

**Electrochemically Assisted Injection for  
Capillary Electrophoresis Time-of-Flight Mass Spectrometry  
- Novel Instrumental and Methodical Developments -**

Dissertation zur Erlangung des Doktorgrades der Naturwissenschaften

(Dr. rer. nat.)

an der naturwissenschaftlichen Fakultät IV

- Chemie und Pharmazie -

der Universität Regensburg



vorgelegt von Peter Josef Johann Palatzky

aus Regensburg

im März 2013



**Electrochemically Assisted Injection for  
Capillary Electrophoresis Time-of-Flight Mass Spectrometry  
- Novel Instrumental and Methodical Developments -**

Dissertation zur Erlangung des Doktorgrades der Naturwissenschaften

(Dr. rer. nat.)

an der naturwissenschaftlichen Fakultät IV

- Chemie und Pharmazie -

der Universität Regensburg



vorgelegt von Peter Josef Johann Palatzky

aus Regensburg

im März 2013

Die vorgelegte Dissertation entstand in der Zeit von November 2009 bis März 2013 am Institut für Analytische Chemie, Chemo- und Biosensorik der naturwissenschaftlichen Fakultät IV - Chemie und Pharmazie - der Universität Regensburg.

Die Arbeit wurde angeleitet von Prof. Dr. Frank-Michael Matysik.

Promotionsgesuch wurde eingereicht am: 12. März 2013

Das Kolloquium fand statt am: 05. April 2013

**Prüfungsausschuss:**

Vorsitzender: Prof. Dr. Arno Pfitzner

Erstgutachter: Prof. Dr. Frank-Michael Matysik

Zweitgutachter: Prof. Dr. Joachim Wegener

Drittprüfer: Prof. Dr. Achim Göpferich

*„Das Denken für sich allein bewegt nichts,  
nur das auf einen Zweck gerichtete und praktische Denken.“*

Aristoteles (384-322 v. Chr.)

# Acknowledgement

First of all, I'd like to thank my supervisor *Prof. Dr. Frank-Michael Matysik* for offering that interesting topic to me and for attending my practical work at the Institute for Analytical Chemistry, Chemo- and Biosensors.

Thanks to all members of the examination board.

I'm also grateful to all present and former members of the Matysik workgroup and the Wolfbeis chair, respectively, for the attractive working conditions and friendly atmosphere. Particularly, I'd like to mention *Stefan Bergner, Jonas Mark and Rebekka Scholz as well as Dr. Heike Mader, Kathrin Hajek, Michael Lemberger* and all others!

Furthermore, I'd like to thank *Dr. Thomas Hirsch* and *Alex Zöpfl* for their support regarding graphene related tasks.

Thanks to my cooperation partners *Susanne Kirchhof* and *Beata Kling*.

The competence of *Peter Fuchs, Herbert Tischhöfer* and all guys of the mechanical and electronic workshop duly deserves to be mentioned here.

Thanks to *Nicole Guber, Gisela Emmert* and all other technicians and secretaries at the institute.

The biggest thank goes to my parents *Helga* and *Helmut Palatzky* for their financial and emotional support through all the years!

Finally I appreciate all my friends who supported me and motivated me over the last decade and, occasionally, were able to stand me: *Stefan O., Markus O., Uli M., Florian D., Daniel R., Markus K., Andi K., Julia S., Therry K., Carina S., Steffi L., Katy K., Winnie G., Michi H., Wurmi, Fluppi...!*

***Thank You!!!***

# Table of Content

<b>1. Introduction.....</b>	<b>1</b>
<b>2. Fundamentals.....</b>	<b>3</b>
2.1. Electroanalytical Chemistry .....	3
2.1.1. Basics and Principles.....	3
2.1.2. Screen-printed Electrodes.....	9
2.1.3. Applications.....	10
2.2. Capillary Electrophoresis.....	11
2.2.1. The Principle of Electrophoretic Separation.....	11
2.2.2. Capillary Electrophoresis and Electroosmotic Flow.....	12
2.2.3. Applications.....	14
2.3. Mass Spectrometry.....	15
2.3.1. General Aspects of Mass Spectrometry.....	15
2.3.2. Electrospray-Ionization Time-of-Flight Mass Spectrometry.....	18
2.4. Hyphenation of Separation Techniques with ESI-MS.....	20
2.4.1. LC/ESI-MS.....	20
2.4.2. CE/ESI-MS.....	21
2.5. Electrochemistry hyphenated to LC- and CE-Techniques.....	22
2.5.1. Hyphenation of Electrochemistry and LC/MS.....	22
2.5.2. Hyphenation of Electrochemistry and CE Techniques .....	23

<b>3. The Author's Original Publications.....</b>	<b>25</b>
<b>4. Experimental.....</b>	<b>29</b>
4.1. Chemicals and Material.....	29
4.1.1. Solutions and Model Systems.....	29
4.1.2. General Handling of Capillary Material.....	31
4.1.3. Screen-Printed Electrodes.....	32
4.1.4. Real Sample Preparation .....	33
4.2. Instrumentation.....	35
4.2.1. Dropsens $\mu$ STAT 100 Potentiostat.....	35
4.2.2. Metrohm $\mu$ AutoLab Potentiostat.....	35
4.2.3. Scanning Electrochemical Microscope CHI 920c.....	36
4.2.4. Lab-built Capillary Electrophoresis Setup.....	37
4.2.5. Time-of-Flight Mass Spectrometer Bruker MicroTOF.....	38
4.3. Instrumental Developments.....	40
4.3.1. Capillary-Based Amperometric Probes.....	40
4.3.2. Time-Gated Electronic Relay.....	41
4.3.3. Semiautomated Injection Cell.....	42
4.3.4. Fully Automated Injection Cell.....	44
4.4. Method Development .....	47
4.4.1. Voltammetric Experiments with Capillary Probes.....	47
4.4.2. Voltammetric Experiments using Screen-Printed Electrodes.....	49
4.4.3. ESI-TOF-MS Settings.....	49
4.4.4. EAI/CE/MS Protocol.....	51



<b>5. Results and Discussion .....</b>	<b>53</b>
<b>5.1. Development of Capillary-Based SECM Probes for the Characterization Of Cell Arrangements for Electrochemically Assisted Injection.....</b>	<b>53</b>
5.1.1. Voltammetry with Capillary-Based SECM Probes .....	53
5.1.2. Electrochemically Assisted Injection Experiments .....	56
5.1.3. Reproducibility of EAI Measurements with Capillary-Based Probes.....	57
5.1.4. Probe Approach Studies .....	59
5.1.5. Conclusions.....	61
<b>5.2. Development and Characterization of a Semiautomated Arrangement For EAI in Combination with CE/ESI-TOF-MS .....</b>	<b>62</b>
5.2.1. Characterization of Screen-Printed Electrodes.....	62
5.2.2. Analytical Performance of EAI in Combination with CE/MS Measurements.....	64
5.2.3. EAI/CE/MS of Nitroaromatic Compounds.....	66
5.2.4. Conclusions.....	69
<b>5.3. EAI/CE/MS using a Fully Automated Injection Device - Mechanistic and Quantitative Studies of the Reduction of 4-Nitrotoluene at Various Carbon-Based Screen-Printed Electrodes .....</b>	<b>70</b>
5.3.1. Analytical Performance of the Fully Automated EAI Arrangement.....	70
5.3.2. Modification and Characterization of Carbon-Based SPEs.....	72
5.3.3. Voltammetric Studies of 4-NT using Different SPE Materials .....	78
5.3.4. Mass Voltammetry of 4-NT by Means of EAI/CE/MS .....	80
5.3.5. Quantitative Determination of 4-NT using Isotope-Labeled 4-NT as an Internal Standard.....	82
5.3.6. Conclusions.....	85

<b>6. References.....</b>	<b>86</b>
<b>7. Summary .....</b>	<b>93</b>
<b>7.1. Summary in English.....</b>	<b>93</b>
<b>7.2. Zusammenfassung in deutscher Sprache .....</b>	<b>96</b>
<b>8. Appendix.....</b>	<b>99</b>
<b>8.1. List of Abbreviations.....</b>	<b>99</b>
<b>8.2. Publications and Presentations .....</b>	<b>101</b>
<b>8.2.1. Peer-reviewed Publications.....</b>	<b>101</b>
<b>8.2.2. Oral Presentations.....</b>	<b>102</b>
<b>8.2.3. Poster Presentations .....</b>	<b>103</b>
<b>8.3. Curriculum Vitae .....</b>	<b>105</b>

## 1. Introduction

Electrochemically Assisted Injection (EAI) was first introduced by Matysik [1] in 2003 and describes a novel injection concept combining electrochemistry with capillary electrophoresis (CE). This approach enables the electrochemical conversion of neutral analytes into charged ones during the injection process. The ions formed are capable of being separated by the help of capillary electrophoresis [2]. Earlier approaches overcame the limitations of neutral analytes in CE with the help of micellar electrokinetic chromatography. Micelle-forming charged tensides were added to encapsulate the analyte molecules and allow for an electrophoretic separation [3]. In capillary electrophoresis commonly UV-, fluorescence-, or less frequently electrochemical detectors are applied. In recent times, a growing interest in capacitively coupled contactless conductivity detection (C<sup>4</sup>D) can be noticed [4]. The hyphenation of CE and mass spectrometry (MS) introduces a significantly higher selectivity with at least the same sensitivity. Both known and unknown analyte species may be verified or identified by MS detection showing the high potential of this technique. The manufacturers have recognized the growing interest in CE/MS coupling and reacted to the market's needs by developing novel coupling solutions [5]. In this context, electrospray ionization (ESI) is the most suitable ionization technique capable of dealing with very small sample volumes and non-volatile, thermally labile compounds [6].

The motivation for EAI/CE/MS development is based on recent requirements in bioanalytical chemistry. Bioanalytical samples are often only available in very small sample volumes. Hence the application of CE in combination with ESI-MS seems to be a very promising approach in bioanalysis. Moreover, the development of EAI cells allows for the implementation of screen-printed electrodes (SPE), as they were designed for sample volumes in the range of a few microliters. The second advantage of SPEs is a wide range of commercially available electrode materials. This fact enables selecting an appropriate electrode material depending on each specific application. Furthermore, ESI is a mild and non-destructive ionization method keeping biological analyte molecules intact during m/z analysis. Oxidative or reductive metabolism studies can be realized by coupling electrochemistry to CE/MS. Moreover, EAI/CE/MS can offer information about the

potential-dependent behaviour of bioanalytes while oxidative or reductive stress is simulated electrochemically during the injection process.

The present thesis covers the development of automated EAI arrangements and their application in combination with CE/ESI-TOF-MS. Preliminary studies have focused on basic geometrical aspects and important electrochemical parameters. The results obtained have been considered in the further instrumental development of automated EAI cells. The second milestone was the fabrication of a semiautomated EAI device that was intensively characterized regarding precision and reliability. Finally the efforts in EAI development resulted in a fully automated, computer-controlled EAI cell that was used for mechanistic studies of nitroaromatics on different SPE materials.

## 2. Fundamentals

### 2.1. Electroanalytical Chemistry

#### 2.1.1. Basics and Principles

The scientific understanding of electricity and magnetism arose in the 16<sup>th</sup> century and formed the basis for electrochemistry. Electrochemistry was first deployed for analytical purposes by Jaroslav Heyrovsky [7] in 1922. Together with Mazuno Shikata, Heyrovsky developed the first polarograph in 1924 and used it for electrochemical studies on mercury drop electrodes. In 1959 he won the Nobel Prize for his contribution to electrochemistry and initiated a fast progress towards modern electroanalytical chemistry.

The typical measurement setup consists of an electrochemical cell with three integrated electrodes (working, reference and auxiliary electrode) connected to a computer-controlled power supply. Depending on whether a potential is applied to the working electrode as a function of time or the system is working in a current-controlled mode, the electrochemical workstation acts in potentiostatic or galvanostatic mode. The following simplified diagram illustrates the standard 3-electrode setup for electrochemical experiments.

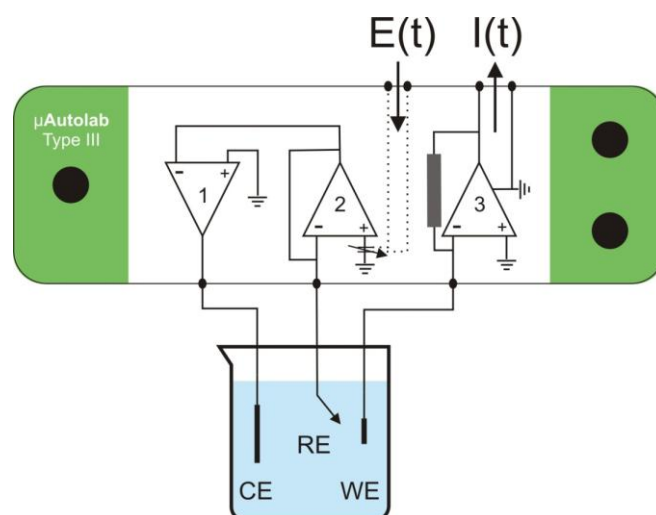


Figure 1: Circuit scheme of a potentiostat in summing amplifier configuration. 3-Electrode setup: working electrode (WE), reference electrode (RE) and auxiliary electrode (AE) are placed in an electrolyte solution. Scheme adapted from [8].

In addition to the WE where the reaction of interest takes place and the AE which acts as an electron source/sink for the redox reaction, a RE is applied to determine the potential between WE and a reference system. The potential between WE and RE is measured very high-ohmic to avoid a certain Faradayic current. Otherwise the resulting voltage drop ( $iR$ -drop) would result in inaccurate measurements. The summing amplifier circuit shown in Figure 1 consists of three operational amplifiers (OA). OA 1 acts as a current amplifier, whereas OA 2 acts as a voltage-follower that provides a constant potential applied to the RE. In combination, OA 1 and OA 2 can be considered as a closed loop in negative feedback mode that provides well-defined currents to the AE to keep the potential between WE and RE constant. OA 3 acts as a current-voltage converter that measures the current response obtained at the WE [8].

Nowadays, often ultramicroelectrodes (UME) in the range of nanometers are applied as WEs, for example in scanning electrochemical microscopy [9, 10]. Due to very small occurring currents at UMEs and a negligible consumption of redox species, the influence of an  $iR$ -drop is negligible in this case. The use of a RE becomes redundant and can be short-circuited to the AE, resulting in a 2-electrode setup with a pseudo-reference electrode [9, 11].

The ability for high-sensitive current measurements allows for a wide range of electroanalytical applications. The most important techniques are potentiometry, voltammetry (derived from Heyrovsky's polarography) and coulometry as well as conductimetry [12]. The techniques can be classified in methods without measurable Faradayic currents (potentiometry) and measurement techniques away from the analytes' redox equilibrium where Faradayic currents result in redox reactions (voltammetry, amperometry, coulometry) [8]. The most frequently applied voltammetric techniques in electroanalysis are described in the following section:

#### *Chronoamperometry:*

A fixed potential is applied to the WE where the former unaffected analyte species are oxidized or reduced. The resulting current is measured and plotted versus time (I-t curve). Due to diffusion limited mass transport, the current decays according to the Cottrell Equation:

$$i(t) = \frac{n \cdot F \cdot A \cdot c \cdot D^{1/2}}{\pi^{1/2} \cdot t^{1/2}} = k \cdot t^{-1/2} \quad \text{Equation (1)}$$

Where n is the number of transferred electrons, F is the Faraday's constant, A the electrode area, c the concentration of the analyte species, D the diffusion coefficient and t the time when the potential is applied. For measurement periods shorter than 50 ms an additional double-layer charging current must be considered. For small UMEs, Equation (1) needs to be modified because of a different mass transport situation. Amperometry is commonly used for determination of diffusion coefficients of redox-active species and in commercial devices for the quantitative determination of human blood glucose [13].

### Cyclic Voltammetry:

Cyclic voltammetry (CV) is the method of choice for investigations of redox mechanisms and analyte-electrode surface interactions. Furthermore, it is well-suited for the determination of oxidation and reduction potentials in the beginning of electroanalytical studies. A voltage ramp is swept to the potential maximum (forward scan) and back to the initial potential (reverse scan). The most common waveforms applied are linear and staircase. The current response depends on the scan rate (slope of the voltage ramp) and several other physicochemical parameters. The resulting I-U-plot is called "cyclic voltammogram". Figure 2 illustrates the case for a fully reversible one-electron transfer reaction:

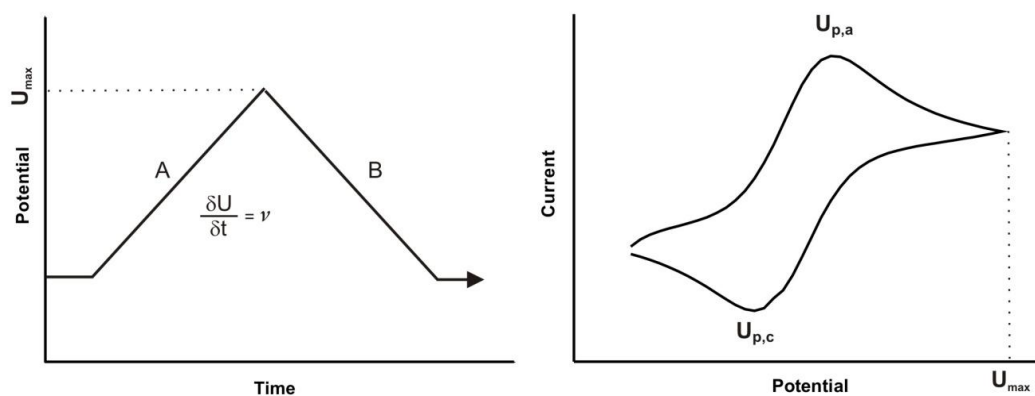


Figure 2: Linear voltage ramp applied in cyclic voltammetry. A: forward scan, B: backward scan (left). Cyclic voltammogram of a reversible one-electron transfer reaction.  $U_{p,a}$  marks the anodic peak potential,  $U_{p,c}$  the cathodic peak potential.  $U_{max}$  indicates the vertex potential (right).



For reversible redox systems the corresponding peak currents can be expressed by the Randles-Sevcik equation for electrodes with linear diffusion behavior. It is derived from Cottrell's Equation (1) and valid for 298.15 K:

$$i_p = (2.69 \cdot 10^5) \cdot n^{2/3} \cdot A \cdot C \cdot D^{1/2} \cdot v^{1/2} \quad \text{Equation (2)}$$

Where  $n$  is the number of exchanged electrons,  $A$  the electrode area,  $C$  the concentration,  $D$  the diffusion coefficient and  $v$  the scan rate.

For irreversible and quasi-reversible redox processes, where the electron transfer is hindered, a transfer coefficient  $\alpha$  must be considered and Equation (2) is modified as follows:

$$i_p = (2.99 \cdot 10^5) \cdot n \cdot (\alpha \cdot n_a)^{1/2} \cdot A \cdot C \cdot D^{1/2} \cdot v^{1/2} \quad \text{Equation (3)}$$

Another important factor is the use of very small UMEs. The diffusion profile in close proximity of an UME changes from linear diffusion behaviour to a more hemispherical diffusion profile. This results in a sigmoidal cyclic voltammogram without any well-expressed oxidation or reduction peaks but with oxidative and reductive steady-state regimes [13]. Considering the different mass transport situation in a hemispherical diffusion profile, the Randles-Sevcik equation can be modified in the following way:

$$i_{ss} = 4 \cdot n \cdot F \cdot C \cdot D \cdot r \quad \text{Equation (4)}$$

$i_{ss}$  is the steady-state current,  $F$  the Faraday's constant and  $r$  is the electrochemically active radius of the UME. Equation (4) is often used in labs for the determination of the effective electrode radius by measuring the steady-state current for a well-studied reversible redox-system like ferrocene and its derivatives [9].

### Square-wave Voltammetry:

Square-wave voltammetry (SWV) is a pulsed voltammetric technique offering high sensitivity at very short analysis times. In SWV experiments the potential ramp applied is superimposed by a square-wave signal of a certain frequency and amplitude. The product of frequency and step potential results in the scan rate and defines the overall analysis time. The current response is measured twice within a potential pulse. One value is recorded at the beginning of the pulse and one at the end. Typically, the difference of forward and backward scan is plotted against the potential as a net curve. Differentiation leads to higher net currents and hence a higher sensitivity can be achieved using pulsed voltammetric techniques like SWV. Additionally, very short pulse durations result in negligible capacitive charging currents and focus solely on the Faraday's current [13, 14]. Figure 3 illustrates a typical potential signal applied in SWV experiments:

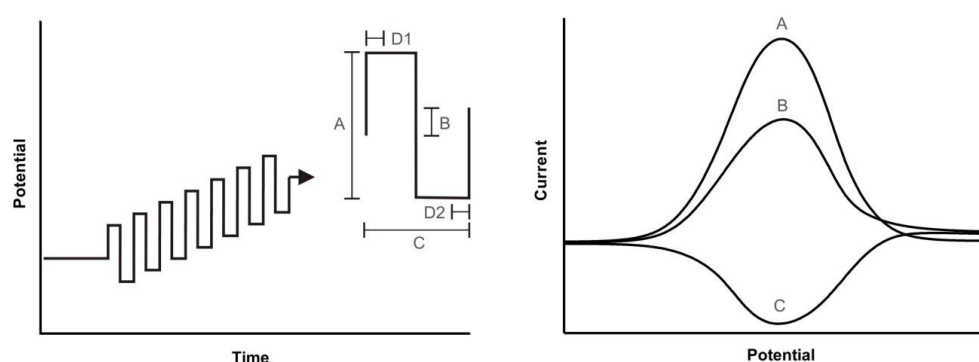


Figure 3: Potential sweep superimposed by a square-wave signal. (A) amplitude, (B) step potential, (C) pulse length (or frequency), (D1) recording window, forward scan; (D2) recording window, backward scan (left). Square-wave voltammogram (A) Net curve, (B) Forward scan, (C) Backward scan (right).

Figure 3 illustrates the applied potential waveform and the resulting current signal for a fully reversible one-electron transfer redox couple. The forward scan (right, B) is measured in the pulse segment D1 (left) and the backward scan (right, C) is recorded in segment D2 (left). Differentiation of B and C results in the net curve A offering a higher peak intensity and thus leads to a better sensitivity of pulsed techniques.

### 2.1.2. Screen-Printed Electrodes

Screen-printed electrodes (SPE) are electrochemical sensors consisting of 2-dimensional three-electrode structures on insulating substrates, for example ceramics or polyester. The electrode structures are defined by the screen-printing technique derived from microelectronics fabrication in the 1990s. An ink containing the suspended electrode material is printed on an insulating substrate to form a thick film layer. Afterwards, the electrode chips are fired in a belt furnace to remove the solvent and harden the printed structures [15-17]. Typically, SPEs are designed as a disk-type, centered WE surrounded by an AE and a (pseudo-) RE in close vicinity. However, interdigitated arrangements have been reported in literature [17-19]. The screen-printing technique allows for fast, cheap and reproducible fabrication of disposable electrochemical sensors offering a wide range of different electrode materials.

Standard materials for WEs are platinum, gold or carbon. Silver or silver/silver chloride electrodes are often applied as RE [20-22]. "State-of-the-art" carbon-based materials are carbon nanofibers, single- and multi-walled carbon nanotubes, graphene, graphene oxide, glassy carbon and boron-doped diamond [21, 23-26]. The following image shows a small selection of commercially available and lab-built SPEs. Additionally, the possibility for the combination of different electrode materials is demonstrated.

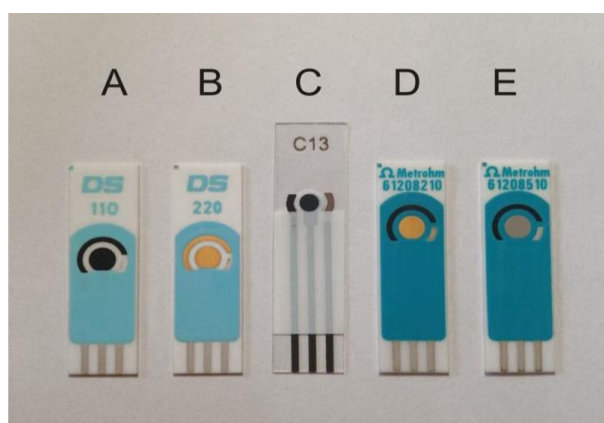


Figure 4: Commercial (Dropsens, Metrohm) and lab-built (C13) SPEs of different electrode material combinations.

Figure 4 shows the commercial SPE models DS110 and DS220 from Dropsens (**A**: WE, AE: carbon, RE: silver; **B**: WE, AE: gold, RE: silver) and Metrohm (**D**: WE: gold, AE: carbon, RE: silver; **E**: WE: platinum, AE: carbon, RE: silver) offering WE diameters of 4 mm. The commercial SPEs were screen-printed on ceramic substrates. In contrast, the lab-built SPE model C13 (**C**: WE, AE: carbon, RE: silver) was built on a flexible polymer substrate with a WE diameter of 3 mm.

Moreover, many efforts have been made to develop sensitive and highly specific biosensors from classical SPEs by immobilization of redox mediators, enzymes and antibodies or microbial agents [16, 27].

### 2.1.3. Applications

Electrochemical methods in combination with SPEs offer a wide range of analytical applications. Portable devices as introduced in section 4.2.1 are very suitable for in-field analysis of toxic substances, e.g. pesticides, herbicides and heavy metals [16]. Classical carbon SPEs were used in combination with differential pulse anodic stripping voltammetry for the determination of Pb. A detection limit of  $2.5 \text{ ng}\cdot\text{mL}^{-1}$  has been obtained with this technique [16, 28]. Du *et al* [29] developed an immunosensor for the cancer biomarker  $\alpha$ -fetoprotein based on graphene-modified carbon SPEs. Considering a certain signal amplification introduced by enzyme-modified carbon nanospheres, a detection limit of  $0.02 \text{ ng}\cdot\text{mL}^{-1}$  has been obtained; the linear range of the calibration plot ranged from  $0.05 \text{ ng}\cdot\text{mL}^{-1}$  to  $6 \text{ ng}\cdot\text{mL}^{-1}$ . Probably best-known is the point-of-care measurement of glucose using glucose oxidase-modified carbon SPEs. Glucose is oxidized to gluconic acid while present oxygen is reduced to hydrogen peroxide. The oxidative or reductive amperometric detection of the hydrogen peroxide formed allows for determination of the glucose level in human blood [16].

## 2.2. Capillary Electrophoresis

### 2.2.1. The Principle of Electrophoretic Separation

In an electric field molecules underlie a certain force  $F_E$  depending on the field strength  $E$  and their own charge  $z$  [30]:

$$F_E = z \cdot e \cdot E \quad \text{Equation (5)}$$

The field strength  $E$  is calculated by dividing the applied potential  $U$  by the overall length of the electrolytic pathway  $L$  [30]:

$$E = \frac{U}{L} \quad \text{Equation (6)}$$

Considering Stokes' Law, a counteracting friction force  $F_r$  results for particles and molecules in an electrolyte solution of viscosity  $\eta$  [30]:

$$F_r = -6 \cdot \pi \cdot \eta \cdot r \cdot v \quad \text{Equation (7)}$$

where  $r$  is the hydrodynamic radius (Stokes radius) and  $v$  is the linear velocity of the molecule or particle. In equilibrium must be considered that  $F_E = F_r$  and the resulting equation can be solved for the migration velocity  $v$  [30]:

$$v = \frac{z \cdot e \cdot E}{6 \cdot \pi \cdot \eta \cdot r} \quad \text{Equation (8)}$$

By elimination of the field strength  $E$ , the electrophoretic mobility  $\mu_{em}$  is introduced and depends only on viscosity  $\eta$ , hydrodynamic radius  $r$  and molecule charge  $z$  [30]:

$$\mu_{em} = \frac{v}{E} = \frac{z \cdot e}{6 \cdot \pi \cdot \eta \cdot r} \quad \text{Equation (9)}$$

Or simplified: The migration velocity only depends on the applied field strength  $E$  and the corresponding electrophoretic mobility  $\mu_{em}$  of each analyte molecule [30]:

$$v = \mu_{em} \cdot E \quad \text{Equation (10)}$$

The following scheme illustrates an electrophoretic separation of cations, neutral analytes and anionic species within an electric field:

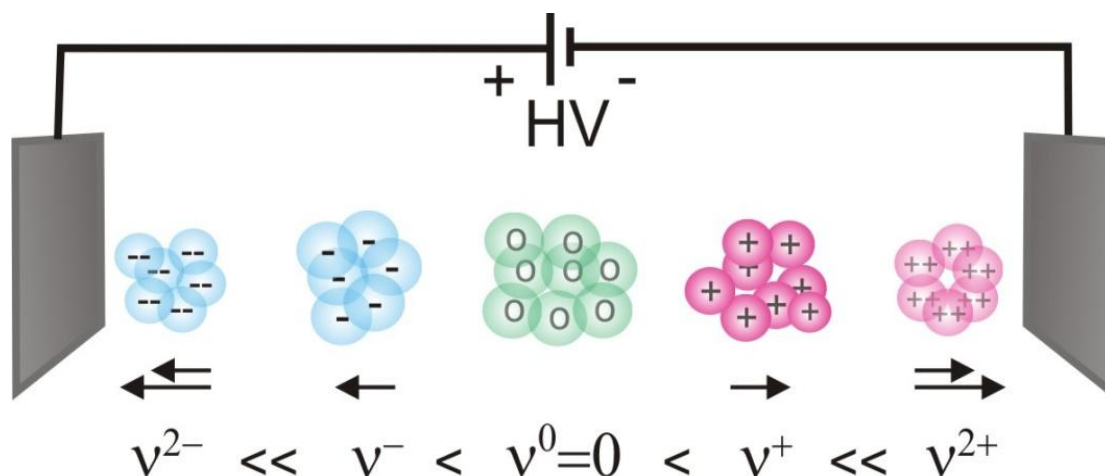


Figure 5: Schematic principle of an electrophoretic separation. Linear velocity relations are valid considering constant field strength  $E$  and same Stokes' radii for all species.

In practice, electrophoretic separations are usually carried out carrier-supported, for example in polyacrylamide gels (PAGE), and are routinely used in protein analysis as well as for DNA and RNA sequencing [30-34].

### 2.2.2 Capillary Electrophoresis and Electroosmotic Flow

Capillary electrophoresis (CE) is a technique where the principle of electrophoretic separation described in 2.2.1. is transferred to fused silica capillaries. Due to very small capillary diameters ranging from  $5\ \mu\text{m}$  to  $75\ \mu\text{m}$  a supporting carrier substrate is needless. Moreover, the use of silica glass as capillary material introduces an effect that affects the electrophoretic separation in a positive way. The phenomenon is called Electroosmotic Flow (EOF) and results from a double layer formed from the negatively charged silanole groups at the inner capillary wall in combination with an externally applied potential. The separation voltage leads the whole plug (including cations, neutral species and anions) migrating towards the cathode. Unlike a hydrodynamic flow situation, where a parabolic

flow profile can be obtained, the EOF causes an almost planar plug front. The planar plug profile results in a considerably higher resolution of capillary electrophoretic separations. Figure 6 illustrates the electrophoretic situation inside a silica glass capillary when a high voltage is applied [30, 31].

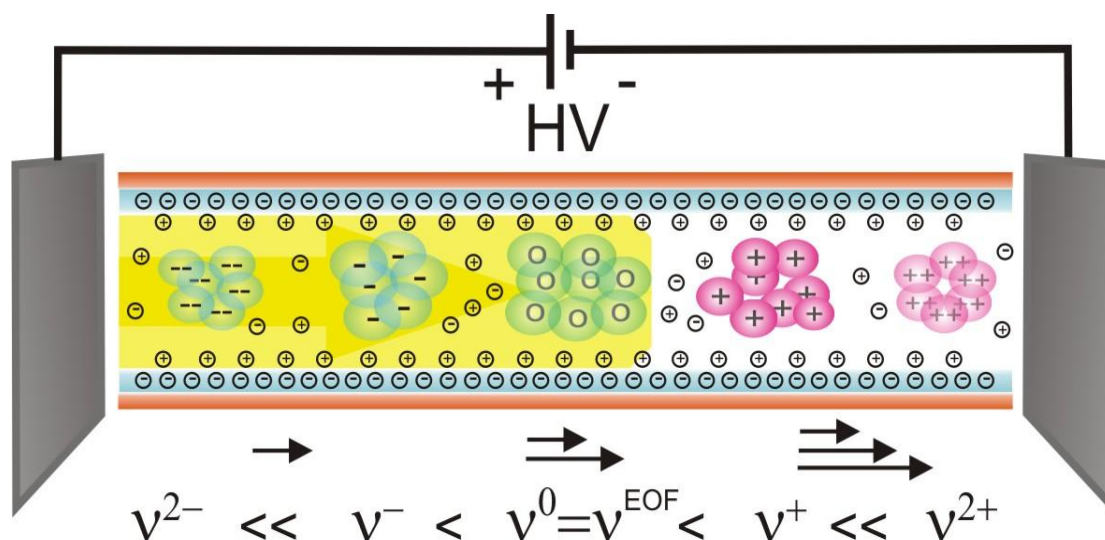


Figure 6: Scheme of a capillary electrophoretic separation. The yellow plug indicates the EOF.

As shown in Figure 6, the EOF superimposes the linear flow velocities of all charged and neutral analytes and hence enables a detection of all analyte species at the cathodic capillary end. Obviously the EOF exceeds the linear velocity of anions. The EOF velocity is calculated using the following equation:

$$v_{EOF} = \frac{\varepsilon \cdot \zeta \cdot E}{4 \cdot \pi \cdot \eta} = \varepsilon_0 \cdot \varepsilon_r \cdot \zeta \cdot \frac{E}{\eta} \quad \text{Equation (11)}$$

$\varepsilon$  is the absolute permittivity,  $\varepsilon_r$  is the relative permittivity,  $\varepsilon_0$  is the permittivity in the vacuum and  $\zeta$  is the Zeta potential occurring where a charged double layer is formed. The EOF velocity depends on several factors. It is linear proportional to the high voltage applied and increases with increasing pH values. Increasing amounts of organic solvents and higher electrolyte concentrations lead to a lower EOF. Another important aspect is the temperature. Temperature changes affect the viscosity by 2-3 % per Kelvin and therefore the EOF might change dramatically during measurements [30, 31].

Typically, CE experiments are carried out in aqueous media which contributes to the EOF effect in a positive way. Another approach is the use of non-aqueous solvents for CE (NACE) offering some additional benefits. The appearance of an EOF in non-aqueous solvents, even without the addition of background electrolytes, has already been intensively studied and reported in literature [35]. The main advantage of NACE is based in low electrophoretic currents. Higher field strengths can be achieved resulting in a better resolution of the separation. Moreover, problems caused by Joule's heating can be avoided when lower Faradayic currents occur during the separation process. Both effects allow for the use of wide bore capillaries and therefore larger sample volumes can be injected whenever needed [36].

The most common detection techniques applied in CE and NACE are UV detection, fluorescence detection and electrochemical detection including the novel C<sup>4</sup>D detection. Mass spectrometry is also widely used in combination with CE and NACE due to its high sensitivity and selectivity. However, MS is very cost-intensive and often of enormous instrumental complexity [30, 31, 37]. The use of CE/ESI-MS coupling is one of the main aspects in this thesis and is discussed in detail in section 2.4.2.

### 2.2.3. Applications

In practice, CE covers a wide range of analytical and bioanalytical applications. For example, CE in combination with atomic spectroscopy has been applied for the detection of metal cations, inorganic anions and carbohydrates in red wine [38]. Furthermore, many different types of antibiotics have been analyzed successfully by the help of CE in combination with UV detection [39]. Another electrophoretic approach that necessarily needs to be mentioned here is chip electrophoresis. Chip electrophoresis plays an important role in mobile in-field analysis. Small glass substrates incorporate an electrophoretic channel of a few centimeters length with small buffer reservoirs at both ends. The USB-powered HV source is mounted in portable racks where the chips are inserted and connected during analysis. Within the last few years many efforts have been made from the instrumental point of view [40]. First devices are now commercially



available and are used, for example, for the determination of volatile aliphatic amines in rotten shrimp tissue. Applying single drop micro-extraction in combination with chip electrophoresis and C<sup>4</sup>D detection, detection limits below 400 ng·mL<sup>-1</sup> can be obtained [41].

## 2.3. Mass Spectrometry

### 2.3.1. General Aspects of Mass Spectrometry

Since Goldstein and Thomson [30, 42] had laid the theoretical and experimental basis by the end of the 19<sup>th</sup> century, mass spectrometry (MS) has turned into the probably most powerful analytical tool in our times. Nowadays, MS is an established high-performance technique used in routine analysis as well as in scientific research. It allows for quantitative and qualitative mass determination of known and unknown substances and, additionally, is able to deliver structural information about a large diversity of analytes. The performance of mass spectrometers is defined by resolving power  $R$  and the mass accuracy:

$$R = \frac{M}{\Delta m} \quad \text{Equation (12)}$$

Where  $M$  is a specific  $m/z$  value and  $\Delta m$  is the  $m/z$  difference of two ions that can even be separated. The mass accuracy defines the significant numbers in elemental mass determination and is given in parts per million (ppm) [43, 44].

The basic principle of MS is that the analyte molecules are first ionized and transferred into the gas phase. In a next step, the charged species are separated according to their individual mass-to-charge ( $m/z$ ) ratio. Subsequently, they are counted electronically and summed up at the detection unit. Hence, a mass spectrometer consists of three sections: *Ion Source, Mass Analyzer and Detector*.

### *Ion Source:*

The efficiency of the ionization process is one of the key points for highly sensitive MS measurements. Hence, a certain number of ionization mechanisms are used in mass spectrometry. The mechanisms can be classified into harsh, destructive processes and in mild, non-destructive ionization processes. Depending on the application, analyte fragmentation under harsh conditions can be a useful tool to get structural information about unknown analytes. Typically, the electron impact (EI) mechanism is used to obtain analyte-specific fragmentation patterns [30, 43]. In contrast, the analysis of biomolecules is carried out preferably under mild and non-destructive conditions. Inhibiting fragmentation by the use of mild ionization techniques allows for the determination of the molar mass of unknown substances. Commonly used mild ionization techniques are chemical ionization (CI), fast atomic bombardment (FAB) and matrix assisted laser desorption ionization (MALDI) [30, 43]. The electrospray ionization (ESI) technique offers many practical advantages when liquid-flow separation techniques (e.g. chromatographic techniques) are hyphenated to MS. Hence, ESI-MS is discussed in more detail in the next chapter.

### *Mass Analyzer:*

After ionization, the ions are transferred into the mass analyzer and are separated according to their individual  $m/z$  ratio. The mass analyzer is kept under high vacuum ( $\sim 10^{-7}$  mbar) to avoid gas-phase collisions that would dramatically limit the resolving power. Mass analyzers are classified according to the working principle. In earlier times the  $m/z$  separation was carried out using electric and magnetic sector fields (or combined in double-focusing MS instruments). "State of the art" developments include orbitrap and (multiple) quadrupole instruments. The preferred technique for the analysis of large biomolecules is the time-of-flight mass analyzer (TOF-MS). The ions are separated in a field-free flight tube according to their individual travel time between homoenergetic acceleration and detection [30, 43, 45-47]. The TOF-MS technique is often combined with an ESI ion source.

*Detector:*

The discrete  $m/z$  portions are detected and summed up in the detection unit. Different instrumental developments allow for sensitive ion detection based on charge multiplication. Commonly used detectors are discrete or continuous dynode electron multiplier or multi channel electron multiplier. The electron multiplication effect bears on an avalanche of secondary electrons triggered by the incoming primary analyte ions. The resulting electric current can be easily measured and evaluated with the help of powerful data acquisition software. More rarely, Faraday cups, Daly detectors and cryogenic detectors are used [43].

### 2.3.2. Electrospray Ionization Time-of-Flight Mass Spectrometry

This section points out instrumental details of ESI-TOF-MS, as this technique was exclusively used in this work. The following image gives a schematic instrumental overview:

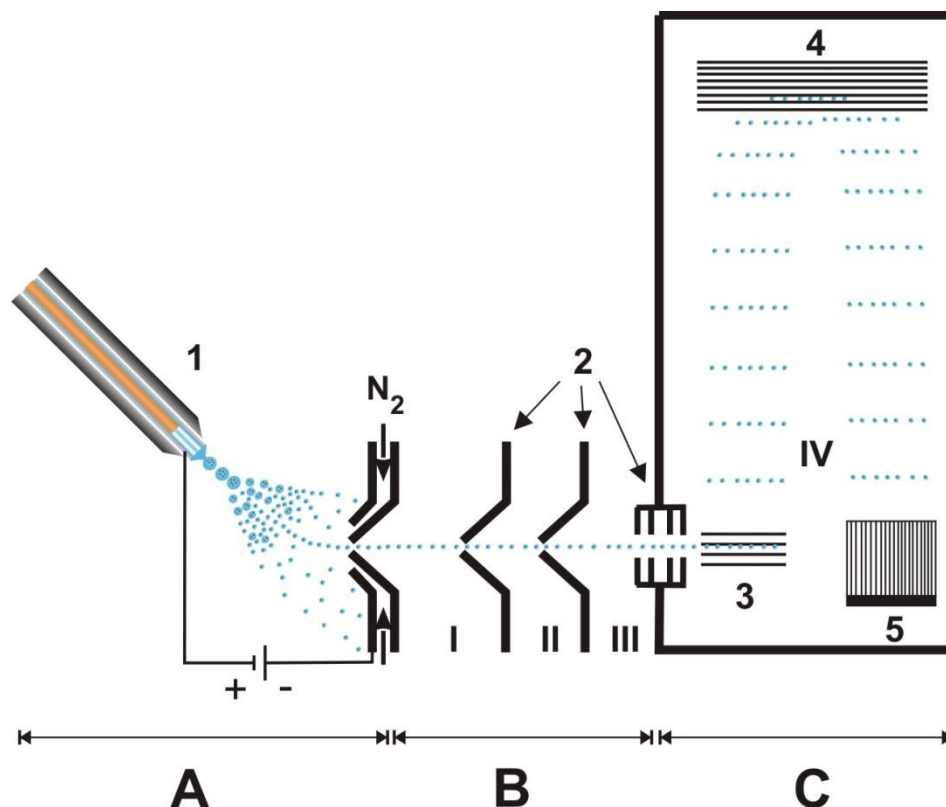


Figure 7: Schematic overview: (A) ESI source, (B) ion transfer optics and (C) time-of-flight mass analyzer with integrated detector. (1) ESI interface, (2) skimmer and ion lenses, (3) orthogonal accelerator, (4) ion reflector and (5) micro channel array detector. (I) to (IV) indicate stepwise increased vacuum stages. (Adapted from "Bruker micrOTOF user manual")

The liquid sample is directly injected into the ESI chamber, using a coaxial sheath liquid sprayer interface. Together with the supporting sheath liquid and the nebulizer gas ( $N_2$ ), the sample eluent forms a Taylor cone within an electric field established between the electrically charged sprayer tip and the countercharged aperture plate [43, 48, 49]. A certain suction pressure and heated  $N_2$  dry gas supports solvent evaporation resulting in

so-called “coulombic explosions” when the repulsion force of the surface charges exceed the droplet’s surface tension. When the charged analyte species are completely desolvated and transferred into the gas phase, the ion stream is focused with the help of skimmers and electromagnetic lenses until it reaches the mass analyzer. Several increasing vacuum stages have been passed when the ion stream enters the ultrahigh-vacuum flight tube. An orthogonal accelerator working in pulsed mode is applied to deflect the ions homoenergetically towards the ion reflector. The potential energy transferred to the ions results in kinetic energy and can be expressed by the following equation:

$$z \cdot eV = \frac{1}{2} m \cdot v^2 \quad \text{Equation (13)}$$

where  $m$  is the mass of the particle and  $v$  is the drift velocity. Solving Equation (13) for  $v$  gives the inverse quadratic relationship between  $v$  and  $m/z$  ratio:

$$v = \left( \frac{2 \cdot z \cdot eV}{m} \right)^{1/2} \quad \text{Equation (14)}$$

Introducing the ions’ travel distance  $L$  between accelerator and detector into Equation (14) gives the flight time TOF:

$$TOF = \frac{L}{v} = L \left( \frac{m}{2 \cdot z \cdot eV} \right)^{1/2} \quad \text{Equation (15)}$$

It can clearly be seen that a homoenergetic acceleration pulse results in an ion separation only depending on the particles’ individual mass-to-charge ratios [43].

The detection of the  $m/z$  equivalent ion portions is realized by a modern micro channel array detector (MCAD). The MCAD consists of hundreds of HV-connected glass capillaries arranged in parallel with ID ranging from 5  $\mu\text{m}$  to 10  $\mu\text{m}$ . The capillary walls are coated with semiconducting material. Incoming ions induce an avalanche of secondary electrons in each single channel and the sum of all channels results in a measureable electronic current. Appropriate hard- and software enables a comprehensive data evaluation [50].

As the ESI technique is a very mild, non-fragmentating ionization technique, it is very suitable for studies on biological and biochemical analyte molecules. A significant advantage of ESI is the formation of multiply charged ions allowing for high-mass analysis exceeding the nominal upper limit of the mass analyzer. Additionally, the TOF mass analyzer hardly shows any limitations regarding high  $m/z$  ratios [43, 51]. Hence, studies of macromolecules like quaternary protein structures of almost 300 kDa (hexamer) have been reported. Protein-protein and ligand-protein equilibria have been investigated by the help of ESI-TOF-MS by Duckworth *et al* [52] in 1998. Literature research in the context of offline ESI-TOF-MS experiments may often remain inconclusively. This is due to one tremendous advantage of ESI in contrast to other ionization techniques. Instrumental developments enable a fast and simple hyphenation of liquid chromatographic separation systems with an ESI source providing significantly enhanced analytical information. Special ESI interfaces allow for direct flow system coupling and enable a continuous flow analysis with real-time data acquisition using an ESI-TOF-MS. The enormous potential of such hyphenated techniques is discussed in detail in the next chapter.

## 2.4. Hyphenation of Separation Techniques with ESI-MS

### 2.4.1. LC/ESI-MS

Commercial atmospheric pressure ionization (API) interfaces of different designs are readily available on the market, allowing for the hyphenation of high performance liquid chromatography (HPLC) systems with ESI-MS devices. API methods include atmospheric pressure chemical ionization (APCI), atmospheric pressure photoionization (APPI) and the ESI technique. Only ESI offers the advantage of an effective ionization of polar, non-volatile compounds in liquid phase. ESI is well-suited for organic analytes of low vapor pressure that are commonly separated by HPLC. Additionally, ESI is the only ionization technique that overcomes ion source limitations caused by the high flow rates applied in HPLC [43]. Hence, HPLC/ESI-MS has developed into a widely used routine analysis technique applied in proteomics, drug determination and many other fields of research. For example, HPLC/ESI-MS has been employed for the determination of chloronicotinyll

pesticides like imidacloprid, acetamiprid and thiacloprid in vegetable samples [53]. Phenolic compounds in olive oils have also been investigated with this technique [54]. Moreover, HPLC/ESI-MS in combination with other analytical focusing techniques is a useful tool in cancer research e.g. for protein mass mapping in tumor identification [55].

#### 2.4.2. CE/ESI-MS

An interface for the hyphenation of CE and ESI-MS was developed in 1988 by Smith and coworkers [56, 57]. The instrumental requirements for CE/ESI-MS coupling, a closed HV-circuit and a conducting capillary tip to establish stable electrospray conditions, can be fulfilled by the use of an aqueous sheath liquid and metal tip coating or an additional stainless steel capillary, respectively. A crucial instrumental aspect in CE/ESI-MS interface development is the separation of the CE high-voltage circuit from the electrospray voltage applied inside the ESI source. The following illustration points out the potential situation when CE is directly coupled to an ESI source:

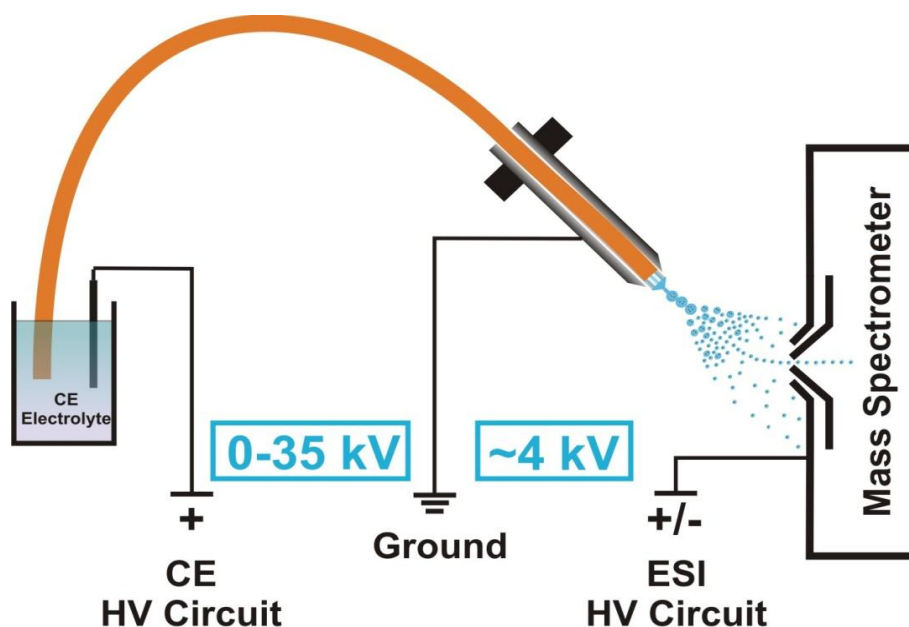


Figure 8: Potential situation in CE/ESI-MS experiments.

Figure 8 illustrates that both CE circuit and ESI circuit have a grounded ESI sprayer needle in common. A closed electric circuit at the sprayer tip is realized using a conducting sheath liquid that is continuously injected with the help of a syringe pump. In the case of CE separation the grounded sprayer tip acts as a cathode. Focusing on the ESI circuit, the sprayer tip works either as cathode or anode, depending on whether the MS works in negative or positive ion mode, respectively.

Sheathless interfaces were developed in combination with nanospray ESI techniques [58]. In recent times, several commercial solutions have been available on the market, for example the Agilent CE-ESI Sprayer kit G1607B [59]. Klampfl *et al* [60] carried out comparative studies of three types of CE/ESI-MS interfaces as they were applied for the determination of nine different fluoroquinolones.

CE/ESI-MS offers a wide field of applications e.g. metabolomics [61]. In drug analysis, the determination of anticancer drugs in human plasma has been reported [62]. A well-suited application with forensic background is the quantification of hallucinogenic amphetamine and morphine derivatives, codeine, cocaine and methadone as they are all protonated at  $\text{pH} < 8$  [63]. In biochemical research, CE/ESI-MS has been applied for plant hormone profiling. Detection limits in the range of a few  $\text{ng}\cdot\text{mL}^{-1}$  have been obtained with the help of a cation-forming derivatisation agent (3-bromoactonyl-trimethylammonium bromide) [64]. Moreover, comprehensive profiling of human hormones like estrogens using CE/ESI-MS has recently been reported [65].

## 2.5. Electrochemistry hyphenated to LC- and CE-Techniques

### 2.5.1. Hyphenation of Electrochemistry, LC and MS

The implementation of electrochemistry (EC) into LC/MS or MS applications provides extended information regarding product formation of redox processes. Direct coupling of EC with MS allows for potential-dependent abundance determination of reactive oxidation products or intermediates. The products formed can often be separated and detected by LC/MS. The electrochemical oxidation allows for the simulation of oxidative



stress and hence the clarification of oxidative degradation pathways [66]. Faber *et al* [67] investigated the phase I metabolism of Diclofenac, a widely used anti-inflammatory drug, with the help of EC/MS and EC/LC/MS. The authors applied EC/MS to figure out reactive oxidation products which are suspected of forming liver-toxic metabolites with proteins and macromolecules [68, 69]. They used a thin layer electrochemical cell equipped with a boron doped diamond electrode and coupled it directly to the ESI source of a TOF-MS [68]. LC was additionally introduced to EC/MS to separate non-reacted trapping agents like glutathione from the trapping products [67]. Reactive triclocarban metabolites have been studied intensively with the same instrumental setup [70]. Furthermore, the experimental approach was used for degradation studies of verapamil, a calcium channel blocker. Microsomal incubation tests were carried out to proof the results obtained in electrochemical oxidation studies [71].

#### 2.5.2. Hyphenation of Electrochemistry and CE Techniques

The hyphenation of electrochemistry and CE has first been described by Matysik [1] in 2003. He presented a concept that enabled the electrochemical conversion of analytes during the hydrodynamic injection process and termed it electrochemically assisted injection (EAI). The glass cell used for EAI incorporated a three-electrode arrangement. The working electrode was positioned close to a fused-silica separation capillary. The electrochemical oxidation of various ferrocene derivatives and their electromigrative behaviour during CE separation had been studied until they were detected via UV detection. In 2010, Gutz and coworkers [72] seized the concept of EAI and developed a flow cell integrated into the CE setup. The system has been capable of preconcentrating trace heavy metals prior to CE separation and C<sup>4</sup>D detection. In 2011 the same workgroup presented an automated two-dimensional CE/C<sup>4</sup>D system with electrochemical preconcentration (1<sup>st</sup> dimension) and staircase potential scanning during EPC (2<sup>nd</sup> dimension) [73]. Instrumental optimization efforts resulted in estimated detection limits of 25 nmol·L<sup>-1</sup>. Further research in the field of EC/CE/C<sup>4</sup>D yielded that the concept enabled the potential-dependent in-situ investigation of reaction products which are

commonly not accessible by applying conventional voltammetric methods [74]. Scholz and Matysik [2] advanced the EAI concept and hyphenated EC/CE with ESI-TOF-MS. First studies indicated that neutral ferrocene derivatives could be separated successfully by CE after oxidative EAI without further addition of micelle-forming tensides. Moreover, the long-term stable cations formed in the EAI glass cell showed a promising ESI efficiency and resulted in a promising MS sensitivity and selectivity.

Based on these results, the motivation for further improvement of EAI cells and the development of new applications has been growing. The efforts made in this context will be summed up and discussed in the following chapters.

### 3. The Author's Original Publications

Parts adapted from the author's original publications form the basis of the following chapters *Experimental* and *Results and Discussion*. The adapted text passages are correspondingly indicated with [P1] - [P3]. This section lists the abstracts of the original publications.

[P1]

#### **Development of Capillary-Based SECM Probes for the Characterization of Cell Arrangements for Electrochemically Assisted Injection**

Peter Palatzky, Frank Michael Matysik

in *Electroanalysis* **2011** 23 (1):50-54.

Abstract:

Electrochemically assisted injection is a new injection concept for capillary electrophoresis. It enables the separation of neutral analyte species by electrochemical ion formation during the injection process. Novel amperometric capillary probes with an integrated microwire electrode have been developed for the characterization of EAI cell arrangements. A scanning electrochemical microscope was used for precise positioning of the capillary probes. The capillary-based SECM probes were characterized regarding their voltammetric behaviour and reproducibility of measurements in the context of EAI injection protocols. These novel SECM probes enabled the study of capillary-to-electrode distances and corresponding dependences on the precision of EAI measurements.

[P2]

**Development and Characterization of a Novel Semiautomated Arrangement for Electrochemically Assisted Injection in Combination with Capillary Electrophoresis Time-of-Flight Mass Spectrometry**

Peter Palatzky, Frank-Michael Matysik

in *Electrophoresis* **2012** 33:2689-2694.

Abstract:

Electrochemically assisted injection is an attractive injection concept for CE that enables the separation of neutral analytes via electrochemical generation of charged species during the injection process. A new semiautomated EAI configuration was developed and applied in conjunction with CE/MS. The EAI cell arrangement consists of an integrated buffer reservoir for CE separations and a compartment holding screen-printed electrodes. A drop of sample solution (50 $\mu$ L) was sufficient to cover the three-electrode structures. A piezo motor provided a fast and precise capillary positioning over the screen-printed electrode assembly. Using ferrocene methanol as a model system, the EAI arrangement was characterized regarding coulometric efficiency, precision and sensitivity of ESI-TOF-MS. The formation of the cationic oxidation product of ferrocene methanol enhanced the sensitivity of CE/MS determination by two orders of magnitude and the electrochemically formed product showed a migration time corresponding to its individual electrophoretic mobility. Preliminary studies of EAI/CE/MS in the field of the analysis of nitroaromatic compounds were carried out. The formation of corresponding hydroxylamines and amines paved the way for selective and sensitive CE/MS determinations without the need of adding surfactants to the electrophoresis buffer.

[P3]

**Electrochemically Assisted Injection in Combination with Capillary Electrophoresis-Mass Spectrometry (EAI/CE/MS) - Mechanistic and Quantitative Studies of the Reduction of 4-Nitrotoluene at Various Carbon-Based Screen-Printed Electrodes**

Peter Palatzky, Alexander Zöpfl, Thomas Hirsch, Frank-Michael Matysik

in *Electroanalysis* **2013** 25:117-122.

Abstract:

Electrochemically assisted injection is a recently introduced injection concept for capillary electrophoresis enabling the separation of neutral analytes by means of electrochemical generation of charged species during the injection process. EAI/CE is particularly attractive in combination with mass spectrometry leading to enhanced performance of MS detection. In this work, a fully automated EAI injection device was developed and applied to mechanistic and quantitative studies of the reduction of 4-nitrotoluene. Three different carbon-based screen-printed electrodes were used including unmodified carbon, carbon nanofiber and reduced graphene oxide SPEs. Under acidic conditions the main products of 4-NT reduction were 4-hydroxylaminotoluene (4-HAT) and 4-aminotoluene (4-AT). The EAI/CE/MS approach enabled the separation and selective determination of both compounds. On the basis of this methodical concept it was possible to study the formation of reduction products of 4-NT in dependence on electrode potential and electrode material. In contrast to conventional electrochemical techniques like cyclic voltammetry EAI/CE/MS provides detailed information regarding changes of the product composition in dependence on various experimental conditions. Over the complete potential range studied the ratio of 4-HAT/4-AT was clearly different for the reduced graphene oxide SPE compared to the unmodified carbon and carbon nanofiber SPE. The construction of mass voltammograms added considerably to the information content of voltammetric experiments. Another aspect of this work was the reliable quantitative

determination of 4-NT by EAI/CE/MS using isotopically labeled 4-NT as an internal standard. In this way the "classical" problem of changing response characteristics at solid electrodes could be eliminated based on the assumption that the target analyte and its isotopically labeled form behave in the same way. A corresponding protocol for quantitative EAI/CE/MS determinations of 4-NT was elaborated and applied to standard solutions and spiked soil samples.

## 4. Experimental

### 4.1. Chemicals and Material

#### 4.1.1. Solutions and Model Systems

##### *Characterization of capillary-based SECM Probes:*

A solution of 1 mM n-butylferrocene (n-BuFc, 99%, ABCR, Germany) in acetonitrile (HPLC grade, Merck, Germany) served as a non-aqueous model system. 500 mM tetrapropylammonium perchlorate (TPAP, >99%, Fluka, Germany) was added as a background electrolyte.

1 mM Ferrocene methanol (FcMeOH, 97%, Aldrich, Germany) in water (Millipore,  $0.055 \mu\text{S}\cdot\text{cm}^{-1}$ ) served as an aqueous model system. The mediator was dissolved in water by sonication and a slightly elevated temperature of  $50^\circ\text{C}$ . 250 mM  $\text{KNO}_3$  (>99%, Merck, Germany) was added to achieve an appropriate background conductivity [P1].

##### *Characterization of screen-printed electrodes:*

A solution of  $10^{-4}$  M FcMeOH was prepared by dilution of a 1 mM stock solution. A 50 mM ammonia/ammonium acetate buffer of pH 9.25 served as background electrolyte. The buffer was prepared by dissolution of 50 mM  $\text{NH}_3$  (25% p.a., Roth, Germany) in water and dropwise addition of acetic acid (100% p.a., Merck, Germany) until pH 9.25 was reached. The pH was adjusted using a pH meter CG 837 purchased from Schott, Germany [P2].

An aqueous solution containing 1 mM and 0.1 mM FcMeOH served as a model system for comparative voltammetric studies of carbon-based SPEs.

### *Separation of Nitroaromatic Compounds:*

Nitrobenzene (NB, >99%), 4-nitrotoluene (4-NT, 99%, both Sigma Aldrich, Germany) and 2,6-dinitrotoluene (2,6-DNT, 97%, ABCR, Germany) at individual concentrations of 100 mg·L<sup>-1</sup> were dissolved in a background electrolyte solution with the help of sonication at an elevated temperature of 50°C. As background electrolyte served 100 mM acetic acid of pH 2.9 [P3].

### *Quantification of Nitroaromatic Compounds:*

Stock solutions of 1 mM 4-NT and 1 mM ring-deuterated 4-nitrotoluene-2,3,5,6-d<sub>4</sub> (4-NT-d<sub>4</sub>, 99%, CDN ISOTOPES, Canada) were prepared for quantitative studies. Due to the poor solubility of the substances, a certain amount was weighted in a glass bottle and filled up with 100 mM acetic acid solution to the corresponding volume. The concentration was verified by HPLC with UV detection [75, P3]

### *EOF-Marker:*

Caffeine (99%, ABCR, Germany) served as an EOF marker in all EAI/CE/MS experiments. Caffeine was added to the sample solutions at a concentration of 10<sup>-4</sup> M by dilution of a 10<sup>-2</sup> M aqueous stock solution [P2, P3].

### *TOF-MS Calibration:*

A 10 mM sodium formate solution was used for TOF-MS calibration in the lower mass range of 50 m/z to 300 m/z. The calibration solution was prepared by dilution of 10 µL of 1M aq. NaOH with 990 µL of solvent containing H<sub>2</sub>O/i-PrOH (50/50, v/v) and 0.1% formic acid [P2, P3].



The following illustration gives structural information about the model systems and analytes used in this work.

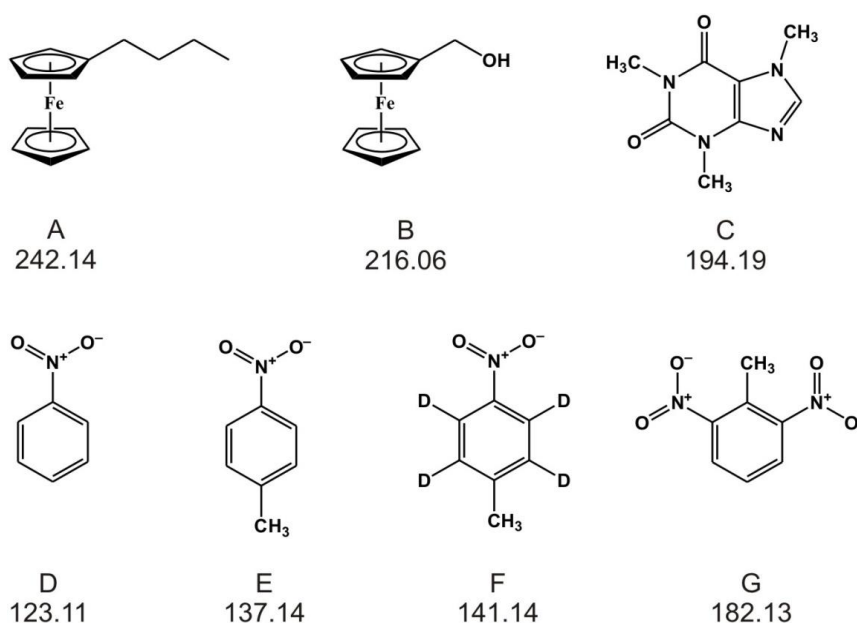


Figure 9: Structural overview of the model systems and analytes used including their molecular weights in g·mol<sup>-1</sup>; **A:** n-BuFc, **B:** FcMeOH, **C:** Caffeine, **D:** NB, **E:** 4-NT, **F:** 4-NT-d<sub>4</sub>, **G:** 2,6-DNT.

#### 4.1.2. General Handling of Capillary Material

All fused-silica capillaries used were purchased from Polymicro Technologies (USA). The capillaries were for 360 µm OD and the chosen ID depended on each application. For the preparation of capillary probes, 75 µm ID capillaries were used and in EAI/CE/MS experiments capillaries of 50 µm ID were obtained to give the best results.

After cutting the capillary to the desired length, the polyimide coating was removed for 1 cm at both ends with the help of a gas burner. Residues were washed away with an acetone wetted cloth. The blank silica ends were polished planar using silicon carbide lapping foils of 15 µm grid size. In the case of the separation capillaries for CE, one end was not polished planar but was beveled to an angle of 15° using a lab-built polishing machine. The polishing residues were removed by purging the capillary in both directions with acetone pressurized in a disposable screw-cap septum vial. The capillary preparation was controlled under the microscope with 40-fold magnification.

After the cleaning process the capillaries were conditioned by purging them with 1 M sodium hydroxide solution for 10 min. Finally, the capillaries were purged with the corresponding CE buffer or mediator solution and fixed in the measurement setup [P1-P3].

#### 4.1.3. Screen-Printed Electrodes

Three different types of SPEs were used in the context of this work. Unmodified carbon SPEs (uc SPE, model: DS110) and carbon nanofiber SPEs (CNF SPE, model: DS110CNF) were obtained from Dropsens (Spain) and used as received. Additionally, uc SPEs were modified by drop coating with a solution of chemically reduced graphene oxide (r-GO) to form a third type of SPEs (r-GO SPE).

Graphene oxide was synthesized according to Hummers' method [76] with slight variations established by Chen *et al.* [77]. Graphite flakes were oxidized using  $\text{KMnO}_4$  as an oxidizing agent to break up the layer-by-layer structure and to form graphene oxide. Finally, chemical reduction of graphene oxide using hydrazine led to the desired r-GO [78]. An aqueous r-GO solution with a concentration of  $0.25 \text{ mg}\cdot\text{mL}^{-1}$  was sonicated for 5 min to obtain a homogenous suspension. A  $20 \mu\text{L}$  drop of the suspension was placed on the working electrode and the solvent was evaporated at a temperature of  $45^\circ\text{C}$  within two hours. The experimental setup is shown in Figure 10.

Additionally, the drop coating procedure was carried out with a  $0.25 \text{ mg}\cdot\text{mL}^{-1}$  graphene oxide solution. For comparison, reduced graphene oxide was electrochemically generated from the drop coated graphene oxide directly at the electrode surface by voltammetric cycling from  $-1.5 \text{ V}$  to  $1 \text{ V}$  at a scan rate of  $100 \text{ mV}\cdot\text{s}^{-1}$  in  $100 \text{ mM Na}_2\text{SO}_4$  for 50 cycles. Afterwards, a constant potential of  $-0.8 \text{ V}$  was applied for 30 min to complete the electrochemical reduction of graphene oxide. The electrochemical reduction protocol was taken from reference [79] but with slight modifications [P3].

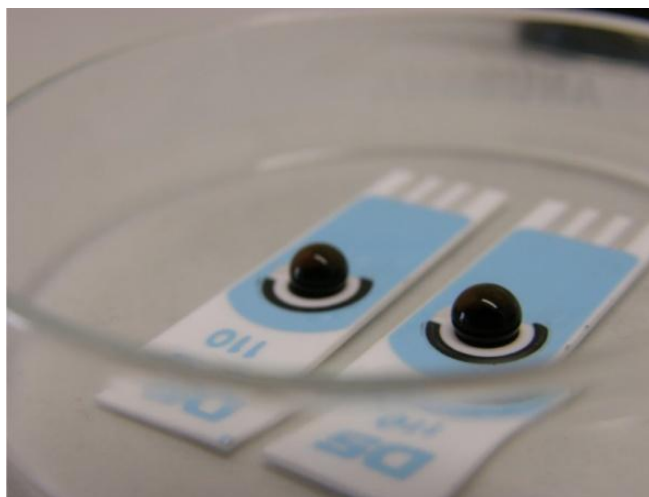


Figure 10: Drop Coating Procedure: A 20  $\mu\text{L}$  drop of a  $0.25 \text{ mg}\cdot\text{mL}^{-1}$  aqueous r-GO solution was placed on the working electrode of a commercially available Dropsens SPE, model: DS110.

Figure 10 illustrates the experimental drop coating procedure of unmodified carbon SPE. The concentric 3-electrode design consists of a disk-type working electrode with an area of  $12.6 \text{ mm}^2$  surrounded by a circular carbon auxiliary electrode. An Ag stripe acts as a pseudo reference electrode.

#### 4.1.4. Real Sample Preparation

Soil and tap water samples were collected at the campus of the University of Regensburg. The samples were spiked with 4-NT and 4-NT- $\text{d}_4$  to establish concentrations in the lower  $\text{mg}\cdot\text{kg}^{-1}$  range and  $\mu\text{mol}\cdot\text{L}^{-1}$  range, respectively. The stock solutions had a concentration of  $1 \text{ mmol}\cdot\text{L}^{-1}$  [P3].

##### *Soil Sample Preparation:*

The sample preparation method was derived from EPA method 8330a with slight variations [80]. Two different samples have been prepared in the same way and compared to each other. In the first case, an amount of 15.746 g soil was homogenized with mortar

and pestle and spiked with 1 mL of 4-NT and 4-NT-d<sub>4</sub> stock solution to achieve mass concentration of 8.71 mg·kg<sup>-1</sup>. The wet soil was again thoroughly mixed and dried in an oven at 50°C for 1 hour. The sample was suspended in 20 mL acetonitrile. After sonication for 10 min, the sample was filtered and washed with 15 mL ACN for two times resulting in a yellowish solution. The solvent was evaporated using a rotary evaporator (T = 40°C, p < 200 mbar) until the volume was reduced to about 4 mL. Finally, the remaining ACN was removed by the help of a nitrogen stream. The residues were taken up in 100 mM acetic acid buffer, again sonicated for 10 min and filtered through a 0.45 µm PTFE syringe filter. The resulting solution had a volume of about 700 µL and was suitable for direct EAI/CE/MS injection. In another experiment, a mass concentration of 2.12 ppm (m/m) was realized in the same way [P3].

#### *Tap Water Sample Preparation:*

The solid phase extraction (SPE) method for tap water samples was derived from EPA method 3535A and adapted to our needs [81]. A sample volume of 90 mL was collected in a 100 mL glass bottle. Each 5 mL of a 1 mM 4-NT and 4-NT-d<sub>4</sub> stock solution were added to achieve a total sample volume of 100 mL with concentrations of 50 µM internal standard and spiking substance. The spiked and isotope labeled sample was used for SPE enrichment without further preparation.

The SPE apparatus used was obtained from J.T. Baker (USA). The apparatus was connected to a water-jet pump to provide an adequate suction pressure. A SPE cartridge (Phenomenex, USA) filled with 500 mg Strata C-18 E (55 µm, 70A) solid phase material was first conditioned with 10 mL methanol and 10 mL H<sub>2</sub>O under gravity flow or a slight suction pressure, respectively. A few mL of the sample solution were immediately filled into the cartridge preventing the cartridge from running dry. A continuous sample flow from the sample bottle towards the cartridge was realized by the help of sealed Teflon cap connected to a small tube. Additionally, a height difference of about 10 cm supported a continuous flow. The extraction was carried out at a flow rate of 5 mL·min<sup>-1</sup> by applying a certain suction pressure. After 20 min the cartridge was washed with 5 mL H<sub>2</sub>O and

eluted with 4 mL ACN under gravity flow. The sample was dried in a certain nitrogen stream and the residues were solved in 1 mL of 100 mM acetic acid buffer (pH 2.9). The solution was sonicated for 10 min, filtered through a 0.45  $\mu\text{m}$  PTFE syringe filter and directly injected to EAI/CE/MS in aliquots of 50  $\mu\text{L}$  [P3].

## 4.2 Instrumentation

### 4.2.1. Dropsens $\mu\text{STAT}$ 100 Potentiostat

The Dropsens  $\mu\text{STAT}$  100 (Dropsens, Spain) was a portable low-cost potentiostat powered via USB connection. In combination with the controller software PSLite 3.0 the  $\mu\text{STAT}$  100 offered a small selection of voltammetric methods (linear sweep-, square wave-, differential pulse- and cyclic voltammetry) and amperometric detection. Moreover, all voltammetric methods could be carried out in stripping mode. The device was capable from measuring currents ranging from 1 nA to 100  $\mu\text{A}$  (divided in 6 current decades) within a potential window of  $\pm 2$  V. The nominal accuracy was  $\leq 1.0$  % for the lowest current range (1 nA),  $\leq 0.5$  % for the 10 nA range and  $\leq 0.2$  % for higher current ranges, all with an additional offset error of 0.2 % [82]. The portable Dropsens  $\mu\text{STAT}$  100 potentiostat with USB connection was available that was applied for preliminary EAI/CE/MS experiments and mass voltammetric studies of FcMeOH.

### 4.2.2. Metrohm $\mu\text{Autolab}$ III Potentiostat

The Metrohm  $\mu\text{Autolab}$  III (Metrohm, Switzerland) was a desktop potentiostat offering versatile electrochemical measurement techniques in combination with the controller software GPES 4.9. It was applied for cyclic voltammetry and square-wave voltammetry of model systems and real samples. The amperometric I-t measurement mode was used in the context of EAI/CE/MS to apply an appropriate oxidation or reduction potential to the substrate electrode. Hence an adaptor was built to connect the SPEs to the device. The following image shows the  $\mu\text{Autolab}$  III Potentiostat.



Figure 11: Metrohm  $\mu$ Autolab III potentiostat.

The device offered a nominal detection range for currents ranging from 10 nA to 10 mA (divided in seven decades) within a potential range of  $\pm 5$  V. The current accuracy was 0.2 % for all current ranges. Additionally, the  $\mu$ Autolab can be used as a powerful electrochemical impedance spectrum analyzer [83].

#### 4.2.3. CH Instruments Scanning Electrochemical Microscope CHI 920c

The scanning electrochemical microscope (SECM) consisted of a high-performance bipotentiostat, a motor controller unit and the measurement stand. The bipotentiostat was suitable for amperometric measurements with a sensitivity between  $10^{-3}$  A·V<sup>-1</sup> and  $10^{-12}$  A·V<sup>-1</sup>. The maximum potential window was  $\pm 10$  V. The bipotentiostat allowed for 3-electrode and 4-electrode measurements. The measurement stand consisted of three orthogonally arranged linear motor stages enabling a three-dimensional capillary positioning. Though the motor stages offered a resolution of 0.1  $\mu$ m. Additionally a three-axis piezo positioner was applied to enhance the lateral resolution to 1.9 nm over a total travel distance of 2.5 cm [84]. Both motor stages and piezo block were controlled by a motor controller unit.

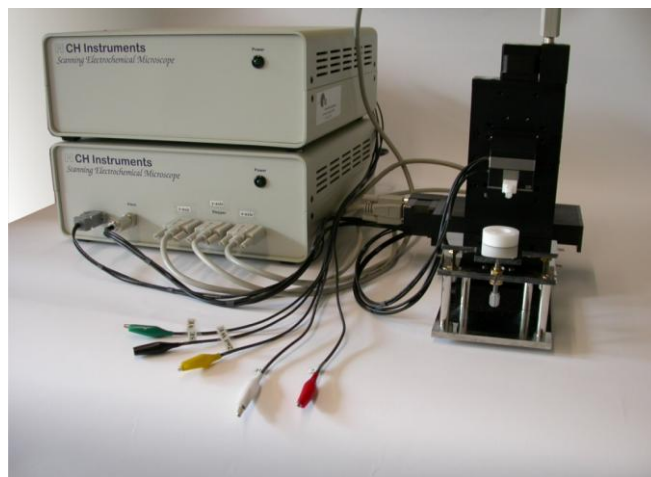


Figure 12: CHI 920c SECM consisting of a bipotentiostat (left, top), the motor controller unit (left, below) and the measurement stand (right). The colored clamps are applied for electrode connections.

The SECM was used for precise vertical capillary probe positioning when probe approach curves were recorded.

#### 4.2.4. Lab-built Capillary Electrophoresis Setup

Electrophoretic separations were carried out applying a HCN 7E-35000 power supply (F. und G. Elektronik, Germany) as a HV source. The HV source was capable of providing an infinitely variable potential of up to +35 kV. The resulting electrophoretic current was monitored by the help of a digital amperemeter. For safety reasons, the anodic HV wire and the ground wire were guided into a Plexiglass box that was equipped with a magnetic HV interrupter switch mounted at the Plexiglass door. The ground wire was connected directly to the electrospray interface to achieve a closed CE circuit. Additionally, the whole CE system was grounded via ground connector of the lab bench. As far as possible all injection and separation procedures were carried out inside the Plexiglass box to prevent the operator and the CE system from dangerous short-circuits. The following image shows the CE setup close to the microTOF MS (Bruker Daltronics, Germany).

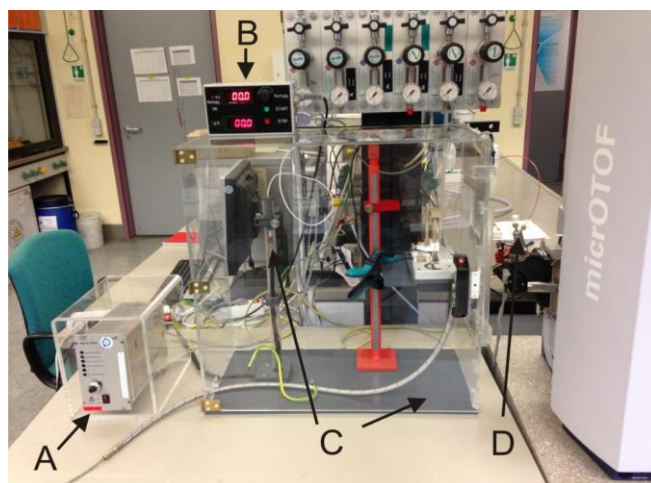


Figure 13: CE components: (A) HV power supply, (B) control unit, (C) Plexiglass box with integrated HV anode and (D) electrospray ionization interface.

Figure 13 shows the complete CE/MS setup placed on a movable table. The HV source (A) is connected to the control unit (B) enabling voltage adjustment, simultaneous current monitoring and start/stop function. Whereas all electronic parts are placed outside the Plexiglass box (C), the anode HV wire (C) is guided inside the box towards the red sample stand. The box is positioned closed to the MS electrospray ionization interface (D) allowing for separations in short capillaries of only 40 to 50 cm. The ESI sprayer needle in the ESI interface is grounded to close the CE circuit. In Figure 13, a fully automated injection cell for EAI is mounted on the sample stand that is later described in detail.

#### 4.2.5. Time-of-Flight Mass Spectrometer Bruker micrOTOF

A time-of-flight mass spectrometer micrOTOF (Bruker Daltronics, Germany) with electrospray ion source was applied for CE detection. The ESI source was capable from direct CE capillary coupling by the help of a grounded coaxial sheath liquid sprayer interface (Agilent, Germany). A stable electrospray containing the CE eluent was achieved by adding a supporting sheath liquid and a nebulizing nitrogen stream to form a Taylor cone at the sprayer tip. The ESI ion source was suitable for analyte flow rates ranging from  $50 \text{ nL}\cdot\text{min}^{-1}$  to  $1 \text{ mL}\cdot\text{min}^{-1}$ . The TOF mass analyzer allowed for positive and negative



ion polarity data acquisition within a mass range of 50 - 3000 m/z and 50 - 20000 m/z (extended mode), respectively. The maximum possible acquisition rate was 20 Hz. The nominal mass resolution was >10000 FWHM and a mass accuracy of 5 ppm (RMS) could be achieved by external calibration [85]. Mass calibration in the lower mass ranges was carried out using 10 mM sodium formate in water/i-propanol solution (50:50, v/v). The following image shows the bench-top micrOTOF ESI-TOF-MS.

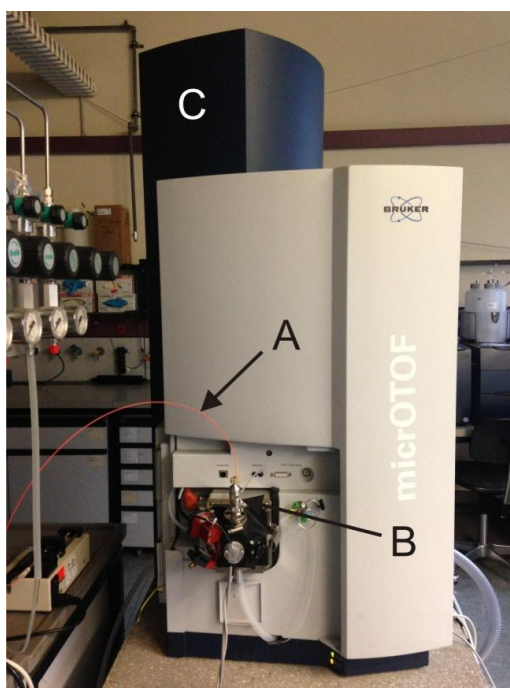


Figure 14: Bruker micrOTOF ESI-TOF-MS: Sheath liquid feed tube (A) from syringe pump is connected to the ESI sprayer needle (B) mounted to the ESI chamber. The flight tube (C) is arranged orthogonal to the horizontally aligned ion optics.

The ESI-TOF-MS was applied as the detector in all EAI/CE/MS experiments. MS method development is explained in detail in section 4.4.3.

### 4.3. Instrumental Developments

#### 4.3.1. Capillary-based Amperometric Probes

The capillary probes were made from fused silica capillaries of 75  $\mu\text{m}$  ID and 360  $\mu\text{m}$  OD (Polymicro Technologies, USA). Capillary pieces of 4 cm and 45 cm in length were used for the probe preparation. One end of each of the capillary pieces was polished to establish a planar mirror finish using silicon carbide lapping foils with a grid size of 15  $\mu\text{m}$  (3 M, USA). The other end were sharpened with an angle of 30° using a lab-built polishing machine. The conically shaped capillary ends were fixed face-to-face on a manual micropositioner below a stereo microscope (40-fold magnification). A 2 cm Pt wire with a diameter of 25  $\mu\text{m}$  (Goodfellow, UK) was manually pushed into the 45 cm capillary for a few hundred micrometers under the microscope. The Pt wire was fixed with a small droplet of grease before the 4 cm capillary was positioned in direct contact to the counterpart. Heating up the grease to 50° C led to the formation of a sealed grease connection between both capillary channels. The arrangement was mechanically fixed and stabilized two times using epoxy resin. After a curing time of one hour the grease was removed by heating the connection section again and flushing the whole capillary with acetone and water. An electrical lead was soldered to the Pt wire. Another layer of epoxy resin and a heat shrink tube ensured a sufficient mechanical stability of the capillary-electrode arrangement. Figure 15 shows a microscopic image of the arrangement before sealing (I) and a schematic drawing of the whole amperometric capillary probe (II).

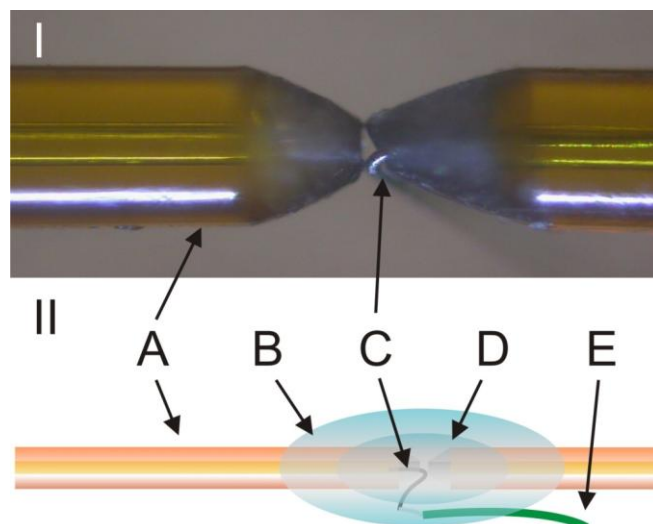


Figure 15: (I) Microscopic image (100-fold magnification) of the capillary arrangement (A) with an inserted 25  $\mu\text{m}$  Pt wire (C). (II) Schematic capillary probe setup additionally showing the primary (D) and secondary (B) epoxy layer and the electric lead (E).

The amperometric capillary probes have been tested regarding leak tightness and chemical stability against organic solvents (acetonitrile). For this purpose the capillary probes were inserted into a screw cap vial with septum and a certain pressure was applied using a disposable 5 mL syringe. In combination with the SECM, the amperometric capillary probes were applied for experiments with respect to the optimum injection distance between capillary inlet and substrate electrode [P1].

#### 4.3.2. Time-Gated Electronic Relay

A time-gated relay was developed in collaboration with the electronic workshop - NWF IV, University of Regensburg. A fast electronic relay G2RL-2 12 V (OMRON, Japan) was combined with a NE556N dual counter IC (STMicroelectronics, USA) acting as a dual timer module. The pulse duration was infinitely variable from 500 ms to 2 s and a pulse delay could be varied from 10 s to 300 s. A trigger button enabled the manual initiation of the delay period. Additionally, an external 5 V TTL signal could be applied for triggering the relay. The maximum relay load was 200 mA at a potential of 30 V.

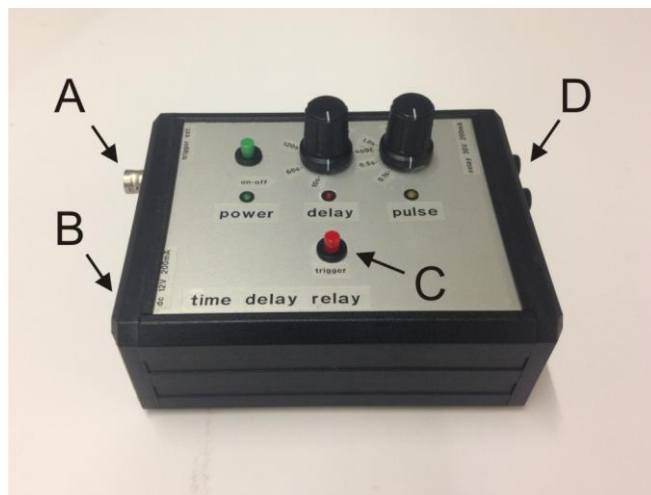


Figure 16: Time-gated relay: (A) external trigger; (B) 12 V power supply; (C) trigger button; (D) relay in/out.

The time-gated relay was used in combination with the SECM and the amperometric capillary probes to investigate the amperometric response of the probes and to determine the flow rates in aqueous and non-aqueous model systems.

#### 4.3.3. Semiautomated Injection Cell

A semiautomated EAI cell was developed in collaboration with the mechanical and the electronic workshop of the faculty. The newly developed EAI configuration is shown in the following illustration.

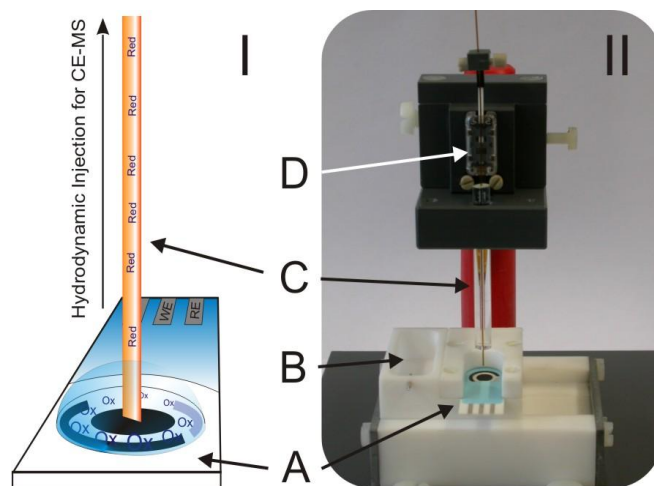


Figure 17: Semiautomated EAI arrangement: Scheme (I) represents the electrochemical analyte conversion on a SPE during hydrodynamic injection. (II) Front-view photograph. EAI components: (A) screen-printed electrode, (B) separation buffer reservoir with integrated Pt electrode, (c) tapered separation capillary ( $\alpha = 10^\circ$ ), and (D) linear Piezo actuator.

The injection arrangement was designed as a movable PTFE carriage with a size of 3.5 cm x 3.5 cm. This carriage incorporates a CE buffer reservoir of 2 mL with a platinum electrode for HV application and a holder for SPEs. A small piezo actuator was fixed on a stand and a glass tubing of 400  $\mu\text{m}$  ID served as a vertical guide for the separation capillary. The piezo motor was purchased from PiezoMotor Uppsala AB (Uppsala, Sweden) and offered a no-load speed of 150  $\text{mm}\cdot\text{s}^{-1}$  at a resolution of 0.5-1.0  $\mu\text{m}$ . The fused-silica capillaries used with the EAI cell were purchased from Polymicro Technologies (Arizona, USA) and had an ID of 50  $\mu\text{m}$  and an OD of 360  $\mu\text{m}$ . In combination with the semi-automated EAI cell, capillary lengths of 50 cm were chosen. By manual displacing the carriage, one could switch the capillary position between the EAI and CE separation modes. The capillary was attached to the piezo motor by means of a PEEK fitting device. A screw mechanism allowed for proper capillary tip adjustment, so that the tip touched the SPE surface in the lowest position. The required precision of capillary-to-electrode distance was achieved by tapering the capillary end to an angle of  $10^\circ$  with the help of a lab-built polishing machine. The resulting shape is depicted in Figure 17 (I). An alumina

lapping foil with a grid size of 30  $\mu\text{m}$  was used. The resulting angle guarantees a capillary inlet positioned about 30  $\mu\text{m}$  above the SPE working electrode surface [P2].

#### 4.3.4. Fully Automated Injection Cell

The fully automated EAI arrangement was a further development of the EAI cell described in the previous section and was also developed in cooperation with the mechanical and electronic workshop. The fully automated construction allowed a microprocessor-controlled vertical and horizontal positioning of the capillary with the help of two high-precision servo motors. A motion sequence included a maximum of 20 single steps. A sequence could be triggered alternately in forward or backward direction. Additionally, the new version incorporated two, removable CE buffer reservoirs of different size (0.2 mL and 2 mL), each with an integrated Pt electrode.

Considering the high-voltage working environment, all electronic microcontroller parts except both servo motors were removed from the EAI stage and housed in a remote manual controller unit that could be positioned outside the Plexiglass box. The control line between controller unit and EAI stage was grounded by the help of a metal tube that was conductively fixed to the HV shield of the servo motors. It was mandatory to connect the cable tubing to the ground jack on the lab bench. In this safety configuration the EAI cell was tested for HV strikes up to 30 kV without damaging the operator or any electronic parts. The following image shows the fully automated EAI cell with the manual controller unit.

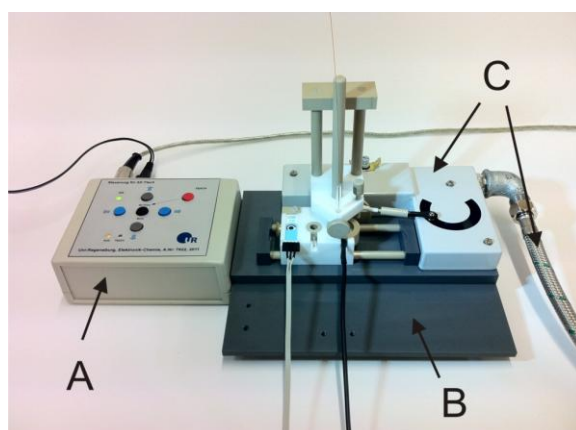


Figure 18: Fully automated EAI cell consisting of manual controller unit (A) and HV-protected Injection stand (B). Servo motors and conducting parts are HV-shielded (C).

Figure 19 gives a more detailed view on the injection compartment including the SPE holder and the CE buffer reservoir. Moreover, the fixation of the separation capillary by the help of a modified PEEK fitting (Upchurch Scientific, USA) is shown in detail.

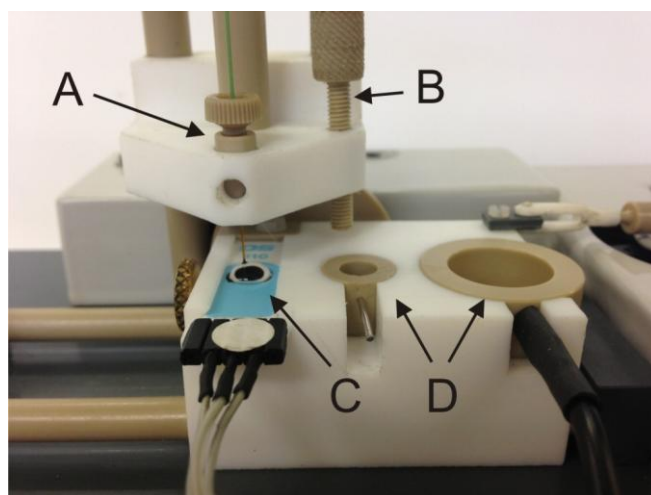


Figure 19: Detailed view on the fully automated EAI cell: (A) Capillary holder, (B) fine adjustment screw, (C) SPE with 50  $\mu\text{L}$  sample drop and (D) buffer reservoirs with integrated Pt electrodes.

The EAI cell could be operated by the manual controller unit or could be programmed via computer software. In contrast to the hand-held controller, the software additionally allowed for variation of the servo motor speed in 100 steps and the programming procedure was more convenient and time-saving. However, the best results were obtained for a motor speed of 95 %. At this speed unintentional air bubble injection could be avoided together with low risk of capillary crashes due to imprecise motor movements.

The connection of controller unit and computer was carried out by USB. A virtual COM port driver was installed automatically. Moreover, a baud rate of 9600 had to be set to ensure proper data communication. The following software screenshot gives an overview over all available functions.

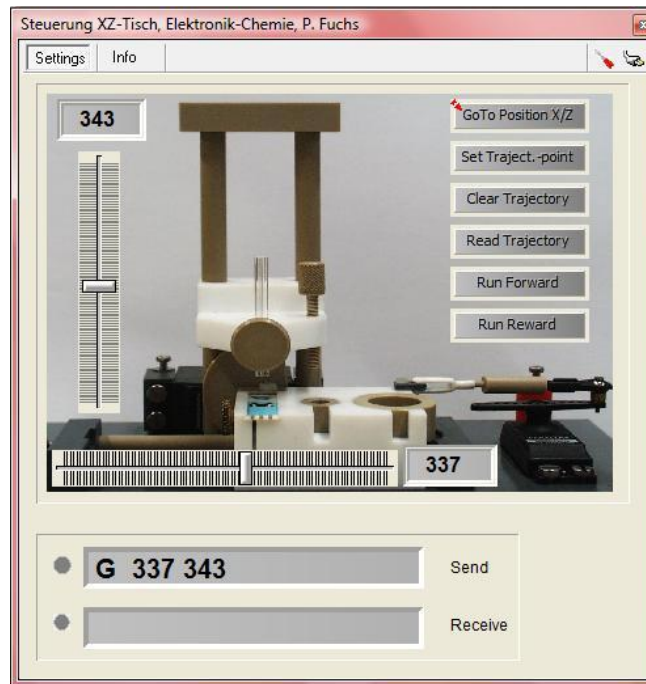


Figure 20: Software screenshot of the fully automated EAI cell.

Two virtual faders and the “Go-to”-button allowed for fast selection of the capillary position. “Set Trajectory Point” saved the point into the flash memory of the controller unit. “Run forward” and “Run reward” triggered the whole sequence saved in the memory. “Clear Trajectory” deleted the sequence saved on the controller unit and “Read Trajectory” retrieved a sequence that was programmed manually into the controller unit.

Besides the ProfiLab software shown in Figure 20 several other commercial available terminal programs (e.g. Microsoft Hyper Terminal) were suitable for the communication between computer and EAI cell controller. However, operating the system manually or by the help of the developed software was much more user-friendly [P3].



## 4.4. Method development

### 4.4.1. Voltammetric Experiments with Capillary Probes

#### *Voltammetry:*

Prior to all experiments the amperometric capillary probes were purged either with aqueous or non-aqueous mediator solution. The hydrodynamic “step-by-step” voltammograms of the capillary probe were recorded with the help of the CHI920c bipotentiostat in amperometric detection mode. A constant hydrodynamic flow was achieved by a height difference of 10 cm. The oxidation potential applied to the capillary probes’ integrated microwire electrode was stepwise increased in 100 mV steps within a potential window ranging from 0 mV to 1000 mV (non-aqueous model system) and from -100 mV to 800 mV (aqueous model system). At each potential step a stabilization period of 100 s was required until the amperometric detection interval of 200 s was initiated. The measurements were carried out in 3-electrode configuration with the help of the CHI920c bipotentiostat. A Pt wire was used as counter electrode and an Ag/AgCl/1 M KCl electrode served as reference system.

Amperometric measurements were carried out for aqueous solution containing 1 mM FcMeOH and 250 mM KNO<sub>3</sub>. The capillary probe was positioned 50 μm over a 2 mm diameter Pt-disk substrate electrode integrated into the SECM sample cell. The CHI920c bipotentiostat was applied for reductive in-capillary detection at 0 mV and simultaneous oxidation at the substrate electrode at 800 mV for 10 s and 600 s, respectively. Moreover, the inverse redox situation was realized by detection at 800 mV and keeping the substrate electrode in open circuit mode.

### *Electrochemically Assisted Injection:*

The CHI920c bipotentiostat was used in combination with the SECM for the optimization of EAI protocols. Additionally, the lab-built time-gated electronic relay was applied to determine the most efficient injection duration. The relay was interconnected between substrate electrode and bipotentiostat because the bipotentiostat only allowed a continuous potential applied to the substrate electrode clamp. A trigger delay of 30 s was achieved by the relay's delay function. EAI durations of 0.5 s, 1 s, 2 s and 10 s were tested for the aqueous and non-aqueous model system. The in-capillary detection potential was set to 0 mV and oxidation potential applied to the substrate electrode was 800 mV in the case of the aqueous model system and 1000 mV for the non-aqueous model system. For reproducibility studies the oxidation pulse at the substrate electrode was triggered consecutively for 6 times. The peak heights and peak areas were evaluated and compared to each other.

### *Probe Approach Studies:*

Probe approach curves were recorded to study the influence of the distance between capillary and substrate electrode on the injection efficiency. Hence, the above described EAI experiments were repeated for successively decreasing distances between capillary probe and substrate electrode. First the capillary probe was fixed to the SECM and positioned in a distance of 150  $\mu\text{m}$  to the substrate electrode. The EAI measurement was carried out and the distance was reduced to 100  $\mu\text{m}$ . The procedure was repeated for distance steps of 20  $\mu\text{m}$  until the capillary probe tip was in contact with the substrate electrode.

#### 4.4.2. Voltammetric Experiments using Screen-Printed Electrodes

All voltammetric SPE experiments were carried out using the  $\mu$ Autolab III or the  $\mu$ Stat 100 as potentiostat. All potentials measured referred to an Ag pseudo-reference electrode placed on the SPE. A sample volume of 50  $\mu$ L was sufficient to cover the 3-electrode arrangement. The scan rates applied in cyclic voltammetry were 50  $\text{mV}\cdot\text{s}^{-1}$  and 100  $\text{mV}\cdot\text{s}^{-1}$ . The model systems and analyte systems were characterized with the help of cyclic voltammetry prior to EAI/CE/MS measurements. The aim was to gather information about electrochemistry, long-term stability and possible counterproductive interactions between redox system and electrode surface ("electrode fouling").

#### 4.4.3. ESI-TOF-MS Settings

Prior to all EAI/CE/MS experiments, an appropriate MS detection method had to be developed for each analyte system. The analyte-specific method development focused on highest sensitivity, in contrast to highest mass resolution, and included the optimization of parameters related to the electrospray ion source and the ion transfer optics as well as an appropriate selection of the corresponding mass traces. Furthermore, an appropriate mass range and a suitable spectra sampling rate had to be defined to gain an optimum in MS performance.

##### *Electrospray Ion Source:*

The capillary outlet was polished planar using a silicon carbide lapping foil with a grid size of 15  $\mu\text{m}$  (3M, USA) and all residues were removed. The capillary was carefully inserted into the coaxial sheath liquid sprayer interface according to the manufacturer's manual. Furthermore, the ESI efficiency depended significantly on the choice of an appropriate sheath liquid. A mixture of  $\text{H}_2\text{O}$ , i-propanol and formic acid at a volume ratio of 50:50:0.2 turned out to give the best results with respect to ESI efficiency, not only in positive ion mode but also in negative ion detection mode.

The instrumental parameters influencing the spray stability were sheath liquid flow rate and nebulizer gas pressure. Once the parameters were optimized for a certain model system or a set of analytes, no further fine-tuning measures during the experiments were necessary to obtain a reproducible ESI efficiency. Further ESI source parameters were capillary voltage and end plate offset voltage as well as dry gas flow and dry gas temperature. The optimized values are listed in Table 1.

#### *Ion Transfer Optics:*

The ions formed in the ESI source were transferred into the mass analyzer with the help of a potential cascade applied to a couple of electromagnetic lenses and skimmers. The ion optics was arranged orthogonally to the flight tube and guided the focused ion beam directly into the TOF mass analyzer. The most important tunable ion transfer parameters were the potentials applied to capillary exit, skimmer 1, hexapole 1, hexapole RF and skimmer 2. Additionally, six further lenses were aligned in the ion optics but had no influence on the MS sensitivity and hence were not further fine-tuned. Lens 1 transfer and lens 1 pre pulse storage time allowed for a certain sensitivity shift within the selected mass range. The chosen parameters are listed in the following Table 1.

Parameter	Method	
	Ferrocene Methanol	Nitroaromatics
<i>General</i>		
Polarity	positive	positive
Spectra Sampling Rate [Hz]	10	10
Mass Range [m/z]	100-400	80-300
<i>ESI Source</i>		
Capillary [V]	4000	4000
End Plate Offset [V]	-500	-500
Nebulizer Pressure [bar]	1.5	1.0
Dry Gas Flow [L·min <sup>-1</sup> ]	4.5	4.1
Dry Gas Temperature [°C]	190	190
<i>Ion Transfer Optics</i>		
Capillary Exit [V]	75.0	75.0
Skimmer 1 [V]	25.3	25.3
Hexapole 1 [V]	23.0	23.0
Hexapole RF [V]	65.0	65.0
Skimmer 2 [V]	23.0	23.0
Lens 1 Transfer [μs]	40.0	40.0
Lens 1 Pre Puls Storage [μs]	12.0	8.0

Table 1: MS method parameters

#### 4.4.4. EAI/CE/MS Protocol

After TOF-MS calibration with 1 M sodium formate, the capillary was inserted into the EAI injection cell. The capillary was vertically fine-adjusted by the help of distance screw in a way that the tapered tip was barely in contact with the working electrode surface of the substrate SPE. After fixation the capillary was moved into the buffer reservoir and purged in reverse flow direction for 5 min by the help of a septum vial containing CE buffer and a certain pressure applied. After purging, the vial was vented and the capillary outlet was fixed in the ESI sprayer needle and inserted in the TOF-MS. A height difference of 5 cm between capillary inlet and ESI sprayer tip was established to achieve a constant flow. Additionally, a certain suction pressure caused by the ESI interface contributed to a

stable hydrodynamic situation that was indicated by a constant total ion current in the MS recordings for at least 30 min. The HV source was switched on, tuned to the desired separation voltage until the measured electrophoretic current was stable for a few minutes and turned off again. A drop of 50  $\mu\text{L}$  of the sample solution was placed on the SPE and the potentiostat was connected to the SPE. For all experiments discussed in chapter 5.2 the  $\mu\text{STAT}$  100 potentiostat was used. The  $\mu\text{Autolab}$  III potentiostat was applied for all EAI/CE/MS experiments in terms of nitroaromatics (chapter 5.3). An appropriate EAI potential was applied for 40 s until the capillary was moved into the sample droplet centered over the working electrode area. During hydrodynamic injection the EAI potential was still applied. After a precise injection time of 5 s or 10 s, respectively, the capillary was moved back into the CE buffer reservoir. The separation voltage of 20 kV or 25 kV was switched on and the TOF-MS recordings were started simultaneously.

For mass voltammetric studies of FcMeOH a series of EAI/CE/MS measurements was recorded for stepwise changing EAI oxidation potentials ranging from -100 mV to 400 mV. The reductive EAI potential windows for the mass voltammetry of nitroaromatics ranged from -0.4 V to -1.4 V and -1.6 V, respectively [P2, P3].

## 5. Results and Discussion

### 5.1. Development of Capillary-Based SECM Probes for the Characterization of Cell Arrangements for Electrochemically Assisted Injection

#### 5.1.1. Voltammetry with capillary-based SECM probes

Voltammetric measurements were carried out to investigate the proper function of the novel probes in aqueous and non-aqueous media. Hydrodynamic voltammograms were recorded stepwise using model redox systems. The potential was varied in steps of 100 mV and the current was registered after a stabilization time of 100 s. A flow rate of  $2.7 \text{ cm}\cdot\text{min}^{-1}$  for the acetonitrile-based system was established by a height difference of 10 cm between the liquid levels in the electrochemical cell and the capillary outlet reservoir. Initial experiments indicated that a rather high supporting electrolyte concentration is necessary to ensure undistorted voltammetric behaviour. For lower concentrations of supporting electrolyte the highly resistive electrolytic path within the capillary results in a significant ohmic potential drop. However, supporting electrolyte concentrations of 0.5 M tetrapropylammonium perchlorate and 0.25 M potassium nitrate provided sufficient background conductivity for measurements in non-aqueous and aqueous media, respectively.

Figures 21 and Figure 22 show hydrodynamic voltammograms recorded with a capillary-based probe positioned in non-aqueous and aqueous model systems. A well defined electrochemical behaviour with an extended limiting current region for the oxidation of *n*-BuFc and FcMeOH were obtained. However, the overall shape of the hydrodynamic voltammograms indicates that there is still some influence of the ohmic potential drop. But the extended region of transport-controlled behaviour was sufficient for the following amperometric measurements.

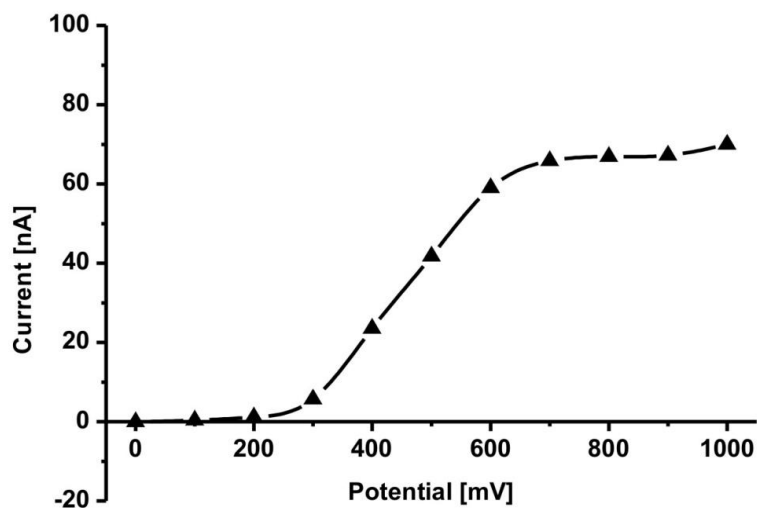


Figure 21: Hydrodynamic “step-by-step” voltammogram recorded with a capillary-based SECM probe with an integrated microwire electrode. An acetonitrile solution containing 1 mM n-butylferrocene and 0.5 M tetrapropylammonium perchlorate was used. The flow rate was  $2.7 \text{ cm}\cdot\text{min}^{-1}$ .

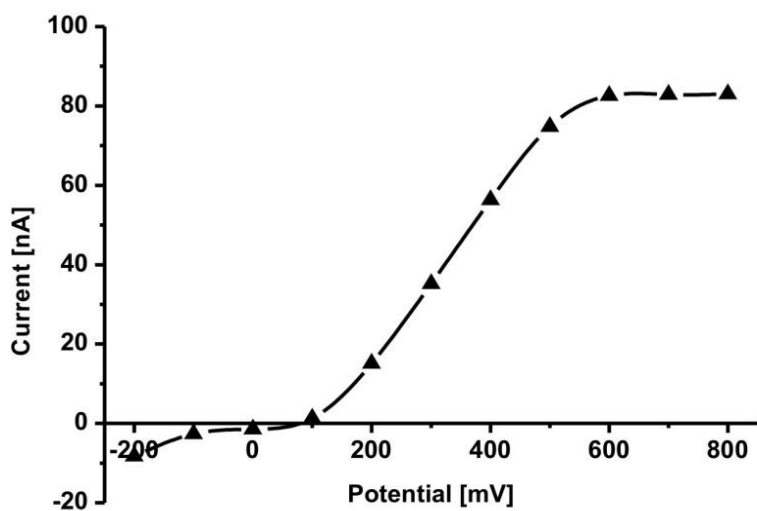


Figure 22: Hydrodynamic “step-by-step” voltammogram obtained for an aqueous solution containing 1 mM FcMeOH and 250 mM  $\text{KNO}_3$ . The flow rate was  $1.6 \text{ cm}\cdot\text{min}^{-1}$ .



According to the results obtained by hydrodynamic voltammetry working electrode potentials of 1000 mV and 800 mV were selected for amperometric recordings of the oxidation of *n*-butylferrocene and ferrocene methanol, respectively. For measurements of the cathodic signals corresponding to the reduction of oxidized species generated at the substrate electrode a potential of 0 mV was applied to the integrated microwire electrode.

Figure 23 illustrates measurements obtained with a capillary-based probe positioned close to the surface of a substrate electrode. Well defined anodic and cathodic steady-state currents could be recorded depending on the potential of the substrate electrode and the duration of potential application. Obviously the integrated microwire electrode enabled a well defined monitoring of species generated at the substrate electrode [P1].

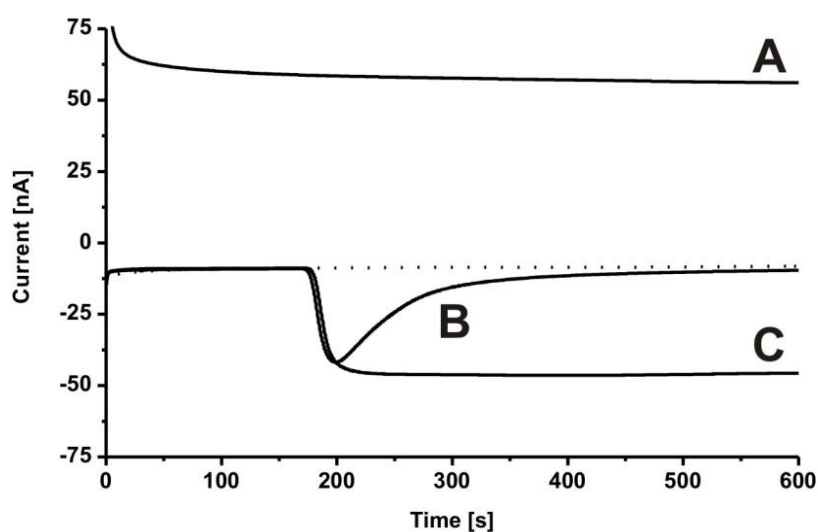


Figure 23: Amperometric measurements with an integrated microwire electrode of a capillary-based probe positioned 50  $\mu\text{m}$  above a substrate electrode. The experiment was carried out using an aqueous solution containing 1 mM ferrocene methanol and 250 mM potassium nitrate and a flow rate of  $1.6 \text{ cm}\cdot\text{min}^{-1}$ . The potentials applied to the substrate electrode (SE) and microwire electrode (MW) were as follows: (A) SE, open circuit potential; MW, 800 mV; (B) SE, 800 mV for 600 s; MW, 0 mV; (C) SE, 800 mV for 10 s; MW, 0 mV. For (B) and (C) the application of the potential of 800 mV to the substrate electrode was started after 30 s.

### 5.1.2. Electrochemically Assisted Injection Experiments

Comparative experiments of EAI were performed for aqueous and non-aqueous media. The capillary probe was positioned 50  $\mu\text{m}$  above the 2 mm Pt substrate electrode at the bottom of the electrochemical cell. The flow rate was as specified in the experimental section. Figure 24 and Figure 25 illustrate the responses for EAI intervals of 10 s for non-aqueous and aqueous solutions. Obviously, the zones of electrochemically generated products are much sharper in non-aqueous solution compared to the aqueous medium. This can be attributed to differences in flow rate and transport characteristics in both media. Due to a lower viscosity of acetonitrile, the flow velocity in the non-aqueous medium is 60 % higher than in the aqueous model system. As a consequence, in aqueous solution it takes longer to remove the electrochemically formed species from the substrate electrode – capillary probe region than in non-aqueous solution. This fact results in a more pronounced peak tailing observed in case of the aqueous system [P1].

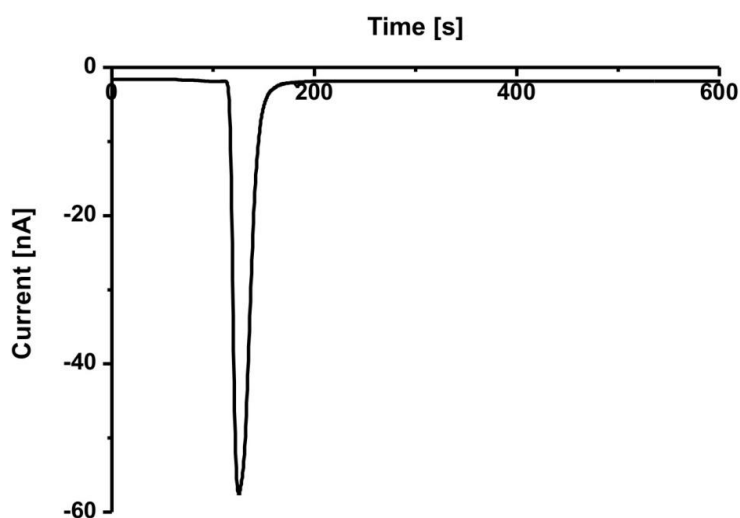


Figure 24: Electrochemically assisted injection performed at a 2 mm Pt substrate electrode in combination with a capillary-based probe positioned 50  $\mu\text{m}$  above the electrode. The amperometric recordings were measured with the integrated microwire electrode. Experimental parameters: acetonitrile solution containing 1 mM n-butylferrocene and 0.5 M tetrapropylammonium perchlorate; potential at the substrate electrode, 1000 mV for 10 s; potential at the integrated microwire electrode, 0 V; flow rate, 2.7  $\text{cm}\cdot\text{min}^{-1}$ .

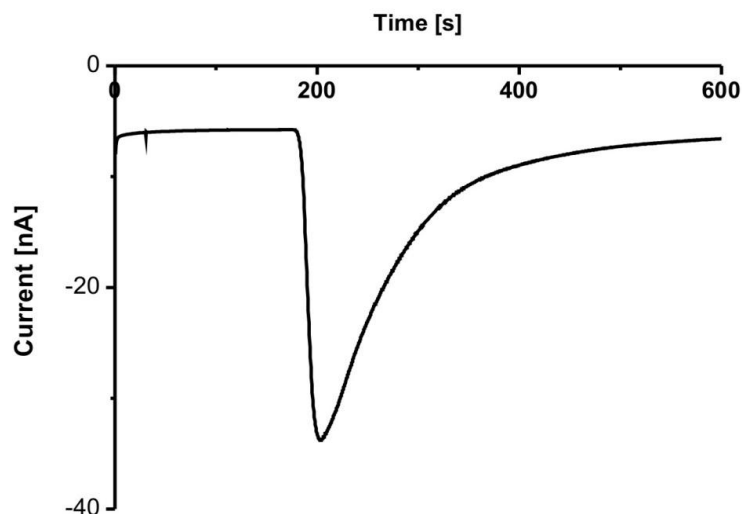


Figure 25: Electrochemically assisted injection performed at a 2 mm Pt substrate electrode in combination with a capillary-based probe positioned 50  $\mu\text{m}$  above the electrode. The amperometric recordings were measured with the integrated microwire electrode. Experimental parameters: aqueous solution containing 1 mM ferrocene methanol and 0.25 M potassium nitrate; potential at the substrate electrode, 800 mV for 10 s; potential at the integrated microwire electrode, 0 V; flow rate, 1.6  $\text{cm}\cdot\text{min}^{-1}$ .

### 5.1.3. Reproducibility of EAI Measurements with Capillary-Based Probes

An important aspect of EAI experiments was the reproducibility of measurements performed with the novel capillary based probes. A typical injection interval for EAI were 10 s. Figure 26 and Figure 27 show recordings of six repetitive EAI experiments for n-BuFc and FcMeOH oxidized at the substrate electrode. The oxidized species formed could be detected at the integrated microwire electrode.

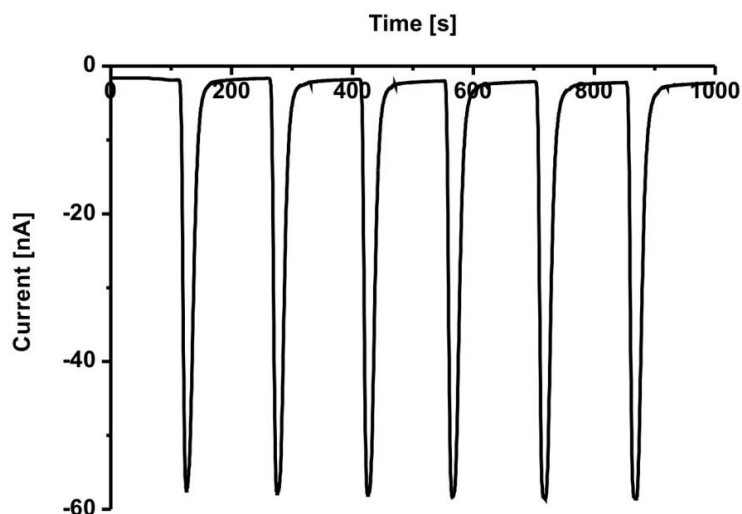


Figure 26: Reproducibility of EAI using a non-aqueous solution of 1 mM n-butylferrocene and 500 mM TPAP in acetonitrile. Six repetitive measurements were performed applying a potential of 1000 mV to the substrate electrode for a period of 10 s. The microwire electrode was set to a detection potential of 0 mV.

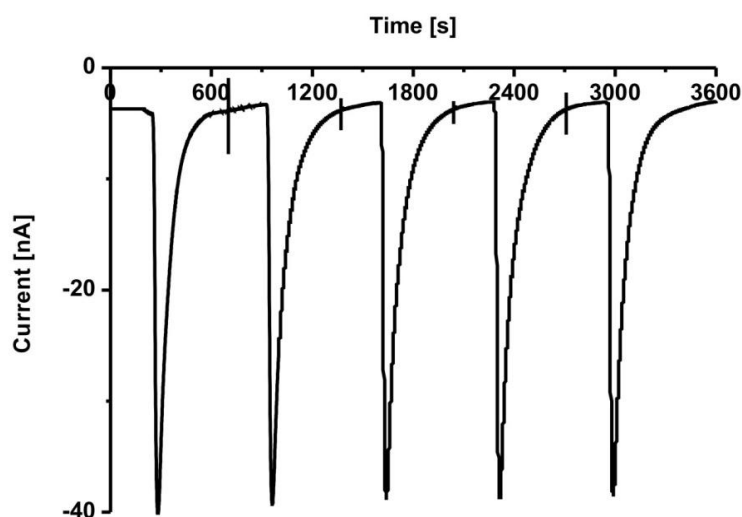


Figure 27: Reproducibility ( $n=6$ ) of EAI using an aqueous solution of 1 mM FcMeOH and 500 mM TPAP. The potential applied to the substrate electrode was 800 mV.

The mean peak height for conditions as shown in Figure 26 was 56.2 nA with a relative standard deviation of 0.4 % ( $n = 6$ ). The corresponding mean peak area was 1.1  $\mu\text{C}$  with a relative standard deviation of 6.6 % ( $n = 6$ ). Shorter intervals of EAI protocols such as

0.5, 1 and 2 s led to less reproducible results. Consequently, EAI duration of 10 s was used in further experiments and the peak height was used as a measure for quantitative evaluation. For the aqueous model system shown in Figure 27 a relative standard deviation of 1.7% (n = 6) was obtained for the precision of peak height measurements and 5.4 % (n=6) for the evaluation of the peak area. The artifacts prior to the signal peak indicate the triggered oxidation potential applied to the substrate electrode [P1].

#### 5.1.4. Probe Approach Studies

Approach curves performed with conventional microdisk SECM probes enabled a detailed characterization of signal dependence on the substrate-probe distance. For further developments of EAI cell configurations it was highly interesting to investigate the analytical characteristics of EAI as a function of the distance between the capillary and the substrate electrode. Using the SECM system approach curves were measured with the capillary based probes. The capillary probe was approached from the bulk solution (150  $\mu\text{m}$  distance) towards the substrate electrode in 20  $\mu\text{m}$  steps. For each positioning the peak height of the EAI signal was recorded. Figure 28 and Figure 29 show the dependence of peak height on the capillary-to-substrate electrode distance tested for non-aqueous and aqueous media.

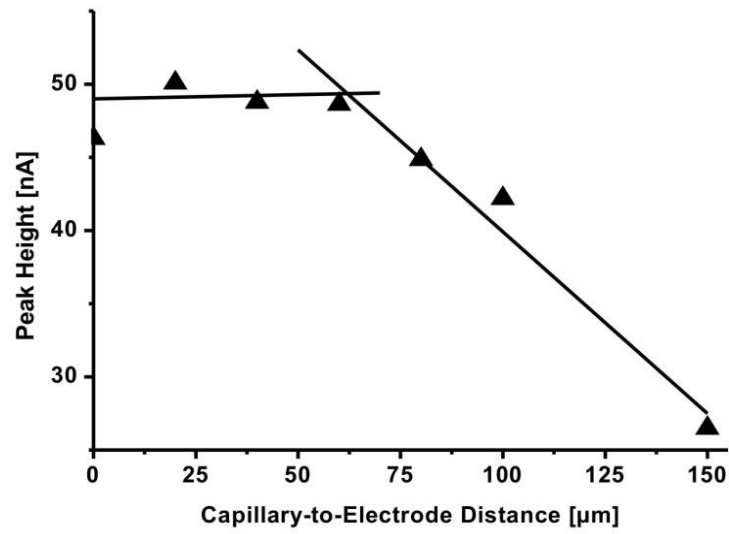


Figure 28: SECM approach plot recorded by a stepwise distance variation between capillary and substrate electrode in non-aqueous media. Experimental conditions were as specified in Figure 24.

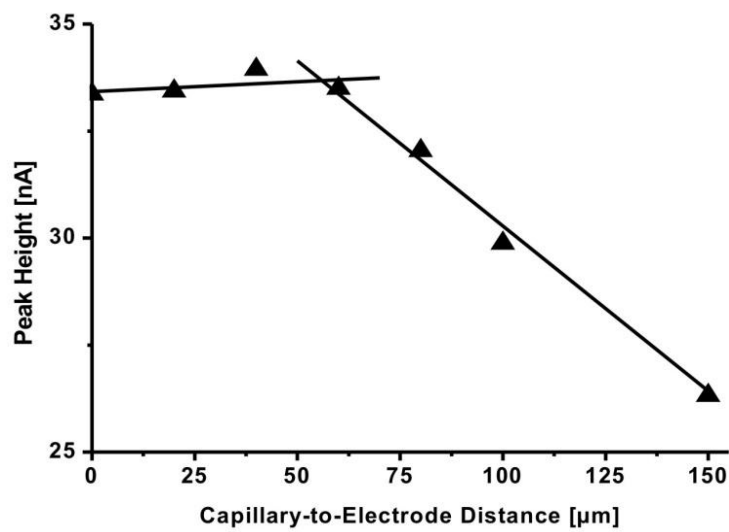


Figure 29: SECM approach plot recorded by a stepwise distance variation between capillary and substrate electrode in aqueous media. Experimental conditions were as specified in Figure 25.

In aqueous and non-aqueous media the recorded signals were nearly constant for capillary-to-electrode distances between 5 and 60  $\mu\text{m}$ . For larger distances a linear decay of the peak height was found. The analytical application of EAI involves repositioning steps between the measurements. Based on the above results obtained for 75  $\mu\text{m}$  capillaries future developments of EAI cell arrangements should realize positioning systems with a precision of  $\pm 30 \mu\text{m}$  to ensure reproducible measurements. Within this range, small variations of the capillary-to-electrode distance should have only minor effects on the precision of the EAI measurements [P1].

#### 5.1.5. Conclusions

Novel capillary-based probes with an integrated microwire electrode were successfully used in conjunction with scanning electrochemical microscopy. It was found that these probes exhibit a well defined electrochemical behaviour. Hydrodynamic voltammetry turned out the capillaries' suitability for amperometric in-capillary detection when sufficient background conductivity is guaranteed. Reproducibility studies pointed out the reliability of the capillary probes developed. The measurements performed enabled a detailed analytical characterization of EAI protocols. Moreover, the probes were successfully applied in combination with a SECM. These novel SECM probes enabled the study of capillary-to-substrate electrode distances and corresponding dependences on the precision of EAI experiment. Based on these results the requirements for further developments of EAI cell arrangements could be derived [P1].

## 5.2. Development and Characterization of a Novel Semiautomated Arrangement for EAI in Combination with CE/ESI-TOF-MS

### 5.2.1. Characterization of Screen-Printed Electrodes

FcMeOH was selected as a model compound for the characterization of the EAI/CE/MS system. The electrochemical behaviour of FcMeOH in conjunction with screen-printed electrodes was studied by cyclic voltammetry and corresponding mass voltammetry. Figure 30 shows the CV recording obtained after applying a droplet of 50  $\mu\text{L}$   $10^{-4}$  M FcMeOH to the screen-printed electrode. Well-defined voltammetric signals with very good long-term stability were recorded.

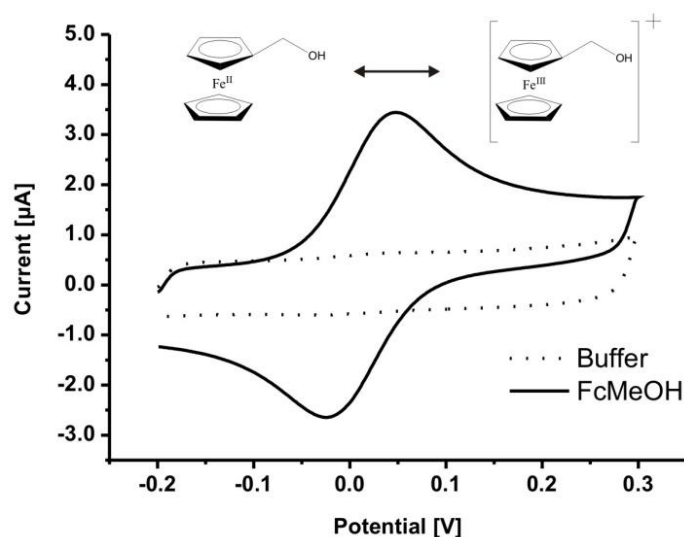


Figure 30: Cyclic voltammetry of a 50  $\mu\text{L}$  of  $10^{-4}$  M FcMeOH in 50 mM ammonia / ammonium acetate buffer of pH 9.25 using screen-printed carbon electrodes. The scan rate was  $100 \text{ mV}\cdot\text{s}^{-1}$ .

After CV studies the EAI/CE/MS system was used for recording mass voltammograms. The potential-dependent formation of  $\text{FcMeOH}^+$  was registered in the migration window of cationic species recording the mass trace of 216.03 m/z. The working electrode potential was increased in 50 mV steps and the peak height was plotted versus the electrode potential. Corresponding results of MV studies are illustrated in Figure 31.



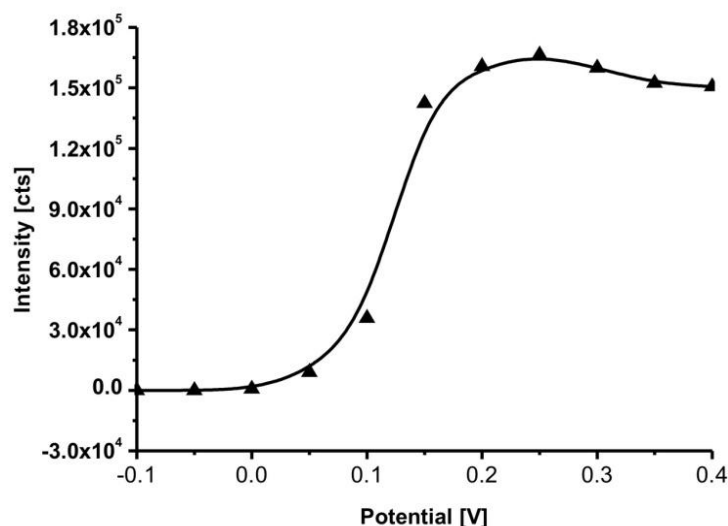


Figure 31: Mass voltammogram obtained by EAI/CE/MS experiments using a  $10^{-4}$  M FcMeOH in 50 mM  $\text{NH}_3/\text{NH}_4\text{OAc}$  buffer at pH 9.25 and screen-printed carbon electrodes. The intensity corresponds to the peak height of the extracted ion electropherogram at 216.03 m/z. The separation voltage was 25 kV.

The potential window for the formation of  $\text{FcMeOH}^+$  is in good agreement with the CV investigations. The different shapes of CV and MV recordings can be attributed to different mass transport situations in both measuring modes. In the case of CV the only mode of mass transport is diffusion. In MV there is an additional mass transport contribution caused by the suction effect. In addition, the presence of the capillary in close proximity to the electrode surface affects the overall mass transport situation. According to the results of CV and MV studies a working electrode potential of 400 mV was selected for EAI experiments to ensure a mass-transport controlled and stable formation of  $\text{FcMeOH}^+$  [P2].

### 5.2.2. Analytical Performance of EAI in Combination with CE/MS Measurements

In previous studies it was found that FcMeOH was a very suitable model system for EAI-CE experiments in aqueous solutions [16]. The electrochemically generated FcMeOH<sup>+</sup> exhibits good stability and can easily be separated from the neutral FcMeOH under typical CE conditions.

Figure 32 illustrates the enhancement of CE/MS by means of EAI. Without EAI a signal at a non-selective migration time (corresponding to the neutral FcMeOH) with poor sensitivity is obtained. The latter aspect results from the poor ionization efficiency of FcMeOH in the electrospray ionization (ESI) process. In contrast, the application of EAI which is associated with the formation of FcMeOH<sup>+</sup> leads to a selective migration time of the cationic species with its individual electrophoretic mobility and an enhancement in sensitivity of about two orders of magnitude.

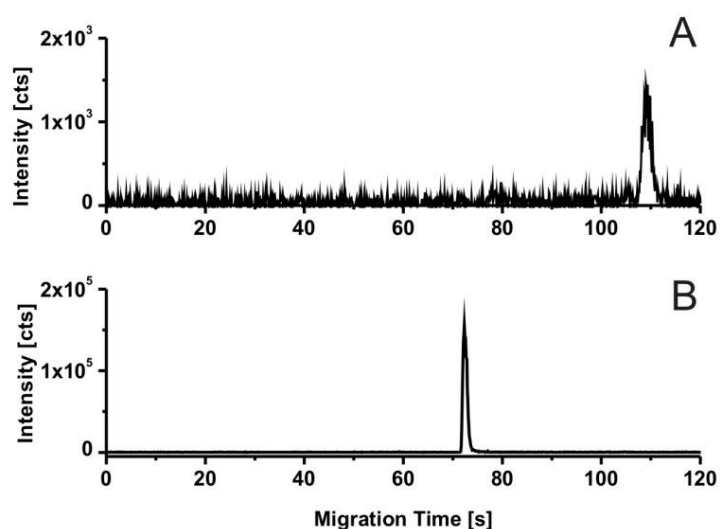


Figure 32: Comparison of CE/MS measurements of  $10^{-4}$  M FcMeOH in 50 mM  $\text{NH}_3/\text{NH}_4\text{OAc}$  buffer (pH 9.25) without (A) and with (B) EAI at 400 mV for 10 s. The separation voltage was 25 kV.

Extracted ion electropherograms were recorded for mass traces 216.03 m/z.

The coulometric efficiency of EAI was determined on the basis of the signals (with / without EAI) obtained for the migration time of the neutral FcMeOH. A coulometric efficiency of  $70 \pm 2\%$  ( $n=6$ ) was calculated. Concentration determinations by EAI/CE/MS are

possible after external calibration. A linear calibration plot for concentrations ranging between  $5 \cdot 10^{-6}$  M and  $5 \cdot 10^{-5}$  M was obtained ( $r^2 = 0.9954$ ,  $n=3$ ). The calibration plot is shown in Figure 33:

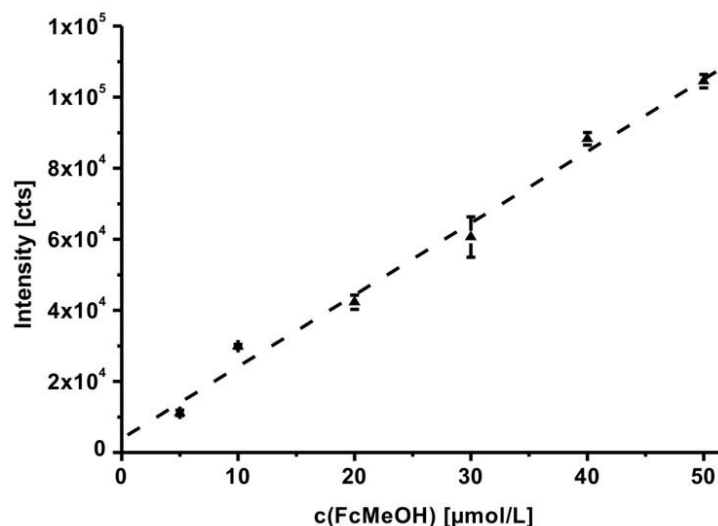


Figure 33: Calibration plot of FcMeOH in 50 mM aqueous  $\text{NH}_3/\text{NH}_4\text{OAc}$  solution of pH 9.25 ( $n=3$ ).

Measurements were carried out using the semi-automated EAI cell.

Experimental conditions: EAI duration 10 s, EAI potential 400 mV, CE voltage 25 kV.

However, the use of isotope-labeled internal standards would be the most reliable way for quantification as this could compensate for changing electrochemical activity at the screen-printed electrodes as well as changes regarding ESI efficiency. The method of internal calibration with the help of isotope-labeled standards is discussed in section 5.3. However, in case of the simple model system a very good long-term stability and repeatability were obtained. Repetitive injections of  $10^{-4}$  M FcMeOH were characterized by a relative standard deviation for peak height measurements of 1.0% ( $n=6$ ) [P2].

### 5.2.3. EAI/CE/MS of Nitroaromatic Compounds

The determination of nitroaromatic compounds is of great interest in the context of security activities to prevent terrorist attacks and environmental concerns related to former ammunition plants or military firing ranges. The variety of explosives and metabolites as well as their different properties and concentration levels form still a challenge for the development of powerful analytical methods. A typical approach for the determination of nitroaromatic compounds is based on the US EPA (United States Environmental Protection Agency) method EPA 8330 [80]. This method suggests the use of two independent columns (C-18 and CN reserve-phase columns) with UV detection. Alternatively, stationary-phase optimized liquid chromatography with segmented columns was used to improve selectivity [86]. In addition, the recently introduced EPA Method 4050 implements an immunoassay for TNT determination [87]. Electrophoretic separations of neutral nitroaromatic compounds are only possible by means of micellar electrokinetic capillary chromatography (MEKC). However, the use of a relatively high concentration of surfactants results in significantly reduced compatibility with ESI-MS. Therefore, alternative detection methods such as electrochemical detection have been applied [88-90].

In this study we show that the electrochemical activity of nitroaromatic compounds on screen printed carbon electrodes can be exploited as a means for enabling CE/MS determinations without the need of adding surfactants to the electrophoresis buffer. The electrochemical reduction mechanism of nitroaromatic compounds is well known and follows a pH-dependent electron-transfer cascade. Nitrobenzene, for example, is first reduced to the phenylhydroxylamine, followed by the formation of aniline, p-aminophenol or azoxybenzene depending on the reaction conditions [91].

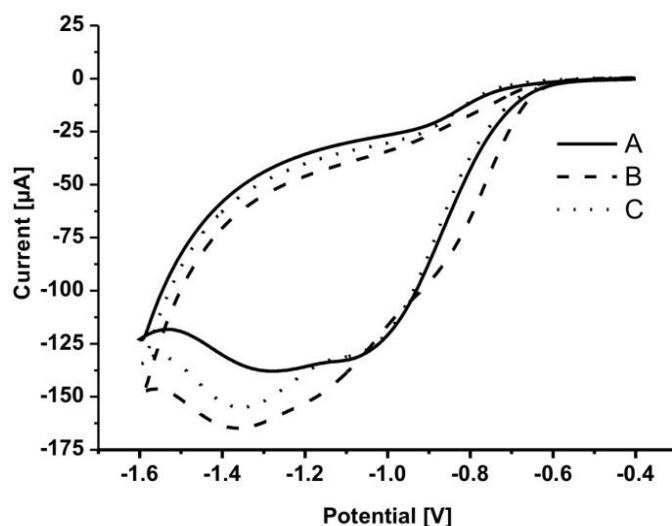


Figure 34: Cyclic voltammograms of  $100 \text{ mg}\cdot\text{L}^{-1}$  of (A) 4-nitrotoluene (4-NB), (B) 2,6-dinitrotoluene (2,6-DNT) and (C) nitrobenzene (NB) in 100 mM acetic acid (pH 2.9) measured with a screen-printed carbon electrode at a scan rate of  $100 \text{ mV}\cdot\text{s}^{-1}$ .

Figure 34 illustrates the CVs for NB, 4-NT and 2,6-DNT using screen-printed carbon electrodes under acidic conditions. Voltammetric techniques are rather limited regarding the selective determination of individual nitroaromatic compounds within complex mixtures. Depending on the electrode potential amines and hydroxylamines are the major reduction products. Both types of compounds are easily protonated and the selectivity of electrophoretic separations can be tuned by varying the pH of the separation buffer. In addition, these electrochemically formed species are much better candidates for an efficient ion formation by the ESI process than the nitroaromatic mother compounds. Applying EAI with a potential of  $-1.6 \text{ V}$  both amines and hydroxylamines are formed and can be separated by CE and detected by ESI-TOF-MS. Figure 35 shows EAI/CE/MS studies of a mixture of the three nitroaromatic model compounds: nitrobenzene (NB), 4-nitrotoluene (4-NT), 2,6-dinitrotoluene (2,6-DNT). Two sets of electropherograms were recorded showing separations of electrochemically formed amines and hydroxylamines. NB was reduced to hydroxylaminobenzene (HAB) and aniline (AN). The monosubstituted 4-NT was reduced to 4-hydroxylaminotoluene (4-HAT) and to 4-aminotoluene (4-AT). The

reduction of the disubstituted 2,6-DNT resulted in major products of 2-amino-6-hydroxylaminotoluene (2-A-6-HAT) and 2,6-diaminotoluene (2,6-DAT).

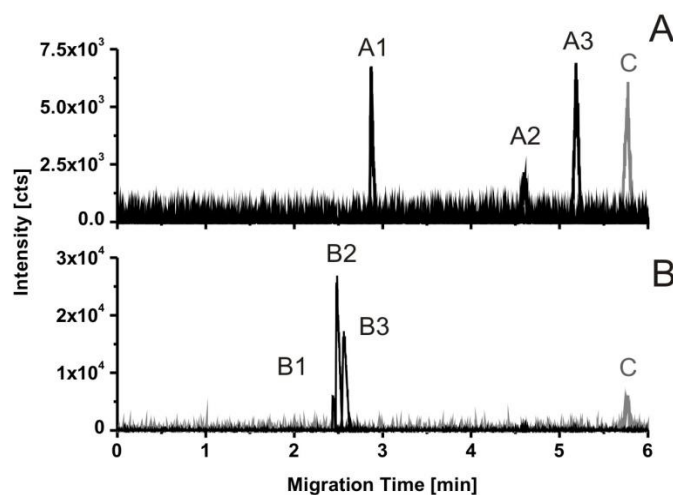


Figure 35: EAI/CE/MS measurements of  $100 \text{ mg}\cdot\text{L}^{-1}$  NB, 4-NT and 2,6-DNT in 100 mM acetic acid (pH 2.9). A: extracted ion electropherograms for hydroxylamine species (A1, 2-A-6-HAT; A2, 4-HAT; A3, HAB); B: extracted ion electropherograms for amine species (B1, AN; B2, 2,6-DAT; B3, 4-AT). The EOF was marked by adding  $10^{-4}$  M caffeine (C). Experimental conditions: EAI parameters, 5 s injection at a potential of -1.6 V; CE separation voltage, 25 kV; ESI-MS, positive mode;  $[\text{M}+\text{H}^+]$  signals for the amines and hydroxylamines with  $m/z$  of 94.07  $m/z$  (AN), 108.09 (4-AT), 123.10 (2,6-DAT), 110.07 (HAB), 124.09 (4-HAT), 139.10 (2-A-6-HAT).

The hydroxylamine species led to clearly separated signals for the three compounds. The amine species have similar migration times under the applied conditions but can still be separated. In addition, determinations based on amine detection are more sensitive than those based on hydroxylamines. The most important parameters for tuning selectivity (and sensitivity) are pH and EAI working electrode potential. The proper choice of both parameters opens the way for very selective determinations of nitroaromatic compounds by means of EAI/CE/MS. The application or hyphenation with alternative detection schemes like UV or electrochemical detection could be a means for further improvements in sensitivity [P2].

#### 5.2.4. Conclusions

A new cell configuration for electrochemically assisted injection (EAI) in combination with capillary electrophoresis (CE) / mass spectrometry (MS) was developed. The use of screen-printed electrodes was found very suitable for a straightforward operation of the EAI/CE/MS system. The analytical performance of the EAI/CE/MS arrangement was characterized using FcMeOH as a model system. Quantitative determinations of the neutral mother compound could be performed via the electro-generated product FcMeOH<sup>+</sup> with considerably enhanced sensitivity and selectivity. In addition, preliminary results could illustrate the potential of EAI/CE/MS for determinations of complex mixtures of nitroaromatic compounds. The application of EAI resulted in the formation of amines and hydroxylamines which are well suitable for CE separations and ESI-MS detection. The EAI/CE/MS approach enables the determination of neutral analytes without the addition of surfactants to the electrophoresis buffer which would deteriorate the performance of electrospray ionization. The EAI working electrode potential is an additional powerful means for selectivity tuning in EAI/CE/MS studies. In case of complex matrices the use of isotope-labeled internal standards would be an ideal means to eliminate problems associated with matrix effects. Even changes in the ratio of several product species could be considered in this way [P2].

### 5.3. EAI/CE/MS using a Fully Automated Injection Device - Mechanistic and Quantitative Studies of the Reduction of 4-Nitrotoluene at Various Carbon-Based Screen-Printed Electrodes

#### 5.3.1. Performance of the Fully Automated EAI Arrangement

As the fully automated EAI cell was especially designed to overcome HV protection requirements resulting from the lab-built CE device, EAI/CE/MS experiments could be realized without any further measures. Initial tests have shown that CE separations with HV potentials up to 30 kV were possible when the EAI cell's HV protection shield was directly connected to the CE/MS grounding. EAI/CE/MS reproducibility tests were carried out using FcMeOH as a model system. The results for 5 repetitive injections are shown in Figure 36.

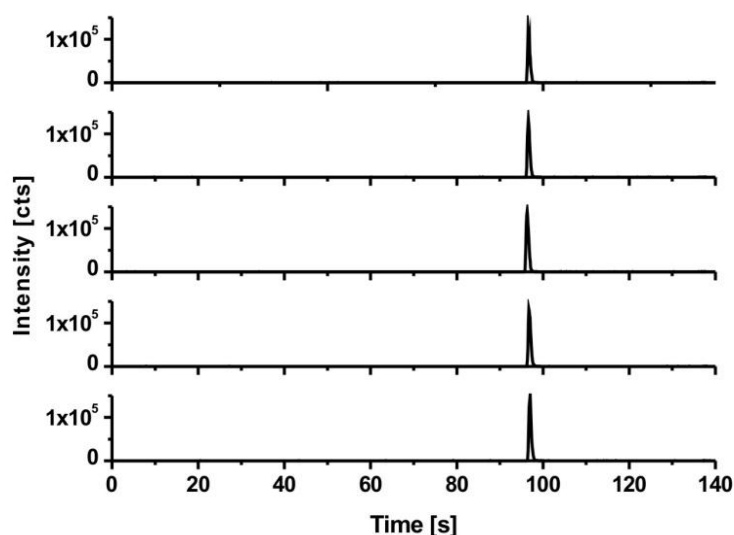


Figure 36: Reproducibility test ( $n=5$ ) for EAI/CE/MS measurements of  $10^{-4}$  M FcMeOH in a 50 mM  $\text{NH}_3/\text{NH}_4\text{OAc}$  solution of pH 9.25. The EAI potential of 400 mV was applied during 10 s EAI. The signals obtained represent the cationic species formed at an uc SPE substrate electrode.

The peak height, peak area and the migration time were evaluated. An RSD ( $n=5$ ) of 5 % was obtained for the peak height. Evaluating the peak area showed an RSD of 9.9 % and a RSD of 0.2 % was calculated for the migration time, respectively.



In further experiments, calibration plots were recorded for a series of dilutions of FcMeOH ranging from 5  $\mu\text{M}$  to 50  $\mu\text{M}$ . The results for three independent measurements are shown in Figure 37.

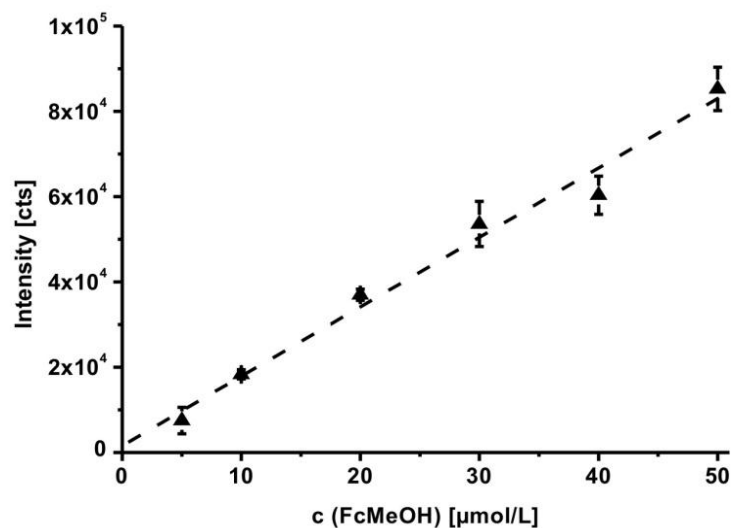


Figure 37: Calibration plot of FcMeOH in 50 mM aqueous  $\text{NH}_3/\text{NH}_4\text{OAc}$  solution of pH 9.25 ( $n=3$ ). Measurements were carried out via EAI/CE/MS using the fully automated EAI cell. Experimental conditions were as specified in Figure 36.

However, a linear calibration plot was obtained offering a linear regression coefficient  $R^2$  of 0.9831. EAI duration of 10 s and an oxidation potential of 400 mV were obtained to give the best results in repeatability tests and for calibration plots. FcMeOH was dissolved in 50 mM aqueous  $\text{NH}_3/\text{NH}_4\text{OAc}$  solution to ensure certain CE buffer conductivity enabling electrophoretic separations. The pH of 9.25 did not influence the redox chemistry of the model analyte but fortunately contributed to a higher EOF.

### 5.3.2. Modification and Characterization of Carbon-Based SPEs

As all previous EAI/CE/MS measurements have been carried out using unmodified carbon (uc) SPEs, the intention was to compare modern carbon-based materials with respect to their influences on the redox behaviour of nitroaromatic compounds. The commercially available SPEs obtained from Dropsens included uc SPEs and CNF SPEs. Additionally, r-GO SPEs were fabricated from uc SPEs. A promising approach was the drop coating procedure described in the experimental part. Figure 10 illustrates the experimental drop coating setup. Drop coating provided a fast, cheap and reproducible possibility for the modification of uc SPEs. Two possible strategies were available to obtain graphene-like structures at the working electrode area.

The first possibility was drop coating with an aqueous graphene oxide solution followed by an electrochemical reduction procedure derived from reference [79]. The procedure included extensive linear sweep cycling from -1.5 V to 1 V and a further potentiostatic reduction at -800 mV. Figure 38 shows the voltammogram recorded during the cycling process. The increasing peak signals indicate the formation of *electrochemically reduced graphene oxide* on the electrode surface.

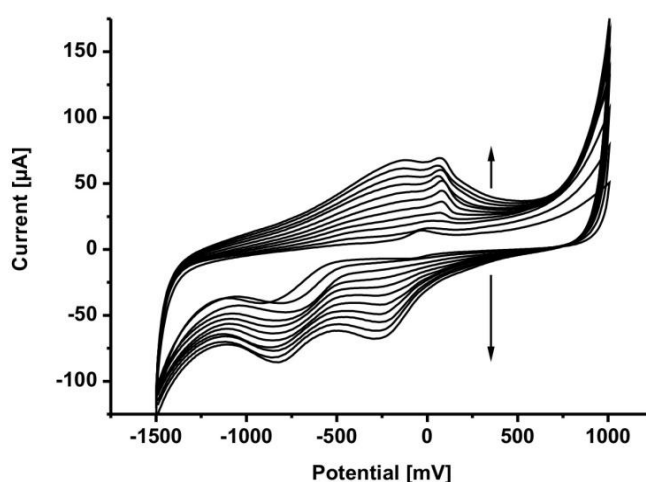


Figure 38: Extended cycling in terms of the electrochemical reduction of graphene oxide drop coated on an uc SPE surface. The electrode was cycled in 100 mM Na<sub>2</sub>SO<sub>4</sub> solution within a potential range from -1.5V to 1 V at a scan rate of 100 mV·s<sup>-1</sup> for 50 times. Every 10<sup>th</sup> cycle is shown in the voltammogram.

When the cycling process was finished, a fixed potential of -800 mV was applied to achieve an almost complete reduction of graphene oxide. In Figure 39, the progress of the electrochemical graphene formation is expressed by cyclic voltammograms of FcMeOH recorded after each process step. Cyclic voltammetry carried out directly after drop coating an uc SPE with graphene oxide (grey line) showed a slight shift to negative potentials compared to uc SPEs. The reductive cycling procedure resulted in a peak potential shift of 50 mV in positive direction indicating that a graphene-like structure is formed at the electrode surface (dashed line). Finally, fixed-potential reduction at -800 mV led to an almost complete electrochemical reduction of graphene oxide, expressed as cyclic voltammogram of little less peak currents (solid line). Additionally, the final reduction product caused some capacitive charging currents expressed in a certain hysteresis.

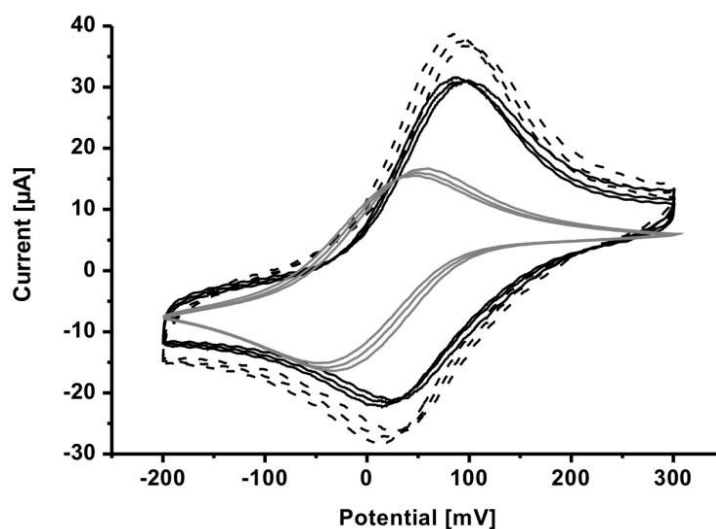


Figure 39: Process monitoring of the electrochemical graphene formation using cyclic voltammetry of 1 mM FcMeOH and 100 KNO<sub>3</sub> in water. The scan rate was 50 mV·s<sup>-1</sup>. (Grey) directly after the drop coating procedure, (dashed) after reductive cycling as described in Figure 40 and (solid) after final amperometric reduction at -800 mV for 30 min.

The second way to obtain graphene-like structures at the electrode surface was drop coating using *chemically reduced graphene oxide* (r-GO). This approach was less time-consuming, led to comparable results and, due to a full availability of r-GO solution, became the preferred modification method. For all further measurements the r-GO SPEs were fabricated in this way.

The drop coated SPEs were first characterized using optical microscopy with 200-fold and 500-fold magnification. The images in Figure 40 illustrate the surface morphology of the SPEs used for EAI/CE/MS experiments with nitroaromatic compounds.

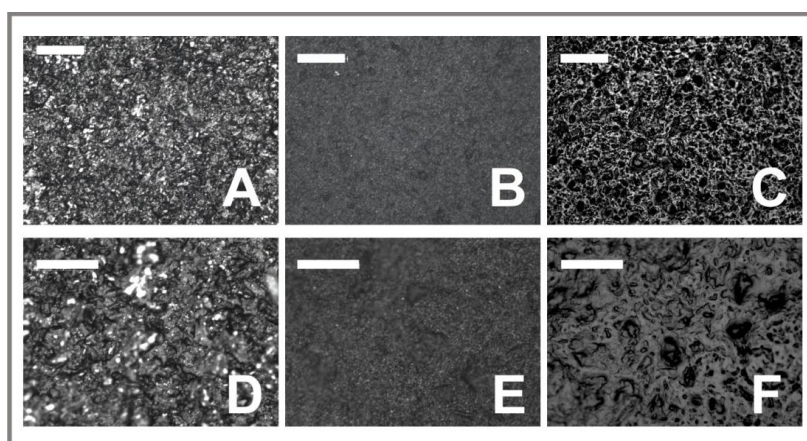


Figure 40: Microscopic surface images of uc SPE (A, D), CNF SPE (B, E) and r-GO SPE (C, F). The magnification was 200-fold (A, B, C) and 500-fold (D, E, F) and the scale bars represent 100  $\mu\text{m}$  (A, B, C) and 50  $\mu\text{m}$  (D, E, F), respectively.

The uc SPEs (A, D) exhibit a rather rough surface whereas CNF SPEs (B, E) show a very fine-structured homogeneous surface. The r-GO drop coating modification of uc SPEs resulted in a rough but more tube-like structure, full of cavities across the surface (C, F). Actually, the r-GO layer is deposited onto the rough surface morphology of the uc SPEs preventing the formation of a homogeneous thin film of r-GO [P3].

Electrochemical characterization was carried out using FcMeOH as model system. Cyclic voltammetry (CV) and square-wave voltammetry (SWV) were the preferred electrochemical methods.

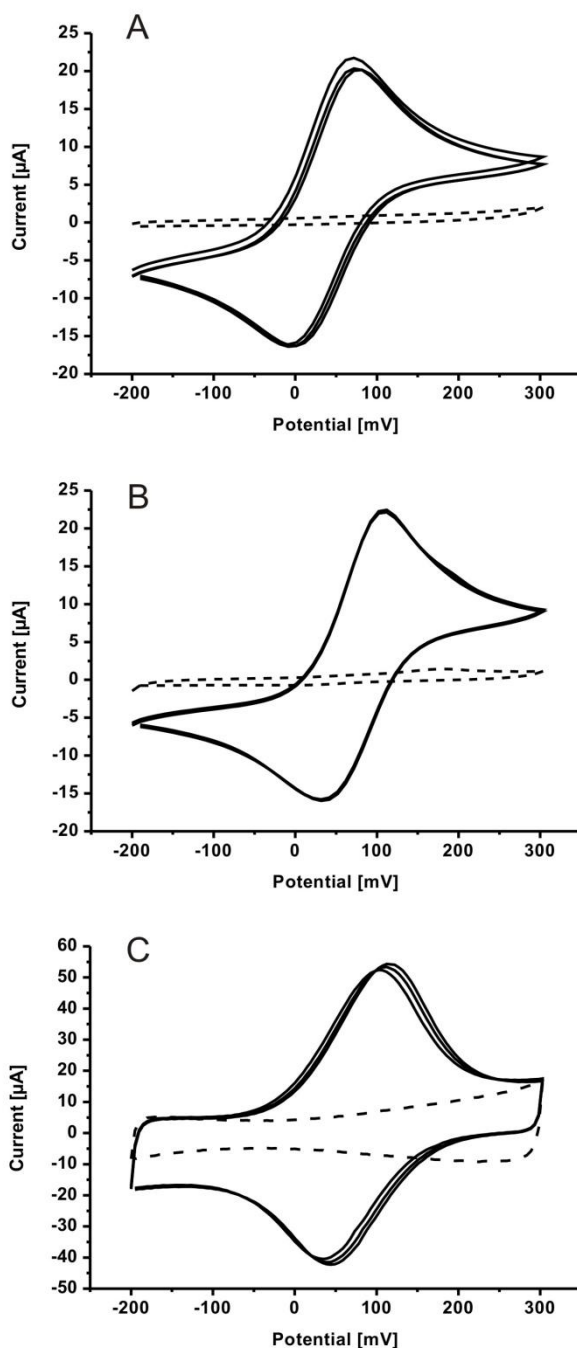


Figure 41: Comparison of commercially available Dropsens SPEs: (A) uc SPE, (B) CNF SPE and (C) r-GO SPE. Cyclic voltammograms were recorded in an aqueous solution of 1 mM FcMeOH and 100 mM  $\text{KNO}_3$ . The scan rate was  $100 \text{ mV}\cdot\text{s}^{-1}$  and the potentials measured referred to an Ag pseudo-reference electrode. Dashed lines represented the buffer solution.

The cyclic voltammograms in Figure 41 compare the electrochemical redox behaviour of FcMeOH on uc SPEs, CNF SPEs and r-GO SPEs. All cyclic voltammograms showed well-expressed oxidation and reduction peaks. In the case of CNF SPEs (B) and r-GO SPEs (C) the peak potentials showed a slight shift of 50 mV towards positive direction. The peak currents measured with the r-GO SPEs (C) were twice as high as in the case of (A) and (B). Moreover, the r-GO electrode (C) showed certain capacitive effects which are expressed as hysteresis and are proposed to be due to thin-layer formation during the drop coating process. The r-GO SPEs were from great interest because of their higher electrochemical activity resulting in significant higher current responses.

Square-wave voltammograms were recorded from a 0.1 mM FcMeOH solution containing 100 mM KNO<sub>3</sub> as a background electrolyte. The square-wave voltammograms are shown in Figure 42. As expected from a fully reversible one-electron transfer model system, sharp and symmetrical oxidation peaks were obtained using uc SPEs (A) and CNF SPEs (B) for SWV. The peak current measured in the case of (B) was twice as high as for uc SPEs and was slightly shifted to more positive potentials. In the case of r-GO SPEs (C) the peak oxidation potential is shifted to 100 mV, confirming the presence of graphene-like structures. Moreover, the oxidation peak in (C) is dramatically superimposed by a very high background signal resulting in a peak maximum almost one magnitude of order higher than in the case of (A) and (B). This is also proposed to be due to capacitive effects caused by formed r-GO surface structures.

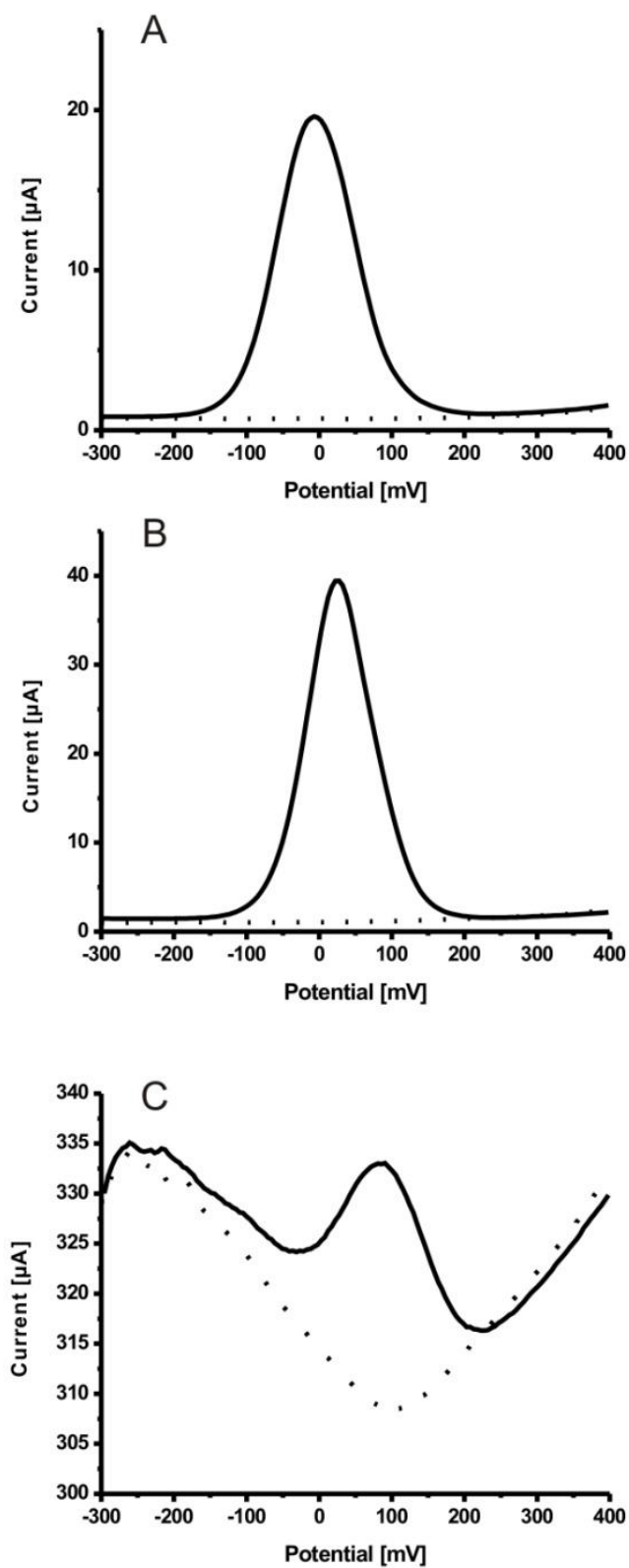


Figure 42: Square-wave voltammetry of 0.1 mM FcMeOH and 100 mM KNO<sub>3</sub> using (A) uc SPE, (B) CNF SPE and (C) r-GO SPE. Amplitude: 50 mV; step potential: 5 mV; frequency: 50 Hz.

The dashed lines represent the buffer solution.

### 5.3.3. Voltammetric Studies of 4-NT using Different SPE Materials

Cyclic voltammograms of 4-NT were recorded using the three types of SPEs. Figure 43 on the next page shows the results for repetitive recordings of CVs. In all cases a considerable decrease in voltammetric signals is observed for successive CV scans. This indicates some progressive deactivation due to the adsorption of reaction products at the electrode surface [92, 93]. In case of r-GO SPEs the reduction starts at less negative potentials compared to uc SPEs and CNF SPEs. In case of r-GO SPEs the negative potential limit was -1.4 V because more negative potentials resulted in a lift-off of the r-GO layer due to hydrogen evolution. In addition, the very large active surface area of the r-GO SPE is reflected by rather high capacitive currents in cyclic voltammogram C [P3].



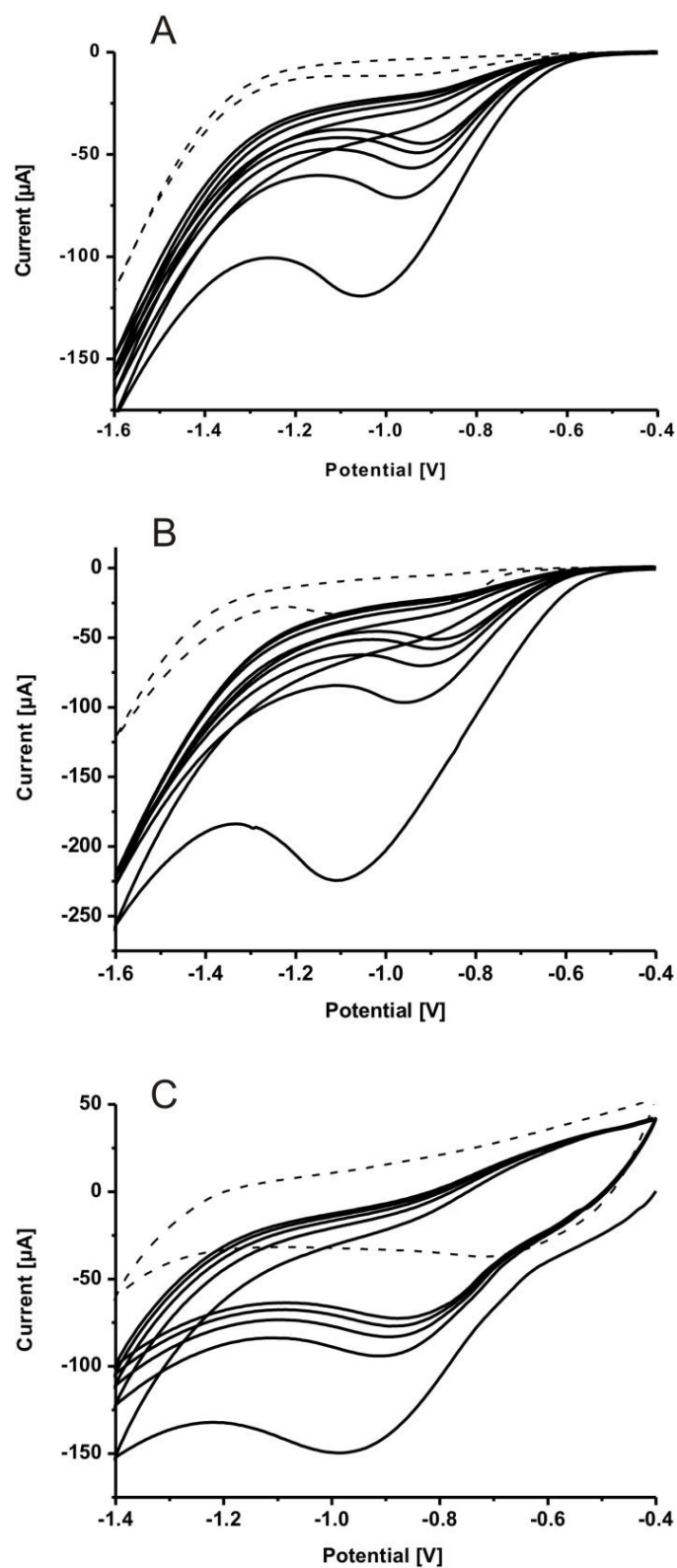
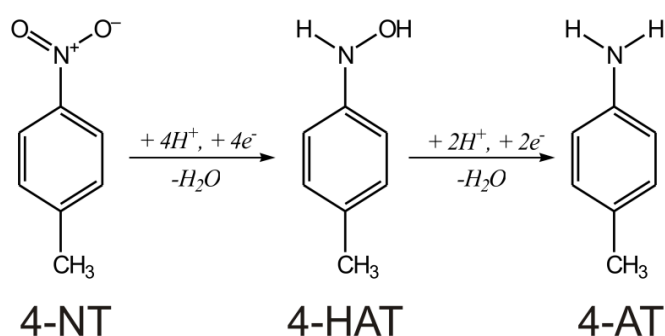


Figure 43: Cyclic voltammograms of 2 mM of 4-NT in 100 mM HOAc at (A) uc SPE, (B) CNF SPE and (C) r-GO SPE. Five consecutive scans were recorded at a scan rate of  $100 \text{ mV}\cdot\text{s}^{-1}$ . The dashed line corresponds to the blank buffer solution.

### 5.3.4. Mass Voltammetry of 4-NT by Means of EAI/CE/MS

It is obvious that CV does not provide clear information regarding the product composition formed during the voltammetric measurement. EAI/CE/MS was applied to generate mass voltammograms describing the intensities of individual mass traces of formed products as a function of electrode potential. It was of interest to investigate if the three different carbon-based SPEs would lead to different product compositions for the reduction of 4-NT. Scheme 1 illustrates the reaction mechanism under acidic conditions as applied in this study (pH 2.9).



Reaction Scheme 1: Consecutive reduction steps of 4-NT forming 4-hydroxylaminotoluene (4-HAT) and 4-aminotoluene (4-AT)

As shown in Reaction Scheme 1, the main reaction products of 4-NT were 4-HAT and 4-AT. Over a rather wide potential range both substances were registered by means of EAI/CE/MS. In the acidic medium used both species, 4-HAT and 4-AT, are protonated allowing their CE separation. In addition, the charged compounds showed much higher sensitivity in ESI-TOF-MS than the neutral 4-NT. For the construction of mass voltammograms the mass traces of 124.08 m/z ( $\pm 0.02$  m/z, 4-HAT) and of 108.09 m/z ( $\pm 0.02$  m/z, 4-AT) were extracted from the total ion electropherogram. An automatic peak integration procedure was applied to determine the peak height of the respective MS signal. Due to different ESI efficiencies of 4-AT and 4-HAT, the absolute MS intensities cannot be used to calculate the ratio of concentrations of both species. Therefore, the intensities were expressed as relative intensities with respect to the highest signal measured. The mass voltammograms were constructed according to a stepwise change of

the electrode potential and EAI/CE/MS determinations of 4-HAT and 4-AT. Each mass voltammogram in Figure 44 shows the mean relative MS intensities calculated from five independent series of measurements.

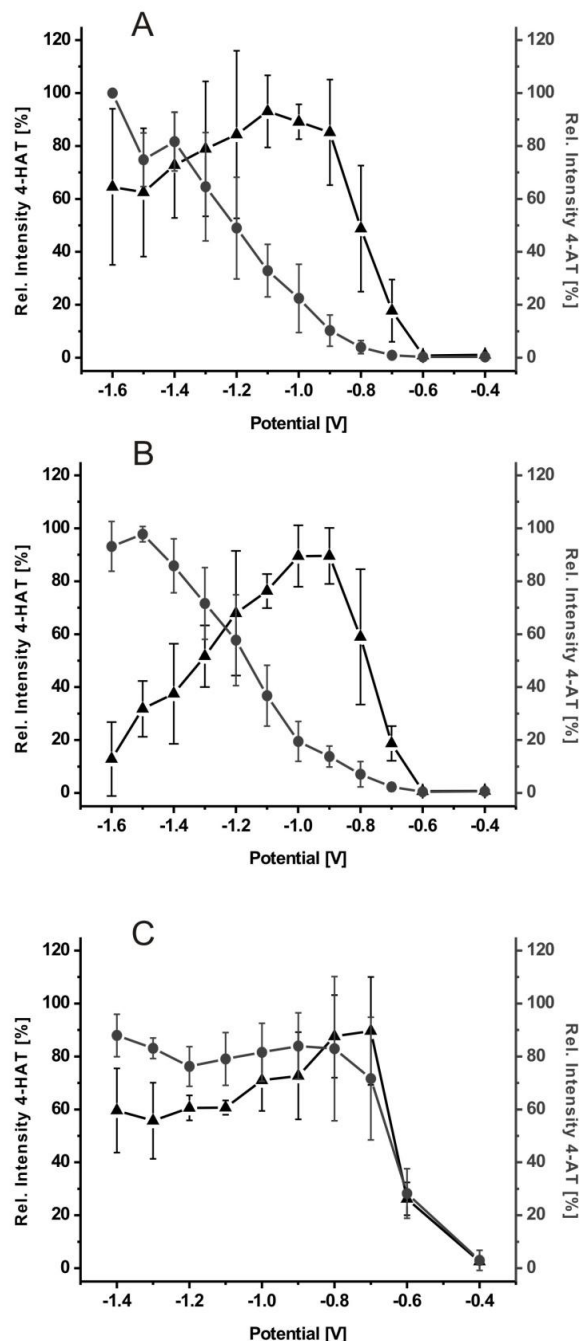


Figure 44: Mass voltammograms for 4-NT reduction at different SPEs based on EAI/CE/MS measurements. (A) uc SPE, (B) CNF SPE and (C) r-GO SPE. Normalized MS intensities of 4-AT (108.09 m/z, grey) and 4-HAT (124.08 m/z, black) are shown in dependence of the EAI potential. The error bars represent the standard deviations of five independent series of measurements.

The voltammetric behaviour and relative product distribution was quite similar for uc SPEs and CNF SPEs. The formation of 4-HAT started at potentials more negative than -0.6 V and approached the maximum concentration at about -1.0 V. At more negative potentials the 4-HAT concentration decreased at both types of electrodes. However, the decrease in 4-HAT concentrations at very negative potentials (less than -1 V) was more pronounced at CNF SPEs than at uc SPEs. The formation of 4-AT followed a similar trend at uc SPEs and CNF SPEs starting at potentials of about -0.7 V and increasing continuously with decreasing potential settings. In contrast to the uc and CNF SEs the situation at r-GO SPEs was clearly different. Both reduction products (4-HAT and 4-AT) were already formed at potentials of about -0.4 V and both concentrations approached a maximum concentration between -0.7 V and -0.8 V. For more negative potentials the 4-HAT concentration tended slightly to decrease whereas the 4-AT concentration remained nearly constant. It can be concluded that the r-GO SPE exhibits a clearly different electrocatalytic behaviour compared to uc and CNF SPEs. It was not possible to investigate potentials lower than -1.4 V using r-GO SPEs because the r-GO layer tended to peel off due to hydrogen evolution [P3].

#### 5.3.5. Quantitative Determination of 4-NT using 4-NT-d<sub>4</sub> as an Isotope-Labeled Internal Standard

Quantitative determinations of nitroaromatic compounds in complex matrices by voltammetry or EAI/CE/MS are associated with the problem of changing response characteristics of solid electrodes usually expressed as progressive electrode fouling. An approach for the reliable determination of 4-NT by EAI/CE/MS was developed using isotopically labeled 4-NT-d<sub>4</sub> as an internal standard. The accuracy of this method was verified by studying standard solutions covering the concentration range between 0.2 mmol·L<sup>-1</sup> and 0.6 mmol·L<sup>-1</sup>. All measuring solutions were spiked with 0.4 mmol·L<sup>-1</sup> 4-NT-d<sub>4</sub>. The ratios of the MS intensities for 4-NT (108.1 m/z) and 4-NT-d<sub>4</sub> (124.1 m/z) signals enabled the calculation of the concentrations of 4-NT (concentrations found). Table 2 shows that recoveries close to 100% were obtained.

Figure 45 illustrates the corresponding linear calibration plot offering an  $R^2$  of 0.9966. The results obtained were independent of the response characteristics of the SPEs, even in the case of massive electrode fouling accurate determinations of 4-NT could be realized in this way.

<b>Internal Calibration of 4-NT Standard Solutions with 0.4 mM 4-NT-d<sub>4</sub></b>			
<b>c<sub>added</sub> [mmol·L<sup>-1</sup>]</b>	<b>c<sub>found</sub> [mmol·L<sup>-1</sup>]</b>	<b>SD [mmol·L<sup>-1</sup>], n=5</b>	<b>Recovery [%]</b>
0.20	0.21	0.03	104.8
0.30	0.30	0.04	99.6
0.40	0.38	0.03	96.2
0.50	0.49	0.04	97.9
0.60	0.62	0.03	102.7

Table 2: Recoveries obtained for the determination of 4-NT by using 4-NT-d<sub>4</sub> as internal standard.

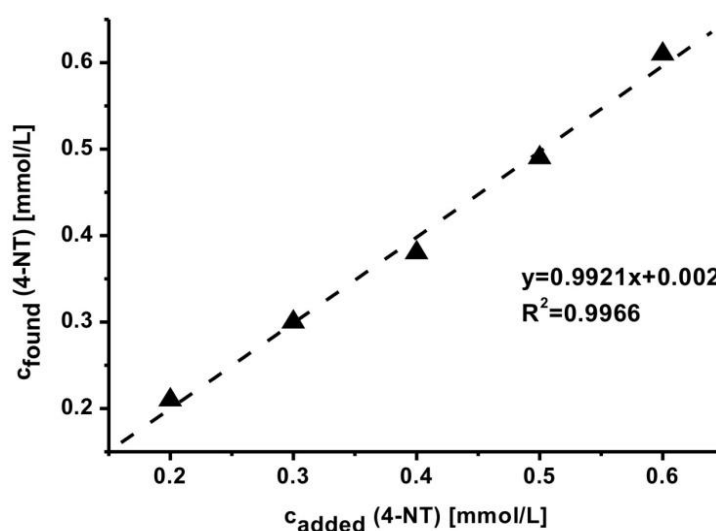


Figure 45: Calibration plot for the determination of 4-NT by using 4-NT-d<sub>4</sub> as internal standard.

Finally, the concept for quantitative determinations of 4-NT by EAI/CE/MS was applied to rather complex real sample matrices. Soil and corresponding water samples represent quite typical matrices for analytical determinations of nitroaromatic explosives [87]. Soil and tap water samples were spiked with well defined amounts of 4-NT and 4-NT-d<sub>4</sub> resulting in the lower ppm (m/m) and  $\mu\text{mol}\cdot\text{L}^{-1}$  range, respectively. An extraction and sample pretreatment protocol including solid phase extraction is specified in the experimental part. EAI/CE/MS was carried out to determine the recoveries for more complex sample matrices. Table 3 lists the recoveries obtained for two independent soil samples and one tap water sample. A crucial point in the sample pretreatment is the homogenization of solid samples and solid phase extraction using commercial available cartridges. Some limitation in this respect could be a source of error [P3].

<b>Simulated Soil Samples spiked with 4-NT</b>			
$\beta_{\text{added}}$ [ $\text{mg}\cdot\text{kg}^{-1}$ ]	$\beta_{\text{found}}$ [ $\text{mg}\cdot\text{kg}^{-1}$ ]	SD [ $\text{mg}\cdot\text{kg}^{-1}$ ], n=6	Recovery [%]
8.71	8.08	0.69	92.8
2.12	2.03	0.24	95.8

<b>Simulated Tap Water Samples spiked with 4-NT</b>			
$c_{\text{added}}$ [ $\mu\text{mol}\cdot\text{L}^{-1}$ ]	$c_{\text{found}}$ [ $\mu\text{mol}\cdot\text{L}^{-1}$ ]	SD [ $\mu\text{mol}\cdot\text{L}^{-1}$ ], n=6	Recovery [%]
50	51	3	102

Table 3: Determination of 4-NT in spiked real samples by EAI/CE/MS using 4-NT-d<sub>4</sub> as internal standard.

### 5.3.6. Conclusions

In chapter 5.3 it was demonstrated that EAI/CE/MS can add valuable information for the study of voltammetric reactions. The construction of mass voltammograms for the reduction of 4-NT enabled the detailed characterization of the product composition. The change in 4-HAT and 4-AT concentrations was determined in dependence on electrode potential and electrode material. It was found that r-GO SPEs led to clearly different product compositions than uc SPE and CNF SPE. The aspect of quantitative determinations of 4-NT was studied using isotope-labeled 4-NT. This approach can overcome the old problem of changing response characteristics at solid electrodes based on the fact that the target analyte and its isotope-labeled form show the same voltammetric behaviour. It could be demonstrated that even in complex matrices like soil or tap water reliable determinations of 4-NT can be performed based on the use of isotope-labeled standards [P3].

## 6. References

- [1] Matysik FM (2003) *Electrochemistry Communications* 5:1021-1024
- [2] Scholz R, Matysik FM (2011) *Analyst* 136:1562-1565
- [3] Terabe S, Otsuka K, Ischikawa K, Tsuchija A, Ando T (1984) *Analytical Chemistry* 56:111
- [4] Kuban P, Hauser PC (2004) *Electroanalysis* 16(24):2009-2021
- [5] <http://www.chem.agilent.com/en-US/promotions/Pages/infinity-cems.aspx>  
[02/2013]
- [6] Ho CS, Lam CWK, Chan MHM, Cheung RCK, Law LK, Lit LCW, Ng KF, Suen MWM, Tai HL (2003) *The Clinical Biochemist Reviews* 24 (1):3-12
- [7] Zuman P (2001) *Critical Reviews in Analytical Chemistry* 31 (4):281-289
- [8] Bard AJ, Stratmann M (2003) in *Encyclopedia of Electrochemistry Vol 3: Instrumentation and Electroanalytical Chemistry*, Wiley-VCH, Weinheim
- [9] Bard AJ (1989) in *Electroanalytical Chemistry - Vol 15: Voltammetry at Ultramicroelectrodes*, Marcel Dekker Inc, New York, NY
- [10] Bard AJ, Denuault G, Lee Ch, Mandler D, Wipf DO (1990) *Accounts of Chemical Research* 23:357-363
- [11] Bard AJ, Faulkner LR (2001) in *Electrochemical Methods: Fundamentals and Applications (2<sup>nd</sup> Ed)*, John Wiley & Sons Inc, New York, NY
- [12] Kellner R, Mermet JM, Otto M, Valcarcel M, Widmer HM (2004) *Analytical Chemistry*, Wiley-VCH, Weinheim, D



- [13] Wang J (2006) in *Analytical Electrochemistry*, Wiley VCH, Hoboken, NJ
- [14] Zoski CG (2007) in *Handbook of Electrochemistry* (1<sup>st</sup> Ed), Elsevier, Oxford, UK
- [15] Newman JD, Turner APF (1992) *Analytica Chimica Acta* 262:13-17
- [16] Dominguez Renedo O, Alonso-Lomillo MA, Arcos Martinez MJ (2007) *Talanta* 73:202-219
- [17] Huang XJ, O'Mahony AM, Compton RG (2009) *small* 5(7):776-788
- [18] Tieman RS, Igo DH, Heineman WR (1991) *Sensors and Actuators B* 5:121-127
- [19] Metters JP, Kadara RO, Banks CE (2011) *Analyst* 136:1067-1076
- [20] Metters JP, Tan F, Kadara RO, Banks CE (2012) *Analytical Methods* 4:1272-1277
- [21] Wang J, Tian B, Nascimento VB, Angnes L (1998) *Electrochimica Acta* 43(23):3459-3465
- [22] Metters JP, Kadara RO, Banks CE (2012) *Analyst* 137:896-902
- [23] Zhang L, Li Y, Zhang L, Li DW, Karpuzov D, Long YT (2011) *International Journal of Electrochemical Science* 6:819-829
- [24] Erdem A, Karadeniz H, Canavar PE, Congur G (2012) *Electroanalysis* 24 (3):502-511
- [25] Kraft A (2007) *International Journal of Electrochemical Science* 2:355-385
- [26] Villalba MM, Davis J (2008) *Journal of Solid State Electrochemistry* 12:1245-1254
- [27] Alonso-Lomillo MA, Dominguez Renedo O, Arcos Martinez MJ (2010) *Talanta* 82:1629-1636
- [28] Honeychurch KC, Hawkins DM, Hart JP, Cowell DC (2000) *Electroanalysis* 12 (3):171-177

- [29] Du D, Zou Z, Shin Y, Wang J, Wu H, Engelhard MH, Liu J, Aksay IA, Lin Y (2010) Analytical Chemistry 82:2989-2995
- [30] Cammann K (2001) in Instrumentelle analytische Chemie: Verfahren, Anwendungen und Qualitätssicherung, Spektrum Akademischer Verlag, Berlin, D
- [31] Schwedt G (2008) in Analytische Chemie - Grundlagen, Methoden und Praxis (2<sup>nd</sup> Ed), Wiley-VCH, Weinheim, D
- [32] Serwer P, Wright ET (2012) Electrophoresis 33 (2):352-365
- [33] Zürbig P, Jahn H (2012) Electrophoresis 33(24):3617-3630
- [34] Marengo E, Robotti E, Bobba M, Milli A, Campostrini N, Righetti SC, Cecconi D, Righetti PG (2008) Analytical and Bioanalytical Chemistry 390:1327-1342
- [35] Valko IE, Siren H, Riekkola M-L (1999) Journal of Microcolumn Separations 11 (3):199-208
- [36] Riekkola M-L, Jussila M, Porras SP, Valko IE (2000) Journal of Chromatography A 892:155-170
- [37] Suntornsuk L (2010) Analytical and Bioanalytical Chemistry 398:29-52
- [38] Rovio S, Siren K, Siren H (2011) Food Chemistry 124 (3):1194-1200
- [39] Garcia-Ruiz C, Marina ML (2006) Electrophoresis 27 (1):266-282
- [40] Mühlberger H, Hwang W, Guber AE, Saile V, Hoffmann W (2008) IEEE Sensors Journal 8 (5):572-579
- [41] Mark JJP, Kumar A, Demattio H, Hoffmann W, Malik A (2011) Electroanalysis 23 (1):161-168
- [42] Thomson SJJ (1912) Philosophical Magazine Series 6, 23 (136):449-457

- [43] Watson JT, Sparkman OD (2007) in Introduction to Mass Spectrometry (4<sup>th</sup> Ed), John Wiley & Sons Ltd, West Sussex, UK
- [44] McLafferty FW (1997) Journal of the American Society for Mass Spectrometry 8 (1):1-7
- [45] Guilhaus M (1995) Journal of Mass Spectrometry 30:1519-1532
- [46] Wollnik H (1993) Mass Spectrometry Reviews 12:89-114
- [47] Mamyrin BA (2001) International Journal of Mass Spectrometry 206 (3):251-266
- [48] Smith DPH (1986) IEEE Transactions on Industry Applications IA-22 (3):527-535
- [49] Kebarle P (2000) Journal of Mass Spectrometry 35:804-817
- [50] User Manual, micrOTOF Mass Spectrometer, Bruker Daltronics (2006)
- [51] Smith RD, Loo JA, Edmonds CG, Barinaga CJ, Udseth HR (1990) Analytical Chemistry 62:882-899
- [52] Ayed A, Krutchinsky AN, Ens W, Standing KG, Duckworth HW (1998) Rapid Communications in Mass Spectrometry 12 (7):339-344
- [53] Ferrer I, Thurman EM, Fernandez-Alba AR (2005) Analytical Chemistry 77:2818-2825
- [54] Garcia-Villalba R, Carrasco-Pancorbo A, Oliveras-Ferraros C, Vazquez-Martin A, Menendez JA, Segura-Carretero A, Fernandez-Gutierrez A (2010) Journal of Pharmaceutical and Biomedical Analysis 51:416-429
- [55] Hamler RL, Zhu K, Buchanan NS, Kreunin P, Kachman MT, Miller FR, Lubman DM (2004) Proteomics 4:562:577

- [56] Smith RD, Olivares JA, Nguyen NT, Udseth HR (1988) *Analytical Chemistry* 60:436-441
- [57] Smith RD, Barinafa CJ, Udseth HR (1988) *Analytical Chemistry* 60:1948-1952
- [58] Bonvin G, Schappler J, Rudaz S (2012) *Journal of Chromatography A* 1267:17-31
- [59] <http://www.chem.agilent.com/en-US/Products-Services/Instruments-Systems/Automated-Electrophoresis/CE-MS-System/pages/ce-ms-ordering.aspx>  
[02/2013]
- [60] Reiter SM, Buchberger W, Klampfl CW (2010) *Chromatographia* 71:715-719
- [61] Ramautar R, Somsen GW, De Jong GJ (2013) *Electrophoresis* 34:86-98
- [62] Elhamili A, Bergquist J (2011) *Electrophoresis* 32:1778-1785
- [63] Gottardo R, Miksik I, Aturki Z, Sorio D, Seri C, Fanali S, Tagliori F (2012) *Electrophoresis* 33:599-606
- [64] Chen ML, Huang YQ, Liu JQ, Yuan BF, Feng YQ (2011) *Journal of Chromatography B* 879:938-944
- [65] Kuehnbaum NL, Britz-McKibbin P (2011) *Analytical Chemistry* 83:8063-8068
- [66] Mark JJP, Scholz R, Matysik FM (2012) *Journal of Chromatography A* 1267:45-64
- [67] Faber H, Melles D, Brauckmann C, Wehe CA, Wentker K, Karst U (2012) *Analytical and Bioanalytical Chemistry* 403:345-354
- [68] Tang W (2003) *Current Drug Metabolism* 4:319-329
- [69] Shen S, Marchick MR, Davis MR, Doss GA, Pohl LR (1999) *Chemical Research in Toxicology* 12:214-222

- [70] Baumann A, Lohmann W, Rose T, Ahn KC, Hammock BD, Karst U, Schebb NH (2010) *Drug Metabolism and Disposition* 38 (12):2130-2138
- [71] Jahn S, Baumann A, Roscher J, Hense K, Zazzeroni R, Karst U (2011) *Journal of Chromatography A* 1218:9210-9220
- [72] Silva Lopes F, Antunes Junior O, Gutz IGR (2010) *Electrochemistry Communications* 12:1387-1390
- [73] Silva Lopes F, Gomes Coelho LH, Gutz IGR (2011) *Electrophoresis* 32:939-946
- [74] Silva Lopes F, Nogueira T, do Lago CL, Gutz IGR (2011) *Electroanalysis* 23:2516-2519
- [75] Environmental Protection Agency EPA  
<http://www.epa.gov/OSW/hazard/testmethods/sw846/pdfs/8330a.pdf> [06/2012]
- [76] Hummers WS, Offeman RE (1958) *Journal of the American Chemical Society* 80(6):1339
- [77] Becerril HA, Mao J, Liu Z, Stoltenberg RM, Bao Z, Chen Y (2008) *ACS Nano* 2(3):463-470
- [78] Li D, Muller MB, Gilje S, Kaner RB, Wallace GG (2008) *Nature Nanotechnology* 3(2):101-105.
- [79] Shao Y, Wang J, Engelhard M, Wang Ch, Lin Y (2010) *Journal of Materials Chemistry* 20:743-748
- [80] Environmental Protection Agency EPA  
<http://www.epa.gov/osw/hazard/testmethods/sw846/pdfs/8330a.pdf> [06/2012]

- [81] Environmental Protection Agency EPA  
<http://www.epa.gov/osw/hazard/testmethods/sw846/pdfs/3535a.pdf> [06/2012]
- [82] <http://www.wonatech.com/ckseo/DropSens/DS.pdf> [12/2012]
- [83] [http://www.metrohm.de/Produkte/Downloads/Autolab\\_Brochure\\_2012.pdf](http://www.metrohm.de/Produkte/Downloads/Autolab_Brochure_2012.pdf)  
[12/2012]
- [84] <http://www.ijcambria.com/secm.htm> [11/2012]
- [85] <http://www.speciation.net/Database/Instruments/Bruker-Daltonics/micrOTOF--benchtop-ESITOF-MS-;i1504> [11/2012]
- [86] Matysik FM, Schumann U, Engewald W (2008) *Electroanalysis* 20:98-101
- [87] Environmental Protection Agency EPA  
<http://www.epa.gov/osw/hazard/testmethods/sw846/pdfs/4050.pdf> [02/2013]
- [88] Wang J, Chen G, Chatrathi MP, Fujishima A, Tryk DA, Shin D (2003) *Analytical Chemistry* 75:935-939
- [89] Pumera M (2006) *Electrophoresis* 27:244-256
- [90] Wang J (2007) *Electroanalysis* 19:415-423
- [91] Marquez J, Pletcher D (1980) *Journal of Applied Electrochemistry* 10:567-573
- [92] Allredge ES, Badescu SC, Bajwa N, Perkins FK, Snow ES, Reinecke TL (2010)  
*Physical Reviews B* 82:125418
- [93] Rochefort A, Wuest JD (2009) *Langmuir* 25:210-215

## 7. Summary

### 7.1. Summary in English

Electrochemically assisted injection (EAI) is a hydrodynamic injection concept applied for CE/MS that enables an electrochemical analyte conversion at a substrate electrode during the injection process. The electrochemical formation of charged species from neutral ones enables an electrophoretic separation in aqueous and non-aqueous media. In some cases, a significant enhancement of electrospray ionization efficiency in mass spectrometry can be achieved.

The first part of the present thesis covers the development and characterization of novel automated injection arrangements for EAI/CE/MS. The stepwise development started with the fabrication of amperometric capillary probes to investigate the dependency of the capillary-to-substrate electrode distance on the injection efficiency. An electrochemical characterization of the capillary probes was carried out with the help of hydrodynamic voltammetry. Probe approach curves were recorded using a scanning electrochemical microscope for the vertical alignment of capillary-based probes over a substrate electrode. The SECM allowed a vertical fine-positioning with a resolution in the micrometer range. In this context the SECM bipotentiostat was exploited for amperometric detection. Probe approach curves turned out that the current response remained nearly constant for distances between 5  $\mu\text{m}$  and 60  $\mu\text{m}$  and decreased significantly for larger distances.

In a further development step a semiautomated injection cell was constructed considering the required accuracy in capillary positioning. A fast and precise piezo motor was chosen for vertical capillary movement over a substrate electrode. Commercially available screen-printed electrodes served as substrate electrodes. A CE buffer reservoir was incorporated next to the substrate electrode holding compartment. The change between injection mode and separation mode was carried out manually by moving the arrangement to the relevant position. The device was hyphenated to a home-built CE/MS system and characterized regarding precision and reproducibility using ferrocene methanol as a model system.

Based on the EAI/CE/MS results obtained with the semiautomated cell, a fully automated EAI cell was developed to enhance the precision of the whole EAI injection process. In contrast to the semiautomated cell, the latest version enabled a fully automated, microprocessor-controlled injection. Two servo motors were responsible for the vertical capillary alignment and the automated change between injection and separation mode. The motion sequence of the servo motors was programmed and triggered either by computer software or a handheld controller unit. The injection cell was characterized in the same way as the semiautomated cell. The fully automated cell was applied for all further EAI/CE/MS experiments.

In the second part of the present thesis, the investigation of screen-printed electrodes in the context of EAI/CE/MS studies of nitroaromatic compounds is described. Screen-printed electrodes consist of a concentric arrangement of three electrodes on a suitable glass or ceramic substrate. They are easy to prepare and modify and a wide range of electrode materials is commercially available. Additionally, sample volumes in the microliter range are sufficient to cover the electrode structures. In the present studies it is focused on carbon-based SPEs. The materials of choice were carbon, carbon nanofibers and reduced graphene oxide. A protocol for the drop coating modification of uc SPEs using reduced graphene oxide was developed. The electrode materials were compared as they were used for mass voltammetric EAI/CE/MS studies of the electrochemical reduction of 4-nitrotoluene under acidic conditions. It was demonstrated that the reduction products 4-hydroxyl-aminotoluene and 4-aminotoluene, are formed at rather negative potentials at reduced graphene oxide electrodes, compared to carbon and carbon nanofiber electrodes. Moreover, the relative abundance of both species formed varied for different electrode materials.

In further experiments, isotopically labeled 4-nitrotoluene- $d_4$  served as an internal standard to investigate the electrodes' liability regarding electrode fouling, a well-known problem when working with solid state electrodes. Both mass voltammetry and cyclic voltammetry turned out that neither 4-nitrotoluene nor its reduction products tended to adsorb at the electrode surface.



Finally, 4-Nitrotoluene-d<sub>4</sub> was exploited as an internal standard for the quantification of 4-Nitrotoluene in soil and drinking water samples. A liquid-solid extraction protocol was developed for soil samples. In the case of drinking water samples, a solid-phase extraction protocol using a C-18 stationary phase was developed. The samples were spiked with a defined amount of 4-nitrotoluene and the internal standard was added. The ratio of the peak intensities recorded in the mass traces of the reduced amine species allowed for the calculation of method recovery values.

In conclusion EAI/CE/MS is a powerful technique that combines the high sensitivity and selectivity of mass spectrometry with capillary electrophoresis. The key point of this work is the electrochemically assisted injection prior to CE/MS measurements. EAI allows CE/MS measurements of commonly inapplicable analytes due to an electrochemical conversion during the injection process. EAI enables the separation of neutral analytes by an electrochemical generation of charged species and, additionally, enhances the electrospray ionization efficiency. It was demonstrated that EAI/CE/MS can be applied for various quantitative and mechanistic studies that are presented in this Ph.D. thesis.

## 7.2. Zusammenfassung in deutscher Sprache

Der erste Teil der vorliegenden Arbeit beschreibt die Entwicklung und Charakterisierung neuartiger automatisierter Injektionszellen für die elektrochemisch assistierte Injektion für die Kapillarelektrophorese-Massenspektrometrie. Die elektrochemisch assistierte Injektion stellt ein Injektionskonzept dar, welches die elektrochemische Erzeugung geladener Spezies aus Neutralanalyten an einer Substratelektrode während des Injektionsvorganges ermöglicht. Auf diese Weise können üblicherweise für die Kapillarelektrophorese ungeeignete Analyte einer kapillarelektrophoretischen Trennung sowohl im wässrigen als auch im nichtwässrigen Milieu zugänglich gemacht werden. Zudem kann durch die elektrochemisch assistierte Injektion die Effizienz der Elektrosprayionisierung bei der Flugzeitmassenspektrometrie für geeignete Analyte signifikant gesteigert werden.

Zu Beginn der Entwicklung dieser automatisierten Injektionszellen wurde insbesondere der Injektionsabstand zwischen Trennkapillare und Substratelektrode untersucht. Um diesen entscheidenden Parameter eingehend elektrochemisch zu untersuchen, wurden amperometrische Kapillarsonden gefertigt welche zunächst mittels hydrodynamischer Voltammetrie charakterisiert wurden. Desweiteren ermöglichte ein elektrochemisches Rastermikroskop eine mikrometeraufgelöste Vertikalpositionierung der Kapillarsonde über einer Substratelektrode und somit die Aufnahme von sog. Annäherungskurven. Dabei zeigte sich, dass die Injektionseffizienz für Abstände zwischen 5  $\mu\text{m}$  und 60  $\mu\text{m}$  nahezu konstant bleibt, während für größere Abstände eine drastische Abnahme zu verzeichnen ist.

Basierend auf diesem Ergebnis wurde zunächst eine halbautomatische Injektionseinheit aufgebaut. Sie besteht aus einem verschiebbaren Teflonschlitten mit integriertem Pufferreservoir und einer benachbarten Halterung für kommerziell erhältliche Siebdruckelektroden. Dadurch kann die Trennkapillare während der Injektion zunächst über der Substratelektrode positioniert werden um sie anschließend für die elektrophoretische Trennung manuell in das benachbarte Pufferreservoir einzutauchen. Zur Vertikalpositionierung dient ein schneller und präziser Piezomotor in Verbindung mit mechanischen Justierungsschrauben. Die Injektionseinheit wurde hinsichtlich der Präzision und Wiederholbarkeit eingehend untersucht. Als Modellsystem diente Ferrocenmethanol.

Die Erkenntnisse aus der praktischen Arbeit mit der halbautomatisierten Zelle bildeten die Grundlage zur Entwicklung eines vollautomatisierten Injektionssystems, bei welchem die horizontale Bewegung des Schlittens ebenfalls automatisiert wurde. Dazu wurden sowohl für die vertikale Kapillarpositionierung als auch für die Schlittenbewegung zwei mikroprozessorgesteuerte Servomotoren integriert. Die Motorbewegungen eines Injektionsvorgangs können somit sowohl mit Hilfe einer manuellen Steuereinheit als auch über eine PC-Software programmiert und auf Knopfdruck getriggert werden. Die Automatisierung der elektrochemisch assistierten Injektion ermöglichte somit eine höhere Injektionspräzision und einfachere Handhabung insbesondere im Hinblick auf die ohnehin sehr komplexen Arbeitsabläufe in Verbindung mit der Kapillarelektrophorese-Massenspektrometrie. Die vollautomatisierte Zelle wurde analog zum Vorgängermodell charakterisiert und für alle weiteren EAI/CE/MS Experimente benutzt.

Im weiteren Verlauf dieses Promotionsprojektes wurden zunächst kohlenstoffbasierte Siebdruckelektroden mit Hilfe der EAI/CE/MS-Technik eingehend untersucht. Es handelt sich dabei um kreisförmige, konzentrisch angeordnete 3-Elektrodenstrukturen, welche über das sog. Siebdruckverfahren auf ein geeignetes Keramiksubstrat aufgebracht werden. Diese Elektroden wurden aufgrund der einfachen Austauschbarkeit, der geringen Anschaffungskosten und der leichten Modifizierbarkeit als Substratelektroden bei den entwickelten Injektionszellen verwendet. Zudem kommen mit einem Probenvolumen von wenigen Mikrolitern aus. Kohlenstoff, Carbon Nanofasern und reduziertes Graphenoxid wurden als Elektrodenmaterialien gewählt und deren Eigenschaften bei der elektrochemischen Reduktion von 4-Nitrotoluol massenvoltammetrisch untersucht. Die potentialabhängige EAI/CE/MS Quantifizierung der unter sauren Bedingungen gebildeten Spezies, 4-Hydroxylaminotoluol und 4-Aminotoluol, zeigte für reduziertes Graphenoxid einen deutlich unterschiedlichen Kurvenverlauf und eine Potentialverschiebung hin zu weniger negativen Reduktionspotentialen im Vergleich zu Kohlenstoff und Kohlenstoffnanofasern.

Um bei Untersuchungen mit dem Modellsystem 4-Nitrotoluol eine Passivierung der Elektrodenoberfläche durch Adsorption von Edukten und Reduktionsprodukten (sog. „Elektrodenfouling“) ausschließen zu können, wurden Messungen mit ringdeuteriertem 4-Nitrotoluol- $d_4$  als internen Standard durchgeführt. In einem weiteren Schritt wurde gezeigt, dass die EAI/CE/MS eine Quantifizierung von nitroaromatischen Explosivstoffen in

Boden- und Trinkwasserproben ermöglicht. Dazu wurde den Realproben 4-Nitrotoluol in definierten Mengen zugesetzt. Das isopenmarkierte Analogon diente als interner Standard. Im Falle der Bodenproben wurde ein Flüssig-Fest-Extraktionsprotokoll entwickelt, im Falle der Wasserproben kam ein Standardprotokoll zur Festphasenextraktion zum Einsatz. Mit Hilfe des Intensitätsverhältnisses beider 4-Aminotoluole wurden die Wiederfindungsraten der Extraktionsmethoden bestimmt.

Abschließend lässt sich sagen, dass mit der elektrochemisch assistierten Injektion in Verbindung mit der Kapillarelektrophorese-Massenspektrometrie eine leistungsstarke Messtechnik entwickelt wurde, die Stärken der Massenspektrometrie (Nachweisstärke und Massenauflösung) mit der Möglichkeit verbindet, neutrale Analytspezies durch elektrochemische Konversion an Siebdruckelektroden einer kapillarelektrophoretischen Trennung zugänglich zu machen. Dies konnte in diversen Anwendungen bestätigt werden.

## 8. Appendix

### 8.1. List of Abbreviations

ACN	Acetonitrile
AE	Auxiliary Electrode
Ag	Silver
AgCl	Silver Chloride
AN	Aniline
n-BuFc	n-Butylferrocene
CE	Capillary Electrophoresis
CNF	Carbon Nanofibers
CV	Cyclic Voltammetry
DA	Dalton
EAI	Electrochemically Assisted Injection
EC	Electrochemistry
ESI	Electrospray Ionization
FcMeOH	Ferrocene Methanol
HAB	Hydroxylaminobenzene
HV	High Voltage
i-PrOH	iso-Propanol
ID	Inner Diameter
KCl	Potassium Chloride
KNO <sub>3</sub>	Potassium Nitrate
LC	Liquid Chromatography
MCAD	Multi Channel Array Detector
MS	Mass Spectrometry

MV	Mass Voltammetry
4-AT	4-Aminotoluene
4-HAT	4-Hydroxylaminotoluene
4-NT	4-Nitrotoluene
4-NT-d <sub>4</sub>	deuterated 4-nitrotoluene
NACE	Non-Aqueous Capillary Electrophoresis
OD	Outer Diameter
PEEK	Polyether Ether Ketone
Pt	Platinum
PTFE	Polytetraflouroethylene, TEFLON®
RE	Reference Electrode
r-GO	reduced Graphene Oxide
SECM	Scanning Electrochemical Microscope
SPE	Screen-Printed Electrode
SWV	Square-Wave Voltammetry
ToF	Time-of-Flight
uc	unmodified carbon
WE	Working Electrode

## 8.2. Publications and Presentations

### 8.2.1. Peer-reviewed Publications

- *“Simulation of Oxidative Stress of Guanosine and 8-Oxo-Guanosine by Electrochemically Assisted Injection-Capillary Electrophoresis-Mass Spectrometry”*

Scholz R, **Palatzky P**, Matysik F-M, in preparation

- *“Electrochemically Assisted Injection in Combination with Capillary Electrophoresis-Mass Spectrometry (EAI/CE/MS) - Mechanistic and Quantitative Studies of 4-Nitrotoluene at Various Carbon-Based Screen-Printed Electrodes”*

**Palatzky P**, Zöpfl A, Hirsch Th, Matysik F-M, *Electroanalysis* **2013**, 25:117-122

- *“Development and Characterization of a Novel Semi-Automated Arrangement for Electrochemically Assisted Injection in Combination with Capillary Electrophoresis Time-of-Flight Mass Spectrometry”*

**Palatzky P**, Matysik F-M, *Electrophoresis* **2012**, 33:2689-2694

- *“Development of Capillary-Based SECM Probes for the Characterization of Cell Arrangements for Electrochemically Assisted Injection”*

**Palatzky P**, Matysik F-M, *Electroanalysis* **2011**, 23:50-54

- *“High-Resolution Imaging of Nanostructured Si/SiO<sub>2</sub> Substrates and Cell Monolayers Using Scanning Electrochemical Microscopy”*

Bergner S, **Palatzky P**, Wegener J, Matysik F-M, *Electroanalysis* **2011**, 23:196-200

Furthermore:

- *“Biodiesel, a Sustainable Oil, in High Temperature Stable Microemulsions Containing a Room Temperature Ionic Liquid as Polar Phase”*

Zech O, Bauduin P, **Palatzky P**, Touraud D, Kunz W, *Energy & Environmental Science* **2010**, 3:846-851

### 8.2.2. Oral Presentations

- *“Development and Application of a Novel Automated Injection Device for Electrochemically Assisted Injection in Combination with Capillary Electrophoresis Time-of-Flight Mass Spectrometry”*

23. Doktorandenseminar - AK Separation Science, Hohenroda, Germany, 2013.

- *“Development and Application of an Automated Injection Device for Electrochemically Assisted Injection (EAI) – A New Approach in Capillary Electrophoresis – Mass Spectrometry”*

6. Interdisziplinäres Doktorandenseminar - AG Prozessanalytik, Berlin, Germany, 2012.

- *„Methodische Entwicklungen und Anwendungen der elektrochemisch assistierten Injektion (EAI) für die Kapillarelektrophorese“*

CE-Forum, Regensburg, Germany, 2011.

- *“Application of Novel Capillary Probes for the Investigation of Electrochemically Assisted Injection (EAI) using a Scanning Electrochemical Microscope for EAI Cell Development”*

7<sup>th</sup> International Students Conference, Prague, Czech Republic, 2011.



### 8.2.3. Poster Presentations

- *“Development and Application of a Novel Automated Injection Device for Electrochemically Assisted Injection in Combination with Capillary Electrophoresis Time-of-Flight Mass Spectrometry”*  
CE-Forum, Aalen, Germany, 2012.
- *“Development and Characterization of a Novel Automated Injection Device for Electrochemically Assisted Injection in Combination with Capillary Electrophoresis Time-of-Flight Mass Spectrometry”*  
ESEAC, Portoroz, Slovenia, 2012.
- *“Separation and Detection of Nitroaromatic Compounds by Electrochemically Assisted Injection in Combination with Capillary Electrophoresis Time-of-Flight Mass Spectrometry”*  
ANALYTICA Conference, Munich, Germany, 2012.
- *“Application of Novel Capillary Probes for SECM Studies of Electrochemically Assisted Injection”*  
ANAKON, Zurich, Switzerland, 2011.
- *“Application of Novel Capillary Probes for SECM Studies of Electrochemically Assisted Injection”*  
ISE, Nice, France, 2010.
- *“Hyphenation of Electrochemically Assisted Injection for Capillary Electrophoresis and Scanning Electrochemical Microscopy for Studies of Mass Transport Behaviour close to Substrate Electrodes”*  
5. Regensburger Elektrochemie-Tage, Regensburg, Germany, 2009.

- *„Hyphenation of Electrochemically Assisted Injection for Capillary Electrophoresis and Scanning Electrochemical Microscopy for Studies of Mass Transport Behaviour close to Substrate Electrodes“*

Wissenschaftsforum Chemie, Frankfurt/Main, Germany, 2009.

### 8.3. Curriculum Vitae

Full Name	Peter Josef Johann Palatzky
Date of Birth	24.11.1981
Place of Birth	Regensburg
Family Status	single

#### ***Scientific Education***

Since 11/2009	Ph.D. Student, Institute for Analytical Chemistry, Chemo- and Biosensors, University of Regensburg  Workgroup: Prof. Dr. F.-M. Matysik
Ph.D. Thesis:	<i>“Electrochemically Assisted Injection for Capillary Electrophoresis Time-of-Flight Mass Spectrometry - Novel Instrumental and Methodical Developments”</i>
10/2007-11/2009	Master of Science in Chemistry, University of Regensburg
Master Thesis:	<i>“Voltammetric Measurement Techniques for Ultramicroelectrode Studies and Applications in Scanning Electrochemical Microscopy”</i>
10/2002-01/2007	Bachelor of Science in Chemistry, University of Regensburg
Bachelor Thesis:	<i>“Stabilization of Alginate Gels via Covalent Cross-Linking Strategies”</i>

### ***Civilian Service***

07/2001-05/2002      Surgical Assistant, Department of Ophthalmology, Hospital of the University of Regensburg

### ***School Education***

09/1992-06/2001      General qualification for university entrance, Werner-von-Siemens-Gymnasium, Regensburg

### ***Work Experience***

2008                      Student trainee, OSRAM Optosemiconductors GmbH

OS TM:                  Testing and Metrology Analytics

OS IR AE1:              Infrared Application Engineering

2009-present            Supervision of lab courses for chemistry, dentistry and medicine students. Individual mentoring of advanced student research work.

2009-present            Private lessons for undergraduate students of chemistry, medicine and dentistry.



Peter Palatzky